TECHNICAL REPORT

CAL No. VJ-2330-G-3

SUMMARY REPORT ON OFF-ROAD MOBILITY RESEARCH

Volume II

3rd TECHNICAL REPORT
NOVEMBER 1968

Sponsored by:

Advanced Research Projects Agency
Department of Defense
ARPA Order No. 841
Dated 7 May 1966

Under Contract DAHC04 67 C 0005
U.S. Army Research Office - Durham
Durham, N.C.

Distribution of this document is unlimited.

CORNELL AERONAUTICAL LABORATORY, INC.
OF CORNELL UNIVERSITY, BUFFALO, N. Y. 14221

THE FINDINGS IN THIS REPORT ARE NOT TO BE CONSTRUED AS AN OFFICIAL DEPARTMENT OF DEFENSE POSITION UNLESS SO DESIGNATED BY OTHER AUTHORIZED DOCUMENTS.

CORNELL AERONAUTICAL LABORATORY, INC.
BUFFALO, NEW YORK 14221

CAL REPORT NO. VJ-2330-G-3

SUMMARY REPORT
ON
OFF-ROAD MOBILITY RESEARCH

3rd TECHNICAL REPORT

VOLUME II

UNDER CONTRACT DAHC04 67 C 0005
WITH
U.S. ARMY RESEARCH OFFICE - DURHAM
DURHAM, N.C.

NOVEMBER 1968

Sponsored by:
ADVANCED RESEARCH PROJECTS AGENCY
DEPARTMENT OF DEFENSE
ARPA ORDER NO. 841
DATED 7 MAY 1966

ABSTRACT

A summary of research and engineering studies conducted on a long-range program of off-road mobility research is presented in Volume I of this two volume report. These studies, some of which are only partially completed, are directed at providing technical knowledge which is required to match off-road vehicles with military mobility requirements.

A hybrid computer model is described which will permit predicting vehicle dynamics performance of simulated vehicles traversing a broad spectrum of off-road situations. A critique of existing soil trafficability theories is made based on a review of the literature which treats the comparison of vehicle performance prediction with experimental results. Analytical and experimental studies of the velocity field and soil fabric in clay soil exposed to dynamic loads are summarized. A general method is discussed for processing mobility related environmental information and for mapping vehicle performance by computer methods. A concept is introduced for testing vehicles in relation to the total environment in order to define the vehicle performance envelope.

Also a method is introduced for displaying potential vehicle performance in selected geographic areas and for producing "testable" specifications for off-road vehicles. Engineering studies of an off-road driving simulator for synthesizing dynamic visual displays and vehicle motion in the laboratory are reviewed.

Recommendations pertaining to future off-road mobility research and engineering studies are presented.

Volume II contains Appendices that complement the material presented in Volume I.

ACKNOWLEDGEMENT

This research was supported by the Advanced Research Projects Agency, Project AGILE, Department of Defense and was contracted through the U.S. Army Research Office, Durham under contract No. DAHC04 67 C 0005. The ARPA Technical Monitor was Mr. A. N. Tedesco. Mr. G. E. Bartlett was ORMR Program Manager.

This report was co-edited by:

George E. Bartlett
Jerome N. Deutschman

The following sections were compiled from material prepared by the following Project Personnel:

Section 3.2 — Manfred R. Belsdorf, Richard Cassidy, Jerome N. Deutschman, Sol Kaufman, Richard L. Pleuthner, John H. Quirk, Dieter Schuring, Robert L. Smith, Rodolfo D. Vergara

Section 3.3 — Robert W. Coakley, Gregory Lewandowski, Richard P. Leonard, Thomas R. Magorian, H. T. McAdams, John H. Quirk, Walter F. Wood

Section 3.4 — Robert E. Baier, Vito A. DePalma, John M. Grace, Patrick M. Miller, Paul Rosenthal, Melvin I. Esrig*, David J. Henkel*, J. Steinback*, Yudbir*, R. D. Japp**, S. J. Windisch**, Raymond N. Yong**, Gideon Dagan***, Marshall P. Tullin***

*Department Geotechnical Engineering, Cornell University
**Department of Civil Engineering and Applied Mechanics, McGill University
***Hydronautics, Inc.

Section 3.5	Nelson M. Isada, Melvin H. Rudov, Robert C. Sugarman, Donald E. Sussman.
Section 3.6	John N. Andrews, Jr., George G. Sexton, Robert L. Smith, William C. Grenke****, Clifford J. Nuttall, Jr.****
Appendix A	Vanig V. Abrahamian, Manfred R. Belsdorf, Sol Kaufman, Robert L. Smith
Appendix B	Richard L. Pleuthner
Appendix C	John H. Quirk
Appendix D	Robert W. Coakley, H.T. McAdams, Walter F. Wood
Appendix E	Richard P. Leonard
Appendix F	Thomas R. Magorian
Appendix G	Peter E. Engler, Francis A. Giori, Phillip J. Joseph, Paul Rosenthal
Appendix H	Vito A. DePalma
Appendix I	Vito A. DePalma, R. D. Japp, Paul Rosenthal, Raymond N. Yong
Appendix J	Dominic F. Morris
Appendix K	Melvin H. Rudov, Robert C. Sugarman

****WNRE Inc.

Appendix L Nelson M. Isada, Robert C. Sugarman

The technical and administrative assistance and guidance provided by Messrs. Fredrick Dell'Amico, Arthur Stein, and Robert M. Stevens is also gratefully acknowledged.

TABLE OF CONTENTS

Table of Contents (continued)

LIST OF FIGURES

VOLUME II

LIST OF TABLES

VOLUME II

GLOSSARY OF ACRONYMS AND CODE NAMES

AMC	Army Materiel Command
ARPA	Advanced Research Projects Agency
ATAC	Army Tank-Automotive Command
CAL	Cornell Aeronautical Laboratory, Inc.
CDC	Combat Development Command
CDOG	Combat Development Objective Guide
IDA	Institute for Defense Analyses
LLL	Land Locomotion Laboratory (of ATAC)
MC	Military Characteristics
MERS	Mobility Environment Research Study
MEXE	Military Engineering Experimental Establishment, Christchurch, England
MTP	Materiel Test Procedure
OPM	Ordnance Proof Manual
ORMR	Off-Road Mobility Research
PSD	Power Spectral Density
QMR	Qualitative Materiel Requirement
RCI	Rating Cone Index
SAE	Society of Automotive Engineers
TACOM	Tank-Automotive Command
TECOM	Test and Evaluation Command
TECP	Test and Evaluation Command Procedures
USCS	Unified Soil Classification System
VDM	Vehicle Dynamics Model
VMEA	Vehicle Mobility Exercise A
VSDM	Vehicle System Dynamics Model
WES	U.S. Army Engineer Waterways Experiment Station
WNRE, Inc.	Subcontractor to CAL (formerly Wilson, Nuttall, Raimond, Engineers, Inc.)

BLANK PAGE

Appendix A: VEHICLE DYNAMICS MODEL FORMULATION

This appendix is composed of two major parts. The first part contains a listing of symbols and a definition of major coordinate systems used in formulating the model.

The second part includes general six degree of freedom equations for a vehicle with a rigid hull and the equations for transforming from an earth-fixed coordinate system to a hull-fixed system. Also included are the equations delimited to five degrees of freedom for the hull, as they have been used in modeling a 4x4 vehicle with two solid axles. Finally, the equations are presented which were used in the model to represent the suspensions, drive system, and wheel-ground interface.

Definition of Coordinate Systems and Nomenclature

Figure A-1 illustrates the two primary coordinate systems used in the VDM. The XYZ system is earth-fixed; the xyz system is hull-fixed, with origin at the hull center of gravity. Positive directions for X,Y,Z; x,y,z; translational velocity u, v, w; components and rotational velocity components p, q, r are indicated by arrowheads in Figure A-1.

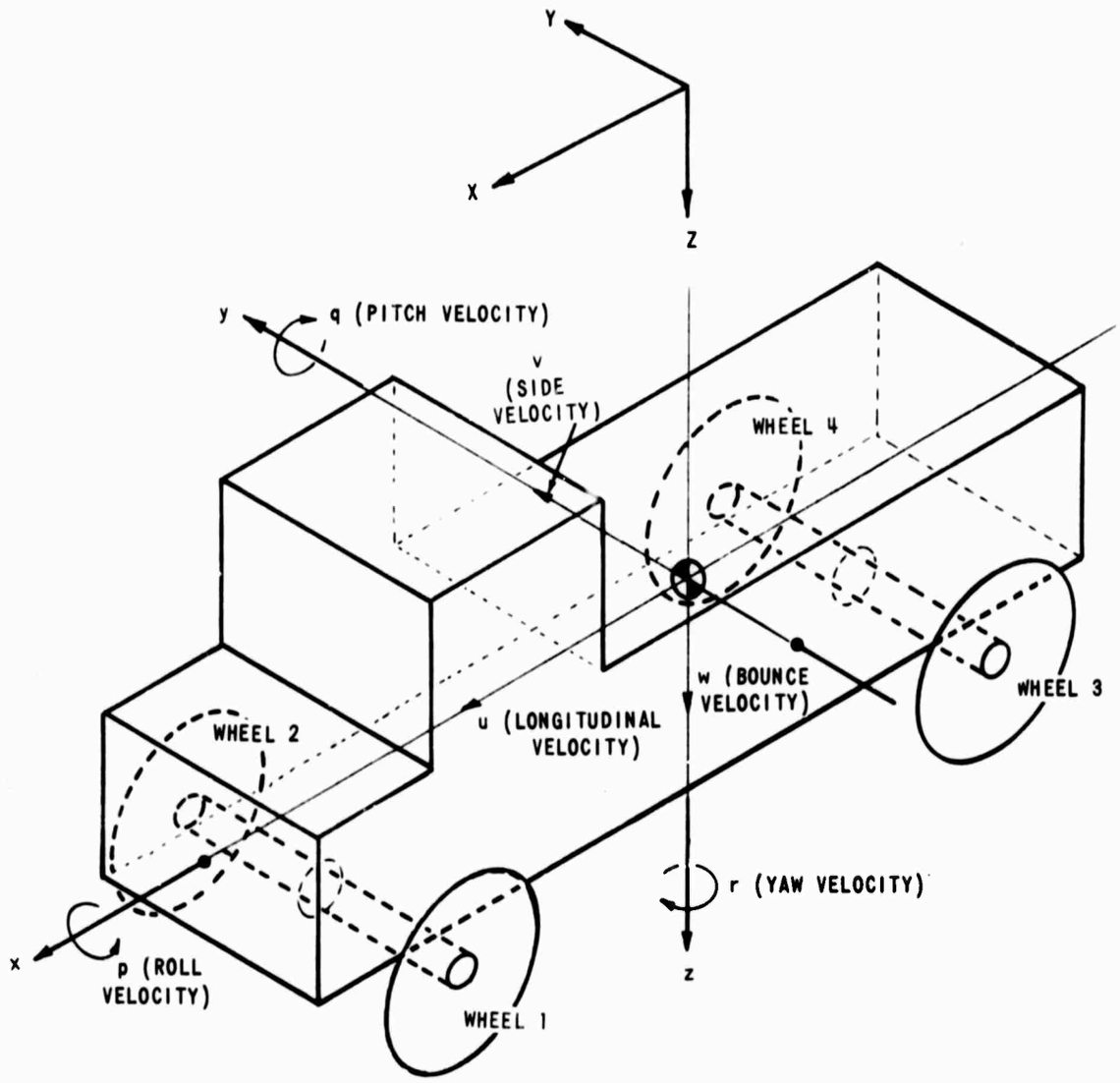

Figure A-1 VDM COORDINATE SYSTEMS

Nomenclature *

a_x, a_y, a_z	Components of absoulte accelerations in hull-fixed axis system.
a_{xij}, a_{yij}, a_{zij}	Components of absolute acceleration of the axle center parallel to hull-fixed axes.
a_{xP}, a_{yP}, a_{zP}	Components of absolute acceleration of any point P on the vehicle in hull-fixed axis system.
b_i	Viscous damping coefficient associated with suspension, for small rates.
b_{ci}	Viscous damping coefficient associated with suspension when compressing at high rates.
b_{ei}	Viscous damping coefficient associated with suspension when extending at high rates.
B_i	Viscous damping force associated with suspension.
$h(X,Y)$	Terrain elevation at point X,Y (positive downward).
H_{xi}, H_{yi}, H_{zi}	Components of wheel-hub forces in hull-fixed axis system.
I_x, I_y, I_z	Roll, pitch, yaw moments of inertia of hull about hull-fixed axes.

---

* NOTE: Subscript i=1,2,3,4 refers to wheel or associated suspension.
Subscript ij=(1,2); (3,4) refers to axle connecting ith and jth wheels.
Superscript dot ($\dot{}$) indicates differentiation with respect to time.
Superscript bar ($\bar{}$) indicates a vector; all distances are treated herein as vector components.

I_{xz}	Hull roll-yaw product of inertia.
I_{xij}, I_{yij}, I_{zij}	Axle-wheel assembly roll, pitch, yaw moments of inertia about axes parallel to the hull-fixed system but with origin displaced to axle cg.
I_{wi}	Effective spin moment of inertia of wheel (plus half an axle).
I_e	Moment of inertia of the engine and transmission input shaft.
K_i	Force associated with suspension spring and bumpstop.
k	Constant in drive torque representation.
k_i	Spring constant of suspension spring.
k_{ei}	Spring constant of bumpstop in extension direction.
k_{ci}	Spring constant of bumpstop in compression direction.
k_{wi}	Tire spring constant.
k_{yi}	Coefficient of tire side force.
m_{ij}	Effective mass of axle-wheel assembly and part of suspension.
M	Total mass of hull plus payload.
M_x, M_y, M_z	Components in hull-fixed axes of total moment acting on hull.

M_e	Total output torque from engine.
M_{di}	Drive torque exerted by engine on wheel.
n	Total gear ratio (transmission and transfer case) between engine and wheels.
n_{wi}	Rotational velocity of wheel--rpm.
n^*_{wi}	Break point in engine torque vs. wheel speed curve.
N_i	Force component at wheel-ground contact, normal to ground.
p, q, r	Roll, pitch, yaw angular velocities of hull about hull-fixed x,y,z axes respectively.
p_{ij}	Component of roll angular velocity of axle about axis through axle cg parallel to hull-fixed x axis.
r	Undeflected radius of wheel.
r_i	Rolling radius of wheel.
S_{zi}	z component of total force transmitted by suspension.
S_{xij}, S_{yij}	x and y components of force transmitted to hull from axle.
s_i	Slip ratio.
T_i	Thrust component at wheel-ground contact, tangential to ground profile in plane of wheel.

$\mathcal{U}$	Matrix transformation from earth-fixed to hull-fixed reference frame.
$\mathcal{T}_{ij}$	Matrix transformation from axle-fixed to hull-fixed reference frame.
u, v, w	Components of hull cg absolute velocity in hull-fixed axis system.
$\overline{V}$	Hull cg velocity.
W_x, W_y, W_z	Components of gross weight of hull in hull-fixed axis system.
W_{xij}, W_{yij}, W_{zij}	Components of effective weight of axle, wheel, and part of associated suspension, in axes parallel to hull-fixed axes, with origin displaced to axle center.
x_{ij}, y_{ij}, z_{ij}	Coordinates of the axle cg in hull-fixed system.
x_{si}, y_{si}	Coordinates of suspension attachment point of axle and hull, in hull-fixed system.
X, Y, Z	Coordinates of hull cg in earth-fixed reference system.
$\dot{X}_i$, $\dot{Y}_i$	Velocity components in earth-fixed system of effective ground contact points.
$\dot{X}_{Ti}$	Velocity component of effective ground contact point in direction of terrain slope.

$\bar{z}_{ij}$	Coordinate in hull-fixed system of axle center when springs are unloaded.
α_i	Slope of terrain in plane of wheel.
β_i	Slip angle of wheel.
δ_{ai}	Displacement of suspension attachment point at axle, measured from reference position $\bar{z}_{ij}$ along body-fixed z axis.
δ_{ei}	Breakpoint of spring rate curve in extension direction.
δ_{ci}	Breakpoint of spring rate curve in extension direction.
δ_{ei}	Breakpoint of damping force curve in extending direction.
δ_{ci}	Breakpoint of damping force curve in compressing direction.
δ_{wi}	Deflection of tire at effective contact point.
μ	Coefficient of rolling friction, often referred to as normalized tractive force.
ψ, θ, ϕ	Yaw, pitch, roll angles of hull (sequence of rotations in order of their occurrence).
ϕ_{ij}	Roll angle of axle relative to hull, about an axis passing through axle cg and parallel to hull-fixed x axis.
ρ	Coefficient of rolling resistance.

σ_i Side force component at ground contact point.

ω_i Rotational velocity of the wheel about its axle.

Vehicle Dynamics Model Equations Formulation

Physical equations which describe the general structure of the VDM are formulated in the following paragraphs. A detailed development of the mechanization equations may be found in Reference A1.

The equations presented here are listed in two different ways. Equations incorporated in the model are assigned numerals preceded by letters; the letters H,S,A,D, and T indicate in which of the five major modules each equation is used: hull, suspension, axle-wheel assembly, drive system, and terrain interface respectively. Equations used only in derivations (usually more general in form than those mechanized) are designated by numerals alone.

Transformations Among Coordinate Systems - Transformation equations representing relative rotation of coordinate systems are written in terms of conventional Euler angles. The sequence of rotations is yaw ψ, pitch θ, and roll ϕ.

The matrix u transforms a vector from the earth-fixed XYZ system to the hull-fixed xyz system, e.g.:

$$\begin{bmatrix} x \\ y \\ z \end{bmatrix} = \begin{bmatrix} u \end{bmatrix} \begin{bmatrix} X \\ Y \\ Z \end{bmatrix} \qquad (1)$$

where

$$[u] \equiv \begin{bmatrix} \cos\psi\cos\theta & \sin\psi\cos\theta & -\sin\theta \\ \cos\psi\sin\theta\sin\phi - \sin\psi\cos\phi & \sin\psi\sin\theta\sin\phi + \cos\psi\cos\phi & \cos\theta\sin\phi \\ \cos\psi\sin\theta\cos\phi + \sin\psi\sin\phi & \sin\psi\sin\theta\cos\phi - \cos\psi\cos\phi & \cos\theta\cos\phi \end{bmatrix} \qquad (2)$$

Since the matrix is orthogonal, its transpose $\tilde{\mathcal{U}}$ equals its inverse, so that, $\tilde{\mathcal{U}}$ can be used to transform vectors from the xyz system into the XYZ system:

$$\begin{bmatrix} X \\ Y \\ Z \end{bmatrix} = \begin{bmatrix} \mathcal{U} \end{bmatrix} \begin{bmatrix} x \\ y \\ z \end{bmatrix} \tag{3}$$

$$\tilde{\mathcal{U}} \equiv \begin{bmatrix} \cos\psi\cos\theta & \cos\psi\sin\theta\sin\phi - \sin\psi\cos\phi & \cos\psi\sin\theta\cos\phi + \sin\psi\sin\phi \\ \sin\psi\cos\theta & \sin\psi\sin\theta\sin\phi + \cos\psi\cos\phi & \sin\psi\sin\theta\cos\phi - \cos\psi\sin\phi \\ -\sin\theta & \cos\theta\sin\phi & \cos\theta\cos\phi \end{bmatrix} \tag{4}$$

The Euler angles are expressed in terms of roll velocity p, pitch velocity q, and yaw velocity r:

$$\dot{\psi} = \sec\theta\,(q\sin\phi + r\cos\phi) \tag{5}$$

$$\dot{\theta} = q\cos\phi - r\sin\phi \tag{6}$$

$$\dot{\phi} = p + \tan\theta\,(q\sin\phi + r\cos\phi) \tag{7}$$

In the present five degree of freedom model where $\psi = 0$, [2] reduces to:

$$\mathcal{U} = \begin{bmatrix} \cos\theta & 0 & -\sin\theta \\ \sin\theta\sin\phi & \cos\phi & \cos\theta\sin\phi \\ \sin\theta\cos\phi & -\cos\phi & \cos\theta\cos\phi \end{bmatrix} \tag{111}$$

and [4] reduces to the transpose of [H1]:

$$\tilde{u} = \begin{bmatrix} \cos\theta & \sin\theta\sin\phi & \sin\theta\cos\phi \\ 0 & \cos\phi & -\cos\phi \\ -\sin\theta & \cos\theta\sin\phi & \cos\theta\cos\phi \end{bmatrix} \tag{H2}$$

Also, since $r = 0$ (6 and 7) reduce to:

$$\dot{\theta} = q\cos\phi \tag{H3}$$

$$\dot{\phi} = p + q\tan\theta\sin\phi \tag{H4}$$

and since ψ is assumed to be very small, monitoring Equation 5 is not required.

In addition to the two major coordinate systems, two others are used, one associated with each axle. These axes are free to roll through an angle ϕ_{ij} with respect to the hull. The matrix T_{ij} which transforms a vector from an axle-fixed axis system into the hull-fixed frame is:

$$T_{ij} = \begin{bmatrix} 1 & 0 & 0 \\ 0 & \cos\phi_{ij} & -\sin\phi_{ij} \\ 0 & \sin\phi_{ij} & \cos\phi_{ij} \end{bmatrix} \tag{A1}$$

and since this is again an orthogonal transformation, vectors may be transformed from hull-fixed to axle-fixed references by the transpose:

$$T_{ij}^{-1} = \tilde{T}_{ij} \tag{A2}$$

The components of absolute acceleration $a_{x_p}, a_{y_p}, a_{z_p}$ in the hull-fixed axis system for any point P on the vehicle are:

$$a_{x_p} = \dot{u} + qw - rv + 2(\dot{z}_p q - \dot{y}_p r) - x_p(q^2 + r^2) + y_p(pq - \dot{r}) + z_p(pr + \dot{q}) + \ddot{x}_p \quad (8)$$

$$a_{y_p} = \dot{v} + ru - pw + 2(\dot{x}_p r - \dot{z}_p) + x_p(pq + \dot{r}) - y_p(p^2 + r^2) + z_p(qr - \dot{p}) + \ddot{y}_p \quad (9)$$

$$a_{z_p} = \dot{w} + pv - qu + 2(\dot{y}_p p - \dot{x}_p q) + x_p(pr - \dot{q}) + y_p(qr + \dot{p}) - z_p(p^2 + q^2) + \ddot{z}_p \quad (10)$$

Hull Motions - Translational motion of the hull is solved from Newton's equations with vector components expressed in the hull-fixed xyz axis system.

$$M\bar{a} = \bar{W} + \sum_{i=1}^{4} \bar{S}_i + \sum_{ij=12}^{34} \bar{S}_{ij} \quad (115)$$

where $\bar{S}_i$ is the force transmitted (z direction only) through the ith suspension to the hull and $\bar{S}_{ij}$ is the vector sum of the y and z components transmitted through the weightless column from the ijth axle (see Figure A-2). The weight components W_x, W_y and W_z in the hull-fixed axis system are computed from:

$$\begin{bmatrix} W_x \\ W_y \\ W_z \end{bmatrix} = \begin{bmatrix} \\ u \\ \\ \end{bmatrix} \begin{bmatrix} 0 \\ 0 \\ W \end{bmatrix} \quad (116)$$

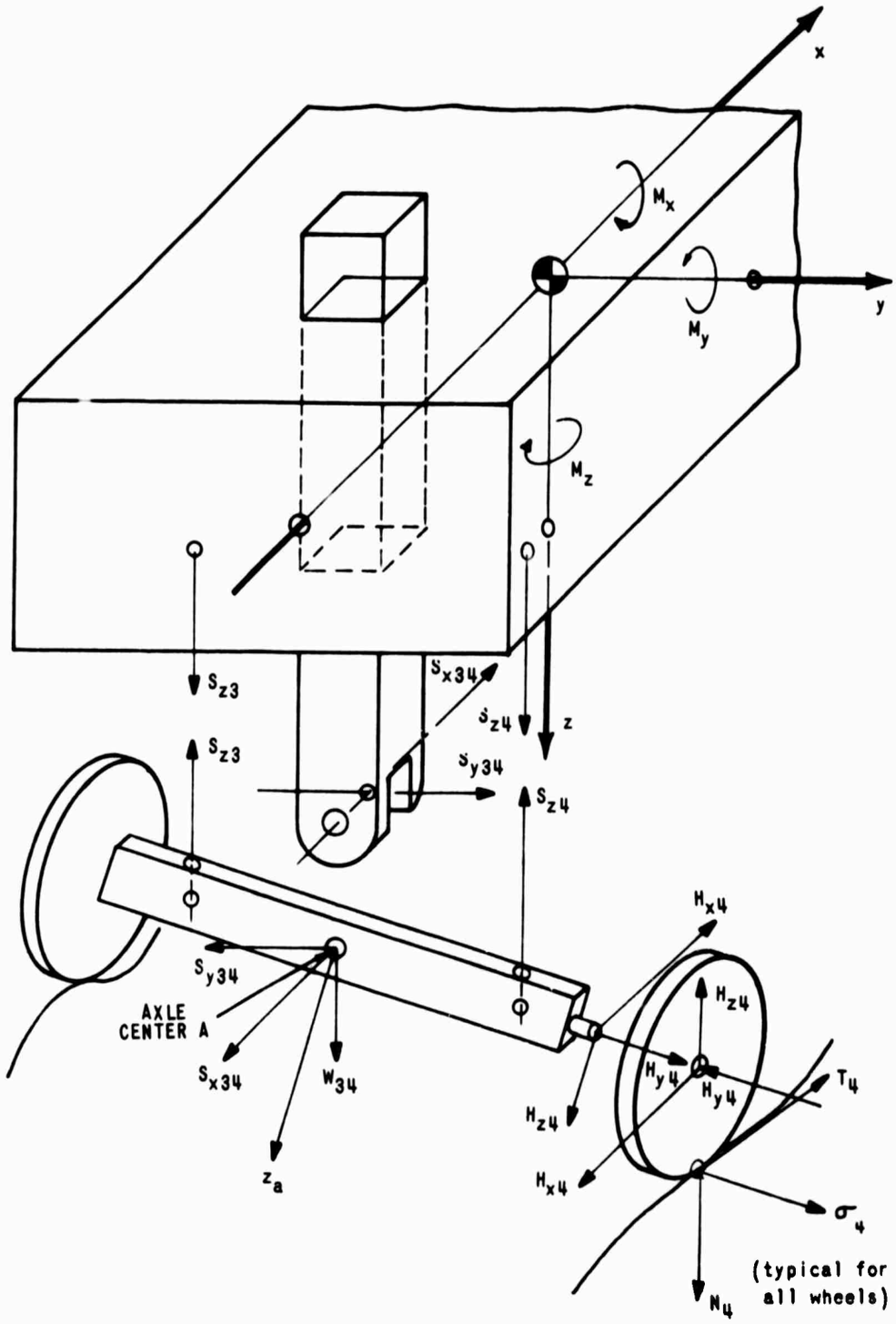

Figure A-2 FREE BODY DIAGRAM (REAR VIEW)

The hull rotational motion is solved from Euler's equations with vector components again expressed in the hull-fixed system.*

$$I_x \dot{p} = M_x + I_{xz} pq \tag{H7}$$

$$I_y \dot{q} = M_y + I_{xz} p^2 \tag{H8}$$

The moments M_x and M_y** acting on the hull are found from:

$$M_x = \sum_{i=1}^{4} S_{zi}\, y_{si} - \sum_{ij=12}^{34} S_{yij}\, z_{ij} \tag{H9}$$

$$M_y = -\sum_{i=1}^{4} S_{zi}\, x_{si} + \sum_{ij=12}^{34} \left(S_{xij}\, z_{ij} + M_{yij} \cos\phi_{ij} - M_{zij} \sin\phi_{ij} \right) \tag{H10}$$

where the moments transmitted from the axle to the hull by the weightless columns are found from:

$$M_{yij} = -I_{yij}\, \dot{q} \tag{H11}$$

$$M_{zij} = p_{ij}\, q \left(I_{xij} - I_{yij} \right) \tag{H12}$$

The hull-fixed velocity components of the hull cg are determined by integrating the following equations which are the delimited version of [8-10] applied to the cg.

---

* These equations assume symmetry with respect to the xz plane $(I_{xy} = I_{yz} = 0)$ and also that $r = 0$. The more general version from which they were derived is not presented here.

** M_z is not computed at the present stage of modeling because yaw motion is not included in the five degree of freedom model.

$$\dot{u} = a_x + wq \tag{H13}$$

$$\dot{v} = a_y + wp \tag{H14}$$

$$\dot{w} = a_z + uq - vp \tag{H15}$$

The u, v, w velocity components are then transformed back into earth fixed components $\dot{X}$, $\dot{Y}$, $\dot{Z}$ through the $\tilde{u}$ matrix. Then the ground speed $|V|$ of the vehicle is computed from the expression:

$$|V| = \dot{X}\cos\theta + \dot{Z}\sin\theta$$

The $\dot{Y}$ (side velocity) contribution to $|V|$ has been negligible in the non-steer problems which have been studied to date.

Axle Motions - In the present model the axles are visualized as attached to the hull in a manner that permits them three degrees of freedom with respect to the hull: (1) motion in the z-direction by means of sliding of the weightless columns, which were discussed in Section 3.2.1.1. (2) roll through an angle ϕ_{ij} relative to the hull, by means of rotation about the pivot point A at the axle center (see Figure A-2) and (3) axle-wheel rotation about the axle axis. Thus, it is assumed that the suspensions are essentially rigid, except in the z direction. The x and y components of the axle-center accelerations can therefore be calculated from the following simplified versions of the kinematic equations (8) and (9):

$$a_{x_{ij}} = a_x + 2q\dot{z}_{ij} - z_{ij}q^2 + z_{ij}\dot{q} \tag{A3}$$

$$a_{y_{ij}} = a_y - 2p\dot{z}_{ij} + z_{ij}pq - z_{ij}\dot{p} \tag{A4}$$

Since the axles have freedom of motion with respect to the hull in the z direction, the axle centers' z acceleration components must be computed from the dynamic equations:

$$m_{ij}\, a_{zij} = W_{zij} + H_{zi} + H_{zj} - S_{zi} - S_{zj} \tag{A5}$$

where the H force components are exerted on the axle by the hubs, the S force components are exerted on the axle by the suspensions, and the axle weight component W_{zij} is found from:

$$\begin{bmatrix} W_{xij} \\ W_{yij} \\ W_{zij} \end{bmatrix} = \begin{bmatrix} \\ \mathcal{T}_{ij} \\ \\ \end{bmatrix} \begin{bmatrix} 0 \\ 0 \\ W_{ij} \end{bmatrix} \tag{A6}$$

The z velocity and displacement component of the axle centers may then be computed by integrating the following version of (10):

$$\ddot{z}_{ij} = a_{zij} - a_z + x_{ij}\dot{q} + z_{ij}(p^2 + q^2) \tag{A7}$$

The relative roll motion of the axles with respect to the hull is found from:

$$I_{xij}\dot{p}_{ij} = \sum_{k=i}^{j} (-S_{zk}\, y_{sk} + H_{zk}\, y_k - \sigma_k r_k) \tag{A8}$$

where σ_k is the side slip force component on the kth wheel.

Since the suspensions have been assumed rigid except in the z direction:

$$q_{ij} = q$$

$$r_{ij} = r = 0$$

and as seen from Figure A-3.

$$\phi_{ij} = p_{ij} - p$$

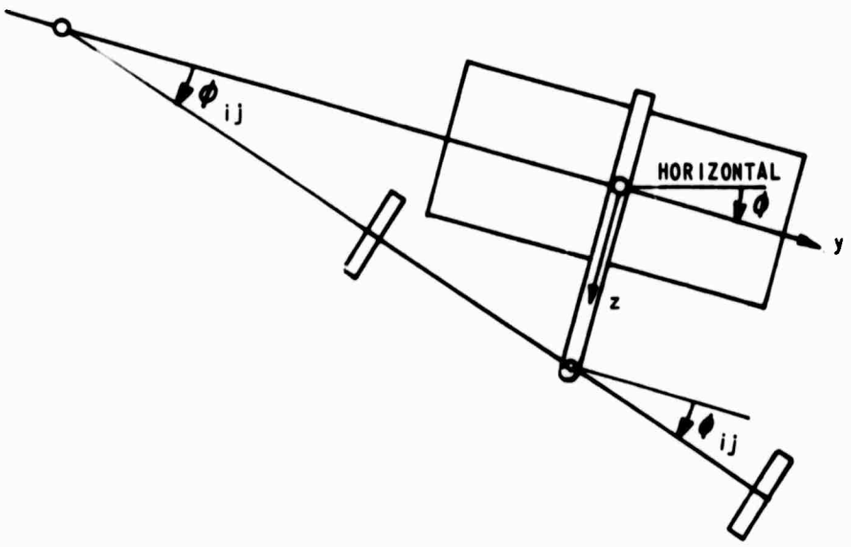

Figure A-3 AXLE-HULL GEOMETRY

Suspension System - From this point on, the equations are directed specifically to a 4x4, two solid axle vehicle. Each of the four suspensions consists of a multi-leaf spring, a shock absorber and a hard rubber bump stop (Figure A-4). In the simulation, this system has been approximated by the combination of a nonlinear frictionless spring* and a nonlinear viscous damper.**

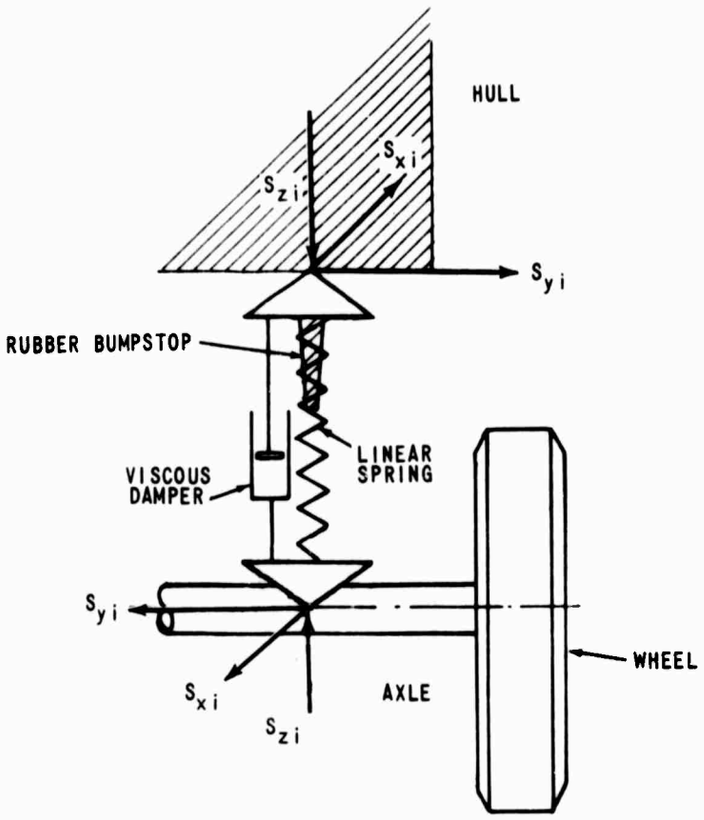

Figure A-4 SUSPENSION SYSTEM (REAR VIEW)

* The spring is represented by linear segments as shown in Figure A-5.

** Coulomb friction, if found to be of significant magnitude, will be introduced as an additional nonlinear term.

The z force components S_{zi} transmitted by the suspension are therefore computed in two parts:

$$S_{zi} = K_i + B_i$$

where K_i is the force associated with the ith spring and B_i with the ith damper.

In the region of small deflection each spring is for the present treated as linear, with stiffness k_i, until compressed to the point where the bump stop is contacted (Figure A-5). At this point the stiffness increases abruptly to k_{ci}. In the extension direction, allowance is made for another abrupt increase in stiffness to a value k_{ei}.

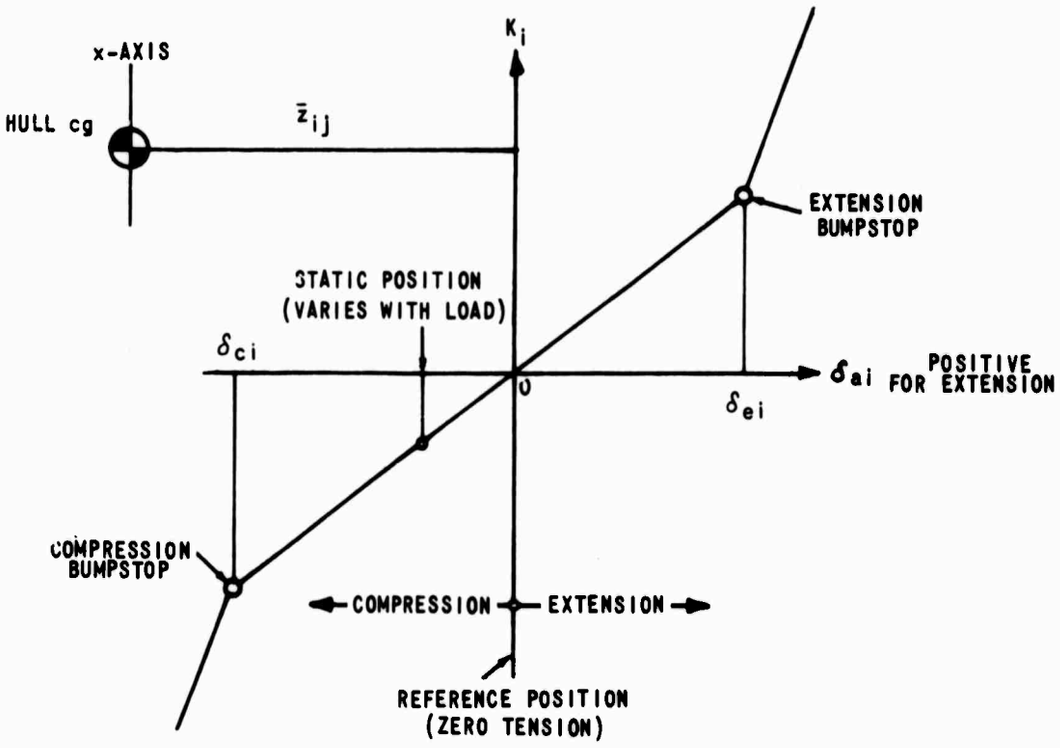

Figure A-5 SPRING FORCE vs. DEFLECTION

The spring force is thus found from:

$$
\begin{aligned}
F_i &= k_i \delta_{ei} + k_{ei} (\delta_{ai} - \delta_{ei}) && \delta_{ei} < \delta_{ai} \\
&= k_i \delta_{ai} && \delta_{ci} < \delta_{ai} < \delta_{ei} \\
&= k_i \delta_{ci} + k_{ci} (\delta_{ai} - \delta_{ci}) && \delta_{ai} < \delta_{ci}
\end{aligned}
\qquad \text{(S1)}
$$

where all the δ's are positive downward (for spring extension). Spring extensions are computed from:

$$\delta_{ai} = (z_{ij} - \bar{z}_{ij}) + y_{si} \phi_{ij} \qquad \text{(S2)}$$

The shock absorber characteristics as modeled are shown in Fig. A-6. The steep slope in the low force region accounts for blow off and creep effects.

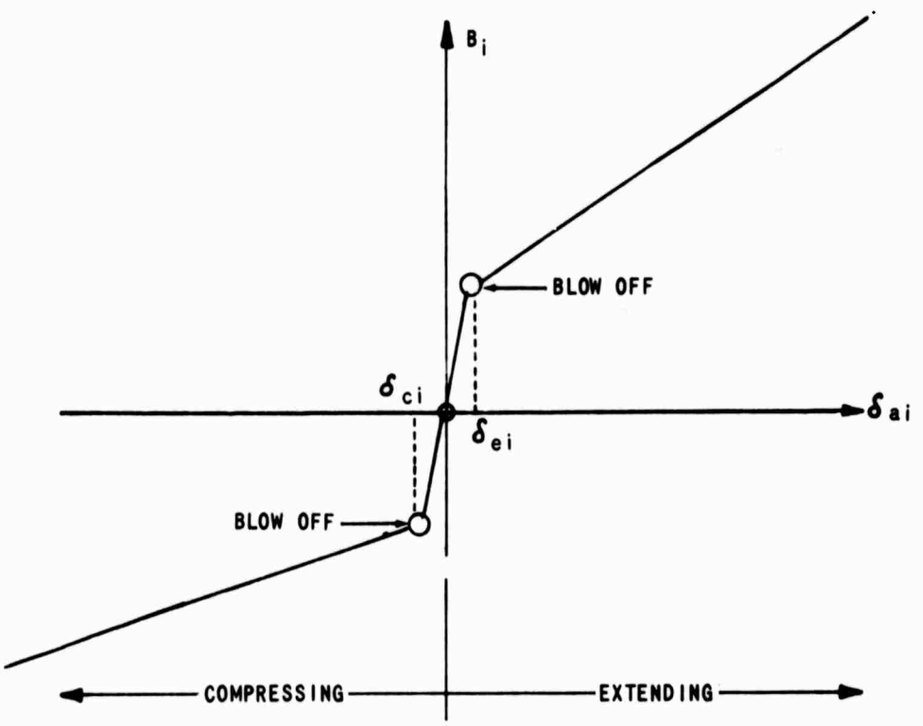

Figure A-6 DAMPING FORCE vs. COMPRESSING/EXTENDING RATE

Damping for B_i is thus computed in the three regions from:

$$B_i = b_i \dot{\delta}_{ei} + b_{ei} (\dot{\delta}_{ai} - \dot{\delta}_{ei}) \qquad \dot{\delta}_{ei} < \dot{\delta}_{ai} \qquad \text{(S3)}$$

$$= b_i \dot{\delta}_{ai} \qquad \dot{\delta}_{ci} < \dot{\delta}_{ai} < \dot{\delta}_{ei}$$

$$= b_i \dot{\delta}_{ci} + b_{ci} (\dot{\delta}_{ai} - \dot{\delta}_{ci}) \qquad \dot{\delta}_{ai} < \dot{\delta}_{ci}$$

and the rate of extension $\dot{\delta}_{ai}$ is found from:

$$\dot{\delta}_{ai} = z_{ij} + y_{si} \dot{\phi}_{ij} \qquad \text{(S4)}$$

The x and y components of forces transmitted to the hull are found from:

$$S_{xij} = W_{xij} + H_{xi} + H_{xj} - m_{ij} a_{xij} \qquad \text{(S5)}$$

$$S_{yij} = W_{yij} + H_{yi} + H_{yj} - m_{ij} a_{yij} \qquad \text{(S6)}$$

Drive System - The schematic diagram (Figure A-7) shows how the driver inputs interact with the mechanical system to produce the torque at the wheels.

In the simulation the power output of the engine is treated as a constant, independent of speed, for $n_w > n_w^*$. This is seen from Figure A-8 to be a reasonable approximation. As a result of this approximation, it is possible to develop a simple relationship for axle drive torque M_{eij} . Since horsepower hp is proportion to the product of drive torque and wheel angular

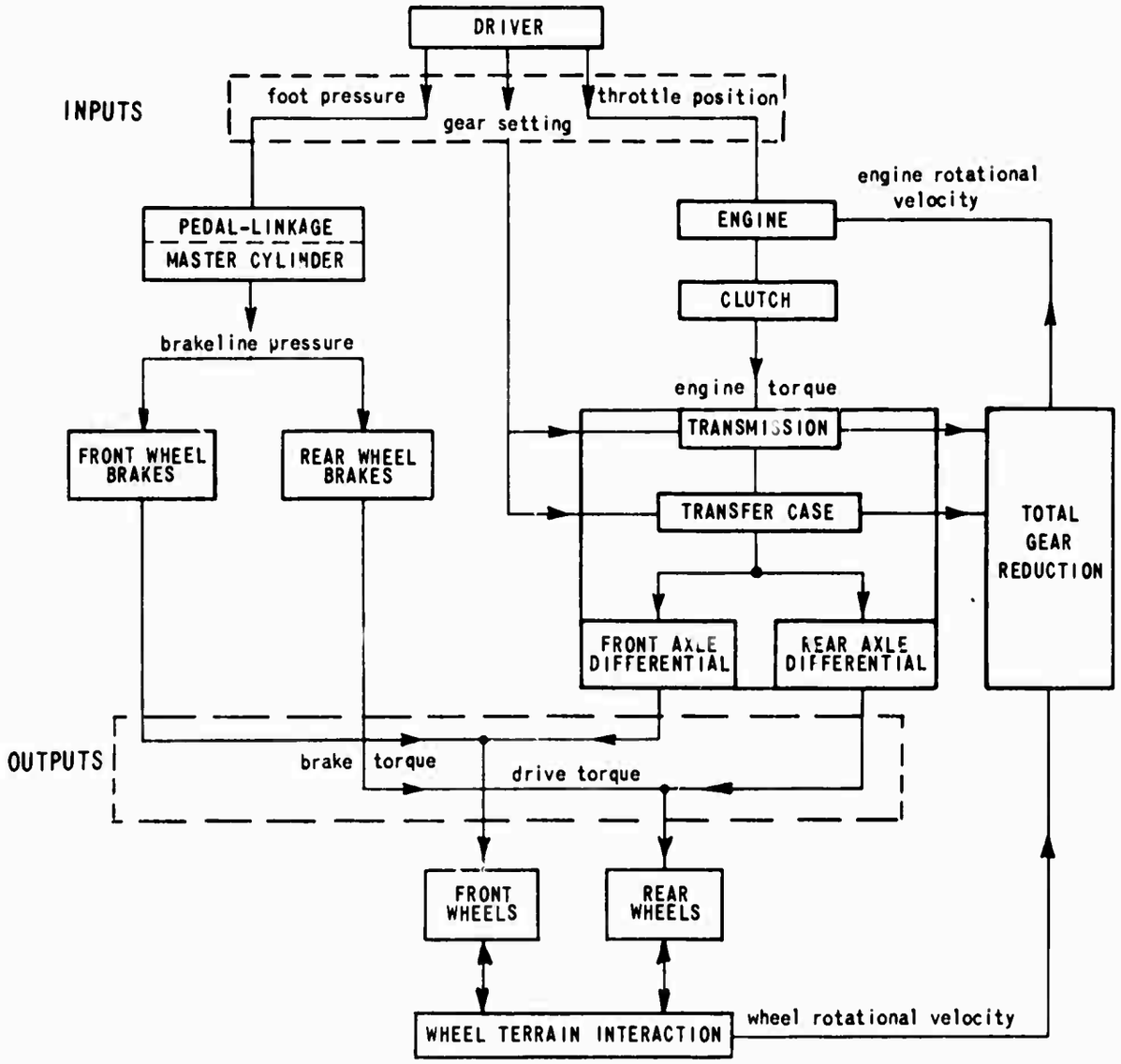

Figure A-7 BLOCK DIAGRAM OF DRIVE SYSTEM

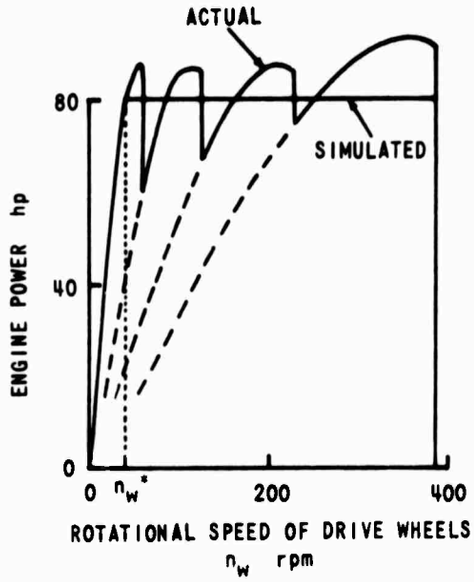

Figure A-8 ENGINE POWER vs. SPEED

velocity n_w (in RPM):

$$hp = \sim M_{eij} n_w \qquad \text{(D1)}$$

and since hp is assumed constant:

$$M_{eij} = \frac{k}{n_w} \qquad (n_w > n_w^*) \qquad \text{(D2)}$$

where the constant k accounts for the conversion of units as well as the division of drive torque between the two axles. At very low wheel speeds (less than n_w^*) it is assumed that maximum drive torque is applied:

$$M_{eij} = M_{eij\,MAX} \qquad (n_w < n_w^*) \qquad \text{(D3)}$$

These approximations are further borne out by Figure A-9, which shows a plot of the net torque delivered by the Kaiser-Jeep engine for all forward gears, with the transfer case set in low. The broken line envelope shows how the model approximates the drive torque at full throttle. The model is thus representative of an ideal driver who shifts gears in an optimum manner.

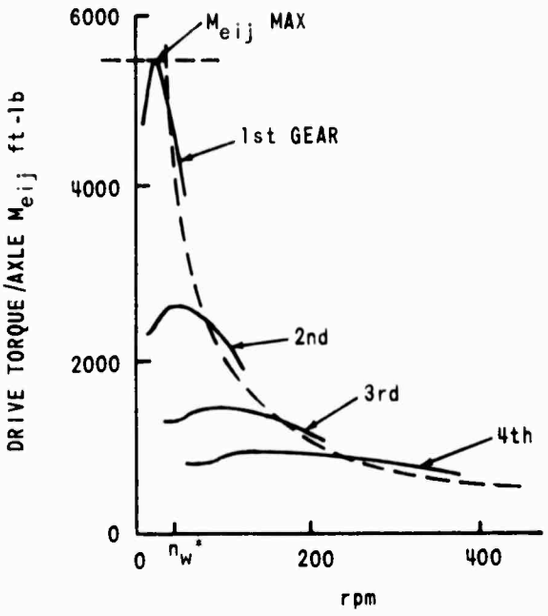

Figure A-9 ROTATIONAL SPEED OF DRIVE WHEELS

Drive torque at partial throttle is assumed to be proportional to throttle position, i.e., at a given rpm of the drive wheels, full throttle torque is multiplied by the fraction of full throttle opening to obtain partial throttle drive torque. The braking torque of the engine occurs only at zero throttle and it is represented as a fixed percentage of the full throttle driving torque at a given rpm. Since the transfer case has no differential, the rotational speed of the front and rear drive shafts are the same. For the present, the differentials in front and rear axle have been neglected, i.e., all wheels rotate at the same speed.

The torque equation is:

$$M_e = \sum_{i=1}^{4} \left(I_{\omega i} \dot{\omega} + T_i r_i - \rho N_i r_i \right) + n^2 I \dot{\omega} \qquad \text{(D4)}$$

where

M_e is the total transmitted engine torque,

ω is the rotational velocity of wheels and axle shafts,

ρ is the rolling resistance coefficient, and

r_i is the rolling radius of the i th wheel.

Engine and transmission inertias have not yet been incorporated into the actual mechanization.

Terrain Interface - The wheel-ground interactions are implemented in the present VDM using the wheel-terrain representation shown in Figure 8 of Section 3.2.1.2. This model has been adequate for treating the profiles of rigid, undulating terrain. The more complex model shown in Figure 9 of the same section will be introduced when required in future studies of traversing sharp, rigid obstacles. Thus, the present simulation of the wheel-ground interaction is based on the force components T_i, σ_i and N_i as illustrated in Figure A-2.

The force component N_i normal to the ground profile, under the i th wheel and in the plane of the wheel, is found from:

$$N_i = k_{\omega i} \delta_{\omega i} \qquad \delta_{\omega i} < 0$$

$$= 0 \qquad \delta_{\omega i} > 0 \qquad \text{[T1]}$$

where δ_{wi} is tire deflection and k_{wi} tire spring rate, and $\delta_{wi} > 0$ represents loss of ground contact. Tire deflection in turn is computed from the following geometric relation based on cg vertical coordinate Z and on local terrain elevation h_i at each wheel.

$$\delta_{wi} = \frac{1}{\cos \alpha_i}(h_i - Z + x_i \sin\theta - y_i \cos\theta \sin\phi - z_i \cos\theta \cos\phi) - r_o \qquad [T2]$$

where α_i is the ground slope under the ith wheel and in the plane of the wheel. Derivation of this expression is presented in Reference A1.

The traction force T_i is then computed as the product of the slip dependent coefficient of traction $\mu(s)$ with the normal force N_i:

$$T_i = -\mu N_i \qquad [T3]$$

The coefficient μ, also referred to as normalized tractive force, is approximated as shown in Figure A-10.

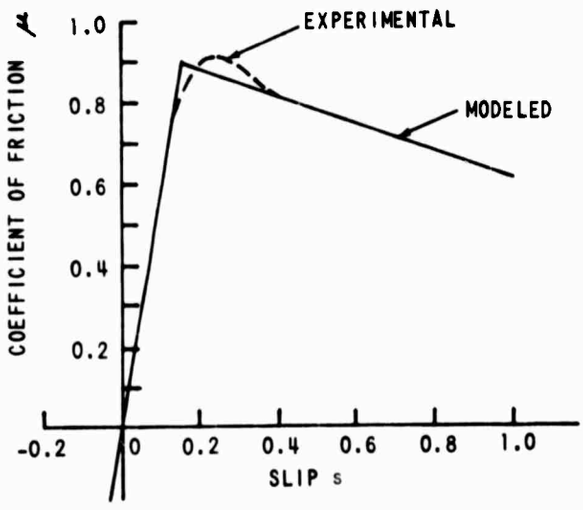

Figure A-10 COEFFICIENT OF FRICTION vs. SLIP

The slip is computed from

$$s = \frac{r_i \omega - \dot{X}_{Ti}}{r_i \omega} \tag{T4}$$

where $\dot{X}_{Ti}$ is the tangential component in earth-fixed axes of the velocity of the effective ground contact point.

The side force σ_i at the tire-ground interface is calculated from a simplified linear relationship between slip angle β_i and elastic force N_i.

$$\sigma_i = k_{yi} \beta_i N_i \tag{T5}$$

where k_{yi} is a coefficient of tire side force. Slip angle β_i is computed from

$$\beta_i = \arctan \frac{\dot{Y}_i}{\dot{X}_i} \tag{T6}$$

where $\dot{X}_i$ and $\dot{Y}_i$ are the velocity components of the effective ground contact point in the earth fixed system.

Finally, the components in the hull-fixed system H_{xi}, H_{yi}, H_{zi} of the forces transmitted to the wheel hub are found from:

$$H_{xi} = T_i \cos(\theta - \alpha_i) - N_i \sin(\theta - \alpha_i) \tag{T7}$$

$$H_{yi} = \sigma_i \tag{T8}$$

$$H_{zi} = N_i \cos(\theta - \alpha_i) + T_i \sin(\theta - \alpha_i) \tag{T9}$$

REFERENCES

A1. Schuring, D., and Belsdorf, M.R., "Analysis and Simulation of Dynamical Vehicle-Terrain Interaction", Cornell Aeronautical Laboratory, Inc., Technical Memorandum No. VJ-2330-G-56, March 1969.

Appendix B: TABULATED SUMMARIES OF VEHICLE TRAFFICABILITY DATA

Table B-1

SUMMARY OF FULL SCALE VEHICLE $\frac{\text{DRAWBAR PULL}}{\text{GROSS VEHICLE WEIGHT}}$ FIELD TESTS

EXERCISE	SOIL	PREDICTION THEORY USED	NO. OF VEHICLES	NO. OF TESTS	$\left(\frac{\bar{\Delta}}{M}\right)$	$\sigma_{\left(\frac{\Delta}{M}\right)}$	RANGE	$\left(\frac{\Delta}{M}\right)$	$\left[\left(\frac{\Delta}{M}\right)^2 + \sigma^2_{\left(\frac{\Delta}{M}\right)}\right]^{1/2}$
WHEEL TRACK I EXERCISE MISSISSIPPI	SAND 2.5%-MOISTURE	BEKKER/LLL - TESTS BY ATAC	24 W	24	-0.89	0.54	-1.84	-0.06	1.04
			3 T	3	-0.59	0.39	-1.07	-0.12	0.71
		BEKKER/LLL - TESTS BY TEA	20 W	20	-0.07	0.29	-0.98	+0.25	0.29
			3 T	3	+0.16	0.17	-0.18	+0.16	0.22
	PEAT 21.0 TO 308.0 % MOISTURE	BEKKER/LLL - TESTS BY ATAC	7 W	7	-0.28	0.40	-0.93	+0.05	0.49
			3 T	3	-0.56	0.19	-0.83	-0.41	0.59
		BEKKER/LLL - TESTS BY TEA	6 W	6	+0.02	0.24	-0.27	+0.34	0.24
			4 T	4	-0.08	0.28	-0.52	+0.23	0.29
SWAMP FOX II EXERCISE PANAMA	SILTY-CLAY 40 TO 50% MOISTURE	ST'D WES CONE INDEX METHOD	13 W	13	-0.12	0.40	-0.96	+0.39	0.42
			3 T	3	+0.09	0.17	-0.15	+0.21	0.19
			10 W	10	-0.85	0.95	-2.82	+0.21	1.27
			5 T	5	-0.46	0.79	-1.98	+0.21	0.91
	CLAY-LOAM 50 TO 60% MOISTURE	BEKKER/LLL - BEVAMETER	11 W	11	-1.54	1.25	-4.36	-0.06	1.98
			2 T	2	-1.65	0.99	-2.64	-0.66	1.93
		BEKKER/LLL - SHEARGRAPH	11 W	11	-0.01	0.12	-0.46	+0.24	0.12
			4 T	4	-0.01	0.10	-0.11	+0.12	0.10
WES ONE-PASS REVIEW BY WNRE, INC.	CLAY & SILTY CLAY	WES-NUTTALL ONE-PASS CONE INDEX ANALYSIS, 1966 NOTES: (1) $\frac{RCI_{(1\text{-SURFACE})}}{RCI_1} \simeq 1.00$	8W, 12 T	53 (1)	-0.06	0.44	-1.00	+1.00	0.45
				80 (2)	+0.05	0.66	-1.56	+1.00	0.66
		(2) " $\simeq 0.50$		40 (3)	-0.12	0.95	-2.39	+1.00	0.96
		(3) " $\simeq 0.25$							
MERS ONE-PASS EXERCISE BY ATAC FOR WES MISSISSIPPI	FAT CLAY	BEKKER/LLL - BEVAMETER	1 T	20	+0.06	0.32	-1.00	+0.56	0.33
			1 T	8	-0.22	0.47	-0.86	+0.35	0.52
			1 T	5	-0.72	0.10	+0.11	+0.14	0.73
			1 T	6	-1.04	0.14	+0.15	+0.17	1.05
	LEAN SILTY-CLAY		1 T	20	+0.22	0.12	-0.11	+0.45	0.25
			1 T	19	+0.12	0.15	-0.19	+0.38	0.19
			1 T	36	+0.25	0.12	0.00	+0.47	0.28
			1 W	21	-0.05	0.30	-0.63	+0.39	0.30
			1 W	13	-0.72	0.86	-2.80	+0.40	1.12
			1 W	21	-0.07	0.52	-1.00	+0.75	0.53
			1 W	31	-0.26	0.47	-1.19	+0.62	0.54
ATAC SNOW TESTS	DEEP MULTI-LAYERED SNOW	BEKKER/LLL - BEVAMETER	5 T	5	-0.09	0.17	-0.40	+0.08	0.19

T - TRACKED W - WHEELED

Table B-1 (CON'T)

NOTES RELATIVE TO $\frac{\text{DRAWBAR PULL}}{\text{GROSS VEHICLE WEIGHT}}$ FIELD TESTS

TEST PROCEDURES	SOIL MEASUREMENTS	DP PREDICTIONS
PROJECT WHEEL TRACK I (1962)		
DUPLICATE DP TESTS MADE (BY TEA AND ATAC) ON SAME LANES USING DIFFERENT DYNOMETER VEHICLES, INSTRUMENTATION AND MEASURING TECHNIQUES. SLIP WAS NOT MEASURED. TEA MEASURED DP WHEN VEHICLE ALMOST STOPPED (APPROXIMATELY 80% SLIP). ATAC MEASURED AVERAGE OF 30 SECOND TEST RUN AT UNSPECIFIED SPEEDS.	ONE SET OF COMPLETE BEKKER/LLL SOIL VALUES (INCLUDING PLATE SINKAGE) LISTED FOR THE TWO TEST SITES (BY BEVAMETER)	BASED ON 1962 BEKKER/LLL STATE-OF-THE-ART METHOD. NOT KNOWN IF SLIP AND/OR SINKAGE ACCOUNTED FOR.
SWAMP FOX II (1962)		
SLIP MEASURED AT ONE SITE, NOT AT SECOND SITE. MAXIMUM DP REPORTED AT 100% SLIP. NO DETAILS OF MEASURING TECHNIQUES AVAILABLE.	ONE SITE USING CONE PENATROMETER, SECOND SITE USING CONE PENATROMETER, SHEARGRAPH AND BEVAMETER. NO SINKAGE TESTS MADE.	ONE SITE BY WES VCI SYSTEM, SECOND BY WES VCI AND SIMPLE COULOMB EQUATION NEGLECTING SLIP FUNCTION AND BOTH SOIL RESISTANCE TERMS.
WES ONE-PASS REVIEW BY WHRE, INC. (1963-1964)		
SOME TESTS MADE WITH 0 TO 80% SLIP, SOME AT 20, 40, OR 100% SLIP. SLIP NOT ALWAYS MEASURED.	BY CONE PENATROMETER. NO SINKAGE TESTS MADE.	BASED ON NUTTALL'S MODIFIED ONE-PASS WES METHOD WHICH ACCOUNTS FOR SOIL RESISTANCE BUT NOT FOR SLIP.
WERS ONE-PASS EXERCISE (1964)		
SLIP WAS MEASURED FOR ALL TESTS.	BY BEVAMETER BUT NO PLATE SINKAGE TESTS MADE.	BASED ON COULOMB EQUATION MODIFIED BY SLIP FUNCTION. SOIL RESISTANCE WAS CONSIDERED NEGLIGIBLE EVEN THOUGH THERE WAS SINKAGE AT ONE TEST SITE.
ATAC SNOW TESTS (1966)		
SLIP WAS MEASURED FOR ALL TESTS.	ALL BEKKER/LLL SOIL VALUES (IN THIS CASE SNOW) INCLUDING PLATE SINKAGE MADE WITH BEVAMETER.	APPARENTLY FULL BEKKER/LLL TREATMENT USED INCLUDING EFFECTS OF SLIP AND SNOW RESISTANCE.

Table B-2

GROUP SUMMARIES OF FULL SCALE VEHICLE $\frac{\text{DRAWBAR PULL}}{\text{GROSS VEHICLE WEIGHT}}$ FIELD TESTS IN SOIL

CLASSIFICATION	TYPE VEHICLE	NO. OF TESTS	AVG $\left(\frac{\bar{\Delta}}{M}\right)$	AVG $\sigma_{\left(\frac{\Delta}{M}\right)}$	RANGE $\left(\frac{\Delta}{M}\right)$		$\left[\left(\frac{\bar{\Delta}}{M}\right)^2 + \sigma^2_{\left(\frac{\Delta}{M}\right)}\right]^{\frac{1}{2}}$
ALL TESTS	W&T	502	-0.16	0.56	-4.36	+1.00	0.52
TESTS IN SAND	W&T	50	-0.48	0.43	-1.84	+0.25	0.65
TESTS IN ALL SOILS EXCEPT SAND (CLAY, SILTY CLAY, FAT CLAY, CLAY-LOAM, PEAT)	W&T	452	-0.12	0.57	-4.36	+1.00	0.58
TESTS USING CONE INDEX THEORY	W&T	204	-0.08	0.68	-2.82	+0.10	0.68
TESTS USING BEKKER/LLL THEORY (BEVAMETER)	W&T	298	-0.21	0.45	-4.36	+0.62	0.50
WHEELED TESTS IN LEAN SILTY CLAY USING BEKKER/LLL THEORY (BEVAMETER)	W	86	-0.23	0.53	-1.19	+0.75	0.58
TRACKED TESTS IN LEAN SILTY CLAY USING BEKKER/LLL THEORY (BEVAMETER	T	75	+0.21	0.13	-1.00	+0.56	0.25
TRACKED TESTS IN FAT CLAY USING BEKKER/LLL THEORY (BEVAMETER)	T	39	-0.27	0.32	-1.00	+0.35	0.42
TESTS IN CLAY-LOAM USING WES CONE INDEX THEORY	W&T	15	-0.72	0.90	-2.82	+0.21	1.15
TESTS IN CLAY-LOAM USING BEVAMETER-BEKKER/LLL THEORY	W&T	13	-1.56	1.21	-4.36	-0.06	1.95
TESTS IN CLAY-LOAM USING SHEARGRAPH-BEKKER/LLL THEORY	W&T	15	-0.01	0.11	-0.46	+0.24	0.11

T - TRACKED W - WHEELED

Table B-3

SUMMARY OF FULL SCALE VEHICLE GRADEABILITY FIELD TESTS

EXERCISE	SOIL	PREDICTION THEORY USED	NO. OF VEHICLES	NO. OF TESTS	$\left(\frac{\bar{\Delta}}{M}\right)$	$\sigma_{\left(\frac{\Delta}{M}\right)}$	RANGE $\left(\frac{\Delta}{M}\right)$		$\left[\left(\frac{\bar{\Delta}}{M}\right)^2 + \sigma^2_{\left(\frac{\Delta}{M}\right)}\right]^{\frac{1}{2}}$
SWAMP FOX II EXERCISE PANAMA	CLAY-LOAM	STD WES CONE INDEX	11 W	11	-0.45	0.52	-1.87	-0.08	0.69
			12T	12	-0.38	0.29	-0.92	+0.31	0.48
		AVERAGE 23 TESTS			-0.42	0.42			0.60
		BEKKER/LLL SHEARGRAPH	11 W	7	-0.08	0.13	-0.21	+0.07	0.15
			13 T	13	+0.02	0.17	-0.29	+0.25	0.17
		AVERAGE 20 TESTS			-0.01	0.15			0.16

T - TRACKED W - WHEELED

Table B-4

SUMMARY OF FULL SCALE VEHICLE $\frac{\text{SOIL RESISTANCE TO MOTION}}{\text{GROSS VEHICLE WEIGHT}}$ FIELD TESTS

EXERCISE	SOIL	PREDICTION THEORY USED	NO. OF VEHICLES	NO. OF TESTS	$\left(\frac{\bar{\Delta}}{M}\right)$	$\sigma_{\left(\frac{\Delta}{M}\right)}$	RANGE $\left(\frac{\Delta}{M}\right)$		$\left[\left(\frac{\bar{\Delta}}{M}\right)^2 + \sigma_{\left(\frac{\Delta}{M}\right)}^2\right]^{\frac{1}{2}}$
WES ONE-PASS REVIEW BY WNRE, INC.	CLAY & SILTY CLAY	WES-NUTTALL ONE-PASS CONE INDEX ANALYSIS 1966	2 W	36	-0.63	1.25	-5.00	+0.46	1.40
			3 T	67	+0.73	0.52	-1.93	+1.00	0.90
		AVERAGE 103 TESTS			0.25	0.85			0.89

T - TRACKED W - WHEELED

Table B-5

SUMMARY OF FULL SCALE VEHICLE SPEED FIELD TESTS

EXERCISE	SOIL	PREDICTION THEORY USED	NO. OF VEHICLES	NO. OF TESTS	$\left(\frac{\bar{\Delta}}{M}\right)$	$\sigma_{\left(\frac{\Delta}{M}\right)}$	RANGE $\left(\frac{\Delta}{M}\right)$		$\left[\left(\frac{\Delta}{M}\right)^2 + \sigma_{\frac{\Delta}{M}}^2\right]^{\frac{1}{2}}$
WES ONE-PASS REVIEW BY WNRE, INC.	CLAY-LOAM	WES-NUTTALL ONE-PASS CONE INDEX ANALYSIS	2 W	6	-0.13	0.43	-0.57	+0.55	0.45
			2 T	10	-0.91	1.36	-4.00	+0.20	1.64
		AVERAGE 16 TESTS			-0.61	1.11			1.27
ATAC KEWEENAW MICH. TESTS	NOTE (1)	ATAC METHOD OF LISTON, SOIL VALUES BY BEVAMETER	5 T	5	+0.37	0.11	+0.24	+0.56	0.39
	NOTE (2)		5 T	5	+0.04	0.33	-0.41	+0.58	0.34
	NOTE (3)		5 T	5	0.00	0.16	-0.26	+0.17	0.16
	NOTE (4)		5 T	5	+0.27	0.11	+0.12	+0.45	0.29
		AVERAGE 20 TESTS			+0.17	0.25			0.31

T - TRACKED W - WHEELED

NOTES: (1) STRONG SOIL (NO SINKAGE), 10% SLOPE; SLOPE & ROLLING RESISTANCE
(2) STRONG SOIL (NO SINKAGE), 40% SLOPE; SLOPE & ROLLING RESISTANCE
(3) ORGANIC SOFT SOIL, 0% SLOPE; SOIL COMPACTION & ROLLING RESISTANCE
(4) SAND ROAD, 0 SLOPE, 0% SLOPE; ROLLING RESISTANCE

Table B-6

SUMMARY OF FULL SCALE VEHICLE $\frac{\text{DRAWBAR PULL}}{\text{GROSS VEHICLE WEIGHT}}$ SOIL BIN TESTS

EXERCISE	SOIL	PREDICTION THEORY USED	NO. OF VEHICLES	NO. OF TESTS	$\left(\frac{\bar{\Delta}}{M}\right)$	$\sigma_{\left(\frac{\Delta}{M}\right)}$	RANGE $\left(\frac{\Delta}{M}\right)$		$\left[\left(\frac{\bar{\Delta}}{M}\right)^2 + \sigma^2_{\left(\frac{\Delta}{M}\right)}\right]^{1/2}$
SOIL BIN	MICHIGAN	BEKKER/LLL	1 T	14	-0.10	0.07	-0.22	+0.08	0.12
TEST AT	FARM	BEVAMETER	1 W	16	+0.17	0.17	+0.07	+0.80	0.24
ATAC-LLL	SOIL		1 W	8	+0.10	0.39	-0.28	+1.00	0.40
	20% MOISTURE								
	DRY SAND		1 T	12	+0.03	0.06	-0.09	+0.11	0.07
			1 T	18	+0.01	0.30	-0.30	+0.07	0.30
		AVERAGE 68 TESTS			+0.039	0.22			0.23

T - TRACKED W - WHEELED

Appendix C: FULL SCALE TEST AND EVALUATION PRACTICE STUDY - DISCUSSIONS OF CONCLUSIONS AND RECOMMENDATIONS

Conclusions Drawn From A Literature Survey*

The literature pertaining to off-road mobility test and evaluation practice which has been surveyed has led to six specific conclusions. These are listed and discussed below.

1. Many recognized authorities are in agreement that current practice in the mobility testing and evaluation of off-road vehicles is unsatisfactory. Opinions vary as to what constitutes "unsatisfactory".

C. J. Nuttall, a recognized authority in off-road mobility, has much to say about the QMR process in his "Ground-Crawling: 1966", [C1] (pp. 133-141). He insists that specifications must be "testable" to be valid and satisfactory. He says, "to be testable, not only must the performance be called out in measurable, engineering terms, but the relevant terrain conditions must also be specified, again in measurable engineering terms. And most important, and difficult, the specifications must give the minimum performance requirements which will satisfactorily do the job where it must be done."

Efforts to "quantify the qualitative" have been going on for the past twenty-three years by such agencies as Waterways Experiment Station (WES), U.S. Army Test and Evaluation Command (TECOM), U.S. Army Tank-Automotive Center (TACOM), Institute for Defense Analyses (IDA), WNRE, Inc., commercial

---

*References C19-C42 were reviewed during the course of the survey but are not cited in the text.

automotive companies as well as universities, and the Society of Automotive Engineers (SAE). While progress has been made, we do not find that the Bekker Soil Value System is accepted as a basis for testing by all concerned. Neither has the Waterways Experiment Station approach been integrated into standard test practice nor been resolved with the Bekker approach. Even though Ordnance Proof Manual 60-85, dated 15 August 1957, provides for taking Bekker and WES soil measurements during vehicle tests on soil, this OPM is not referenced in specific test procedures where mobility tests are specified. Current conversion of OPM's to Test and Evaluation Command Procedures (TECP) should provide an opportunity to rectify this deficiency.

A. W. Jones, [C2] decries his findings in checking performance tests of the M113. He notes that most tests were conducted on hard surfaces and that where off-road tests were conducted, vague terms such as "dry snow, river bank, muskeg, or wet muskeg", were used to describe the environment. His report of observations of field tests in Thailand [C3] is also quite critical of the test methods and the manner in which they were performed.

R. A. Liston, of TACOM, concludes in a 1966 report [C4], the "data from a limited number of vehicle tests conducted in snow indicate that the drawbar-pull to weight ratio is a relatively insensitive measure of off-the-road vehicle performance." He also points out the failure by others in tests on soft soil to correlate DP/W with time required to complete a test course in a field exercise, though DP/W has long been a recognized vehicle evaluation parameter. See also Reference C5 where drawbar pull wasn't as important to overriding vegetation as were vehicle shape and dimensions.

Test facilities under TECOM at Aberdeen,[C6] Yuma [C7] and Ft. Greely are primarily designed to measure performance other than the ability to negotiate off-road terrain, at least in a quantitative sense. There are either discrete obstacles (all on firm terrain), a mud "hole", or "cross-country courses". There is no disagreement here with endurance, reliability, maintainability and service testing. The approach to testing the ability of

a vehicle to negotiate off-road terrain, however, is questioned. The ability of a vehicle to negotiate most fixed obstacles on firm terrain can be determined from geometrical and power parameters. The ability to negotiate the same obstacles -- or combinations of obstacles -- on other than firm terrain is the real problem, and is more representative of actual field conditions. Where this is attempted (as on cross-country courses), the environmental descriptors and vehicle performance parameters are usually given in qualitative rather than quantitative terms.

2. Specific programs that have been proposed at the conclusion of extensive projects have either not been acted upon (to our knowledge) or are slow in being implemented and reported upon.

In a Project MERS report, "Research Plan for Development of a Quantitative Cross-Country Mobility Prediction System", [C8] it is indicated that a comprehensive and well-planned effort was initiated, but never completed. Provision was made to deal with the major environmental obstacles encountered and to obtain quantitative data for the first time. Preliminary tests on firm ground were encouraging, but the project was terminated before all the obstacles and soft soil conditions could be investigated.

Nuttall's excellent review [C1] contains many suggestions and recommendations which--to our knowledge--have neither been acted upon, followed up, nor expanded upon.

Vicksburg Mobility Exercise A [C9, C10] represents another important project. This project is distinguished by the fact that the list of those involved in it is a "Who's Who" of off-road mobility. This is quite encouraging since it indicates a physical convergence of recognized authorities which can potentially lead to a resolution of divergent philosophies and opinions.

However, even in this latest project one wonders if the stated general purpose of the exercise will be terminated once the principal specific purpose is achieved. "The general purpose of the exercise was to consider quantitatively the various elements of the entire mobility problem and to suggest an approach to achieve a substantial degree of solution...the principal specific purpose was to design a number of vehicle test bed concepts that would be capable of operating in remote areas of the world where extremely soft-soil conditions predominate, and to develop a test program for these vehicles." The test program alluded to is in two parts. The first part is quite modest, aimed only at Go/No-Go, maneuver tests, speed tests, and drawbar-pull tests. Soil classification, strength, moisture, density, and profile will be "collected" and "measured", though control of these factors is not mentioned. The second part of the testing program which, it is stated, "if implemented, would be a major step toward developing ultimate means of assessing the apparent mobility of vehicles in more complex terrains", bears a remarkable resemblance to the tests proposed in Project MERS three years before and never carried out.

3. A communications gap exists between the theorists and/or experimenters and the volume testers and/or users.

This situation is not peculiar to off-road mobility, but is found--and probably always will be in varying degrees--in all lines of endeavor. In the off-road mobility area this gap appears to be a chicken and egg proposition. In the absence of a general unifying theory, the theorists are divided within their own ranks in regard to which theory to follow or how to resolve the differences in the theories extant. Field tests conducted thus far still result in large differences between predicted and observed results.* Furthermore, many more extensive projects that the theorists and experimenters have proposed have not been carried out to their final conclusion. Consequently, they feel helpless to advise the volume testers and users how they should proceed to improve their testing [C1, C2, C4, C5, C8].

*This topic has been treated in some detail in the section 3.2.2.

The volume testers and/or users, on the other hand, are continually presented with vehicles that must be tested and used. Since they receive what they consider little credible guidance from the theorists, they have no alternative but to design and conduct their own tests in a manner which is "practical" and which will handle the volume of vehicles to be tested expeditiously, but fails to generate data of the type and precision which might be of help to the theorists [C6,C7].

4. Testing by the "experimenters" suffers from diversification of effort, "special case" testing, and too little concrete data upon which to confirm results.

Diversification of effort can take several forms. One is the human desire to prove that the theory one espouses is correct and to direct work only in this direction. Consequently, there are as many potential directions of effort as there are theories. Another form results from directives from higher authority. The military situation is dynamic and under pressure. The visit of a very important person to a test site can result in a sudden diversion of priority that can delay, if not reorient, the direction of a formerly controlled course of action. Yet another form is the desire to evaluate a new component or field expedient which doesn't advance the state-of-the-art, but may provide something "a little better".

Since the experimenter must keep within the funding allowed for his project, he must frequently run fewer tests than are statistically required to validate his hypotheses. In this area in particular, "error variances" are known to be high, and significant differences can be detected under these conditions only by increasing the number of tests. Hence, many reports are terminated by "indications" rather than firm conclusions. Also, field data are frequently useless because there are either gaps in the data or the environmental conditions under which the tests were conducted were not measured. Even where experimenters are present during field mobility exercises, they are frequently not given enough time to make the measurements they require for a complete picture [C3, C11, C12, C13].

5. Testing by "volume testers" suffers from poor definition of the environmental profile for which the vehicle is intended.

Part of this situation is due to the lack of "testable specifications" which have been discussed under the first conclusion. Except for "fixed obstacles" as at Aberdeen, environmental descriptors and vehicular performance are generally expressed in qualitative rather than quantitative terms. We quote, for example, from Reference C11: "This study is based on the results of three years of field tests in Thailand. No attempt has been made to equate the results with theoretical mobility formulas." This report covers 13 vehicles, took three years to perform, was conducted in the field, yet contributed little to the state-of-the-art knowledge in the sense of resolving theory with practice.

Another aspect of this problem is typified in Reference C14. The purpose of this program was to conduct a series of tests in paddy fields and on roads. The results are couched in terms of the types of obstacles which were surmounted, either not at all, or with "most", "increasing" and "least" difficulty. Quantitative data reported were ambient temperature, relative humidity, barometric pressure, time of day, times to traverse three of the six courses, and average speed. Cone index data were also given, and three replications of the courses were made. This report is characterized by some irrelevant data and some good data and test practice. However, judgements by which the final conclusions and recommendations were arrived at were qualitative rather than quantitative. Other test programs on specific vehicles or groups of vehicles in specialized environments have shown various degrees of achievement, in terms of useful results [C3, C11, C12, C13, C15].

Recommendations for Improvement of Test Practices

Studies of methods by which test practices might be improved have resulted in six recommendations which are discussed below.

1. Standardize Current Test Methods and Practices

The only comprehensive body of published test procedures that was found in the literature search was Ordnance Proof Manual, Vol. II, Automotive Testing [C16]. Since the U.S. Army Test and Evaluation Command assumed the function upon its organization in 1962, it has been republishing these "OPM's" under the new name of TECP 700-700 series. Under this terminology they are called "U.S. Army Test and Evaluation Command Materiel Test Procedures". It is our understanding that MTP's are being prepared at 14 different TECOM facilities. They are then forwarded for review and editing to the Test Analysis and Operations Office at TECOM Headquarters.

It is recommended that during this revision process those tests relevant to mobility be sub-grouped under a "Mobility" heading to emphasize this aspect of testing as opposed to engineering and endurance tests, even though both may be conducted simultaneously.

It is also recommended that other agencies conducting "mobility" tests be directed to do so in accordance with the appropriate TECP or that any new test requirement follow the TECP format and be coordinated with TECOM. In this manner TECOM would be the central repository for all vehicle test methods, would be aware of all new developments, and could maximize control of standard tests.

Finally, test requirements in Army Regulations and in vehicle MIL-C and MIL-T specifications should reference TECP methods or be consistent with them.

A word about SAE J939, "Recommended Practice on Off-Road Vehicle Mobility Evaluation" [C17] is in order here. The chief value of SAE J939 is that it officially presents to civilian industry under the sponsorship of a civilian engineering society a limited number of individual test procedures that have been standard procedures in the military for a long time. Practically all seven vehicle performance tests and all seven soil tests in SAE J939 can be found in OPM's dating back as much as ten years. It is stated that, "the tests and test procedures described attempt to indicate the major elements comprising an evaluation of off-road performance". The careful wording certainly leaves room for the inclusion of further "major elements" such as standard obstacles, center of gravity determination, braking, steering, gradeability and side slope performance, fording, etc. which have also been in OPM's for a long time.

2. Specify Environmental Profile for Vehicles

QMR's should specify in as much quantitative detail as possible the environmental parameters and their limits which the vehicle is to be designed to meet as well as the level of performance expected, since these will be the basis for future test methods. Perhaps a "check list" of environmental descriptors should be furnished those who prepare QMR's to help them in selecting appropriate descriptors, to insure that applicable ones are not inadvertently left out, and to standardize the method and terminology of presenting them in QMR's.

3. Generate Reliable Environmental Data During Testing

The results of a vehicle test are the vehicle responses that result from the interaction between vehicle characteristics and environmental parameters, as modified by driver influence. Generally speaking, many of the vehicle characteristics are known prior to a test. Driver influence, if not well known in a specific case, is potentially controllable through selection and rotation of drivers. Environmental parameters, however, are generally the least known and the paucity of reliable environmental data in conjunction with vehicle testing is the chief despair of the "experimenters" and a major roadblock to progress in the field of off-road mobility. Much

money is invested in testing, and the small additional cost entailed in obtaining sufficient reliable data would more than justify the entire test since it can be used in many more ways long after the specific test has been completed.

Reliability of data involves several facets. Required instruments must be available, calibrated, and in good condition. Personnel must be instructed in their correct use. The location, time, and number of observations must be specified and provided for in the test procedure. The number of observations required of a given characteristic is related to the error variance of the repeated readings, the difference in the value one wants to be sure of detecting, and the confidence level with which one wants to detect it. Statistical assistance should be sought in planning for data reliability.

4. Reduce the subjectiveness of Mobility Reporting

Following is a quote from a typical off-road mobility report: "The vehicle operates well off roads, except in heavy, sticky mud. The latter condition hinders mobility due to mud buildup in and above the tracks. Otherwise, its agility, maneuverability, and ease of steering and braking are very good. The ride is bouncy, which is due to the small size of the vehicle. Size again causes it to be stopped by large holes which larger tracked vehicles can traverse. Sixty percent longitudinal and 40% side dry dirt slopes were negotiated without difficulty. Maneuverability in close woods is very good." [C18]

Such a report may be informative from a driver's viewpoint, but yields little quantitative information either in regard to the particular path taken at the time, or to other areas which may contain "holes, woods, or dirt slopes" that are not dry. Even without soil property measuring instruments, one could improve such a report by giving approximate dimensions of holes that could and could not be traversed; tree diameters and spacing estimates;

how long it took to traverse, say, 100 ft. of these woods; at what speed the slopes were negotiated, etc. The point is, that even where idealized measurements cannot be taken, reports can be presented in quantitative terms which are more meaningful and useful.

5. Plan Field Mobility Exercises to Provide Meaningful Measurements

Many exercises studied in the literature indicate that once a test program is underway, few environmental measurements are obtained. In Swamp-Fox I [C12], for example, only 2-1/2 miles per day were covered, yet it was stated that there was insufficient time to take cone penetrometer readings. Firm but slippery slopes were encountered which slowed down the vehicles, yet no readings were taken of the soil and moisture conditions on these slopes. The recommendation here is that test plans allow sufficient time for test personnel to make significant environmental measurements. Such data will aid materially in bringing theory and practice closer together.

6. Establish Stream Crossing Test Facilities

This recommendation may be premature in light of the state-of-the-art of knowledge on the subject. However, stream crossing and exiting appear to be a major problem in the field and we find no evidence that suitable standard test facilities exist for vehicle evaluation, especially in regard to the problem of exiting onto stream banks. It is, therefore, recommended that work be initiated to develop such a test facility. Perhaps an initial effort on a modest scale would consist merely of determining Go/No-Go or of timing exits from streams onto natural ramps of various percent slopes and a few soil types.

REFERENCES

C1. Nuttall, C.J., Jr., "Ground Crawling: 1966, State-of-the-Art of Designing Off-Road Vehicles," U.S. Army Waters Experiment Station, C.E., Contract Report No. 3-162, May 1967.

C2. Jones, A.W., "The Problems of Off-Road Mobility," Institute for Defense Analysis, Research Paper P-189, July 1965.

C3. Jones, A.W., "Tests and Measures for Ground Mobility," Institute for Defense Analysis, August, 1965.

C4. Liston, R.A. and Hanamoto, B., "The Drawbar Pull-Weight Ratio as a Measure of Vehicle Performance," U.S. Army Tank-Automotive Command Technical Report No. 9349 (LL107), August 1966.

C5. Anonymous, "Environmental Factors Affecting Ground Mobility in Thailand; Soil Trafficability," Technical Report No. 5-625, Appendix C, U.S. Army Engineer Waterways Experiment Station, CE, May 1963.

C6. Anonymous, "Automotive Field Test Facilities, Development and Proof Services," Aberdeen Proving Ground, OPM 60-140, May 1966.

C7. Anonymous, "Test Capabilities-Yuma Proving Grounds," Yuma Proving Ground, September 1967.

C8. Anonymous, "Research Plan for Development of a Quantitative Cross-Country Mobility Prediction System (Project MERS)," U.S. Army Engineer Waterways Experiment Station, CE, April 1965.

C9. Anonymous, "Vicksburg Mobility Exercise A; Vehicle Analysis for Remote-Area Operation", Miscellaneous Paper No. 4-702, U.S. Army Engineer Waterways Experiment Station, CE, February 1965.

C10. Anonymous, "Vicksburg Mobility Exercise A; Report of Second Meeting; Design of Field Test Program," U.S. Army Engineer Waterways Experiment Station, CE, February 1967.

C11. Borris, R.V., "Vehicle Characteristics Affecting Mobility in Thailand," Report No. 66-023, Military R&D Center, Bangkok, Thailand, May 1966.

C12. Schreiner, B.G., and Rula, A.A., "Operation Swamp Fox I; Terrain and Soil Trafficability Observations," Technical Report No. 3-609, U.S. Army Engineer Waterways Experiment Station, CE, August 1962.

C13. Anonymous, "Report of Environmental Operation - Vehicle Evaluations in Subarctic Environment (Alaska 1961-62)," U.S. Army Transportation Board Report TCB-61-073-EO, December 1962.

C14. Hall, A.T., "Comparative Tests of the XM-571, Spryte, M-116 and M-37 in Thailand," Military R&D Center, Bangkok, Thailand, Report No. 66-009, February 1966.

C15. Devereaux, R.H., "Integrated Engineering Service Test of Truck, Cargo, 1-1/4 Ton, 6x6, XM561, Under Arctic Winter Conditions," U.S. Army Test Evaluation Command, Project No. 1-3-4140-60, April 1966.

C16. Anonymous, "Ordnance Proof Manual - Volume II - Automotive Testing," Army Test and Evaluation Command, Interim Pamphlet No. 60-05, January 1967.

C17. Anonymous, "Off-Road Vehicle Mobility Evaluation," SAE Recommended Practice Handbook Supplement, SAE J939, March 1967.

C18. Anonymous, "Service Test of Armored Personnel Carrier T114 (C&R Version)," First Partial Report of Project No. 2112, U.S. Army Armor & Engineering Board, Report ATBBJ P-2112, May 1961.

C19. Anonymous, "Water-Crossing Requirements for Future Combat and Tactical Vehicles," Department of the Army, Combat and Tactical Vehicles, AR 705-2300-S, 11 August 1960.

C20. Holdridge, L.R., "A Critical Evaluation of Environmental/Mobility Prediction Methods and Recommendations for the Future," Swamp Fox II, Final Report, Vol. II, Environmental Research, U.S. Army Materiel Command.

C21. U.S. Army Materiel Command

MIL-C-45317C	21 May 1962	Carrier, Light Weapons, Infantry: 1/2 ton, 4x4, 17274
MIL-C-45355B(MO)	19 July 1963	Carrier, Personnel, Full-Tracked: M113
MIL-C-45364B(MO)	10 Feb 1965	Carrier, Cargo, Amphibious: M116
MIL-C-46724B(MO)	13 Aug 1963	Carrier, Command Post: Light Tracked, M577
MIL-C-46753(MO)	18 Mar 1963	Carrier, Command & Reconnaissance: Armored, M114A1
MIL-C-62013(MO)	3 Dec 1964	Carrier, Cargo, Full-Tracked: XM 548E1
MIL-T-45079(ORD)	28 May 1958	Tank Recovery Vehicle, Medium, 74
MIL-T-45308A(ORD)	27 Dec 1960	Tank, Main Battle, 105mm Gun, M60

MIL-T-52509(MO)	11 Apr 1966	Tractor, Full-Tracked, Low Speed
MIL-M-45396A(MO)	16 Dec 1963	Mortar, 107mm, Self-Propelled: XM106
MIL-V-62008(MO)	8 Sept 1964	Vehicle, Combat Engr., Full-Tracked: 165mm Gun, T118E1
MS-500023	10 Dec 1965	Carrier, Command Post, Lt. Tracked, M577A1
MS-500033	24 Jan 1966	Carrier, Personnel, Full-Tracked, Armored M113
MS51985	7 May 1964	Howitzer, Lt., Self-Propelled 105mm, M52A1
MS-53080	26 Aug 1964	Tank, Combat, Full-Tracked, Flame-Thrower, M67A1

C22. Logistical Vehicle Off-Road Mobility; Project TCCD 62-5, Final Report, U.S. Army Transportation Combat Development Agency, February 1963.

C23. Rettig, G.P. and Bekker, M.G., Obstacle Performance of Wheeled Vehicles; Report 29; U.S. Army Tank-Automotive Command, March 1958.

C24. Rymiszewski, A. J. and Theis, W.A., "Evaluation of Past and Present Vehicles Capable of Performing in Adverse Terrain," Appendix A., U.S. Army Tank-Automotive Command, 15 November 1965.

C25. Service Test of Universal Engineer Tractor-Crawler, Maj. J.J. Lendvay, U.S. Army Test and Evaluation Command, U.S. Army Armor & Engineering Board RD&E Task No. 1M643324D59615, February 1966.

C26. Final Report of Service Test of Carrier, Utility, Articulated XM571, Project 1-3-550-31-D, U.S. Army Test and Evaluation Command, U.S. Army Armor & Engineering Board, February 1965.

C27. Robinson, R.M. and Pascua, R.M.,"Engineer/Service Test (Desert All Seasons) of Truck, Cargo, 2-1/2 Ton, 8x8, XM410E1," U.S. Army Test and Evaluation Command, U.S. Army Armor & Engineering Board, Project 1-4-4210-70, Yuma Proving Grounds, YPG Report 6001, January 1966.

C28. Murphy, N.R., Jr., "Performance of Soils Under Tire Loads; Effects of Test Techniques on Wheel Performance," Technical Report No. 3-666, Report No. 6, U.S. Army Engineer Waterways Experiment Station, CE, October 1967. (Also: Murphy, N.R., Jr., and Green, A.J., "Effects of Test Techniques on Wheel Performance," Journal of Terramechanics, Vol. 6, No. 1,1969).

C29. Rush, E.S., and Temple, R.G., "Trafficability Tests in Fine-Grained Soils with Two Vehicles with 9- to 10-Ton Wheel Loads," Miscellaneous Paper No. 4-879, U.S. Army Engineer Waterways Experiment Station, CE, March 1967. (Also published in Journal of Terramechanics, Vol. 4, No. 1 No. 1, 1967, pp 31-48.

C30. Liston, R.A., Czako, T., Haley, P., Harrison, W.L., Hanamoto, B. and Martin, L., "Mobility Environmental Research Study; Mobility Testing Procedures," Contract Report No. 3-153, U.S. Army Engineer Waterways Experiment Station, CE, February 1966.

C31. Cheaney, E.S., Riley, G.R., Goldgraben, J.R. and Swan, J.C., "Preparation of Testing Procedure Standards With Which to Rate Vehicle Performance," Batelle Memorial Institute, April 1962.

C32. Bourassa, P., Leher, E.G., Dickson, W.J., "The Influence of the Shear Strength of Muskeg Terrains on the Trafficability of a Few Selected Vehicles," Canadian Armament R&D Establishment, Technical Report 434/65, June 1965.

C33. Perloff, W., "Mobility of Tracked Vehicles on Soft Soils," Proceedings of the 2nd International Conference of the International Society for Terrain-Vehicle Systems, August 1966.

C34 Berlage, A. and Buchole, W., "Mechanics of Tractor Operation on Tilled Soils," Proceedings of the 2nd International Conference of the International Society for Terrain-Vehicle Systems, August 1966.

C35. Masuda, S. and Tanaka, T., "Traction of the Tractor Based on Soil Parameters," Proceedings of the 2nd International Conference of the International Society for Terrain-Vehicle Systems, August 1966.

C36. Okamura, A., "Application of Rubber Crawler 'Ohtsu Mighty Pillar' for Engined Tillers," Proceedings of the 2nd International Conference of the International Society for Terrain-Vehicle Systems, August 1966.

C37. Janosi, Z.J., "Obstacle Performance of Tracklayer Vehicles," Proceedings of the 2nd International Conference of the International Society for Terrain-Vehicle Systems, August 1966.

C38. Society of Automotive Engineers

SAE J857	Roll-over tests with collision
SAE J850	Barrier collision tests
SAE J688	Truck ability prediction procedure
SAE J695	Turning ability and off-tracking
SAE J708A	Agricultural tractor test code
SAE J872	Reserve tractive ability
SAE J873	Vehicle drag
SAE J950	Gradeability
SAE J897	Vehicle slope operation
SAE J893	Vehicle fuel consumption

C39. Clark, J.M. Jr., Simon H.P., and Roma, C., "Correlation of Prototype and Scale Model Vehicle Performance in Clay Soils," SAE Automotive Engineering Congress, Paper No. 782J, January 13-17, 1964.

C40. Szten, E.M., Billion, W.E., Inglis, E., Miller, K., Simmons, K.R., Tarkin, R.A., "Analysis of Cross-Country Surface Vehicles for South Vietnam," Research Analysis Corp., Report T-474, March 1966.

C41. Nye, A.R., "Scaled Vehicle Mobility Evaluation by Field Type Methods," Southwest Research Institute, April 1966.

C42. Persson, S.P.E. and Chang, B.S., "Viscous Properties of a Slippery Soil Surface," Paper No. 66-145, ASAE Summer Meeting, Amherst, Mass., June 26-29, 1966.

BLANK PAGE

Appendix D: WATER BALANCE IN S.E. ASIA

Contained in Cornell Aeronautical Laboratory's second semi-annual technical report on off-road mobility research is a map which delineates the world-wide regions which exhibit relatively distinct seasonal soil moisture levels which influence the movement of off-road vehicles.[D1] A similar map of wet season soil strength ranges has been prepared by Waterways Experiment Station.[D2] These maps are of use in strategic planning. They delineate regions within which vehicles with soft soil capabilities are needed for some season(s) of the year. When we desire to ascertain more specifically those months of the year in which soft soil conditions have a high probability, more detailed analysis is needed.

Presented here is a method by which monthly rainfall in excess of potential evapotranspiration can be estimated from climatic records for individual months of the year. The method is demonstrated for Southeast Asia, although data is available for application to many countries of the world. It can be assumed that where there is an appreciable excess of precipitation over evapotranspiration, the soils in flat and moderately sloping topographic positions will present soft soil problems.

Thornthwaite Method

In 1958 a report was published jointly by the Laboratory of Climatology and the Air Force's Geophysics Research Directorate [D3] which described and demonstrated a method for converting temperature and precipitation data into "tractionability" information.

The senior author, C.W. Thornthwaite, had previously done considerable research in the problem of climatic water balance. He developed a simple

empirical method for estimating the amount of moisture in soil. Independent variables used are temperature, precipitation, latitude, time of year, and water-holding capacity of the soil. The method had wide application in many parts of the world.

A book of instructions for applying the method, together with tables, has been published which makes it possible for anyone to apply the Thornthwaite method [D4]. Either monthly or daily data can be used. Recently the National Science Foundation financed a month-by-month tabulation of water balance for the entire world [D5]. Virtually all available and suitable weather records were used. These tables could provide a valuable input to the study of off-road mobility.

Data on water-holding capacity of soils is even less available than climatic data. When the Thornthwaite method is used in a small area such as an irrigation district, the water-holding capacities of the different soils can be measured. Such capacities vary considerably. The set of tables used for applying the method makes provision for capacities ranging from 25 to 400 mm field capacity for the first four feet of soil. In applying the method to large areas, a field capacity is chosen for the whole area. In the case of Asia, it is assumed that the field capacity of the soil is 300 mm. No assumptions are made in this discussion with regard to soil water-holding capacity. The soft-soil problem is as much one of climate as of soil and topographic position.

When there is a surplus of water during any particular month, the soil is wetted from the top down. When there is deficit, the top layers become dry first except under a forest cover where drying out occurs more nearly evenly in the entire root zone.

Application of Thornthwaite Method to S.E. Asia

To demonstrate the applicability of the Thornthwaite method to monthly assessment of soft-soil conditions, a study was made of data from Southeast Asia. The area included in the study extends from the equator to 25° north latitude and from 93° to 111° east longitude. Use is made of a base map from a previous study of Southeast Asian Climatology [D6]. Countries treated are all of Singapore, Malaya, Thailand, Cambodia, Laos, North Vietnam, South Vietnam, and part of Burma.

The maps shown in Figure D-1 are made from tabulated water-balance data of 106 weather stations. Monthly precipitation-evapotranspiration data were recorded on a transparent base superimposed on a map showing station locations. This transparent overlay was then superimposed on a map showing elevations, and isolines were drawn with reference to both the plotted data and the elevations. This resulted in more accurate maps than if strict linear interpolation had been assumed between stations, but little can be known for certain about the climate of places not close to and about the same elevation as a weather station. The difficulties of assessing the affects of elevation on evapotranspiration are quite complex. Temperatures decrease in a predictable manner with altitude and therefore potential evapotranspiration does also. Air mass characteristics and wind direction act to complicate the distribution of rainfall. Windward slopes are rainier than leeward. Upper parts of leeward slopes may be nearly as wet as windward ones if the onset of precipitation produces an unstable condition in the air mass which leads to convection. Usually, though, in Southeast Asia rainfall increases with elevation up to near the crests of relatively low mountains and then tapers off quite rapidly on the lee side. The northeast monsoon which blows on the east-facing coasts of Vietnam in winter is wet and unstable in its lower layers only, and, after producing rain along the coast, loses almost all of its remaining moisture on the first seaward-facing slope. It is believed that the maps of evapotranspiration are reasonably accurate, in view of the small amount of data available. Large areas of highland with no weather stations are probably wetter than indicated. Although such land could be

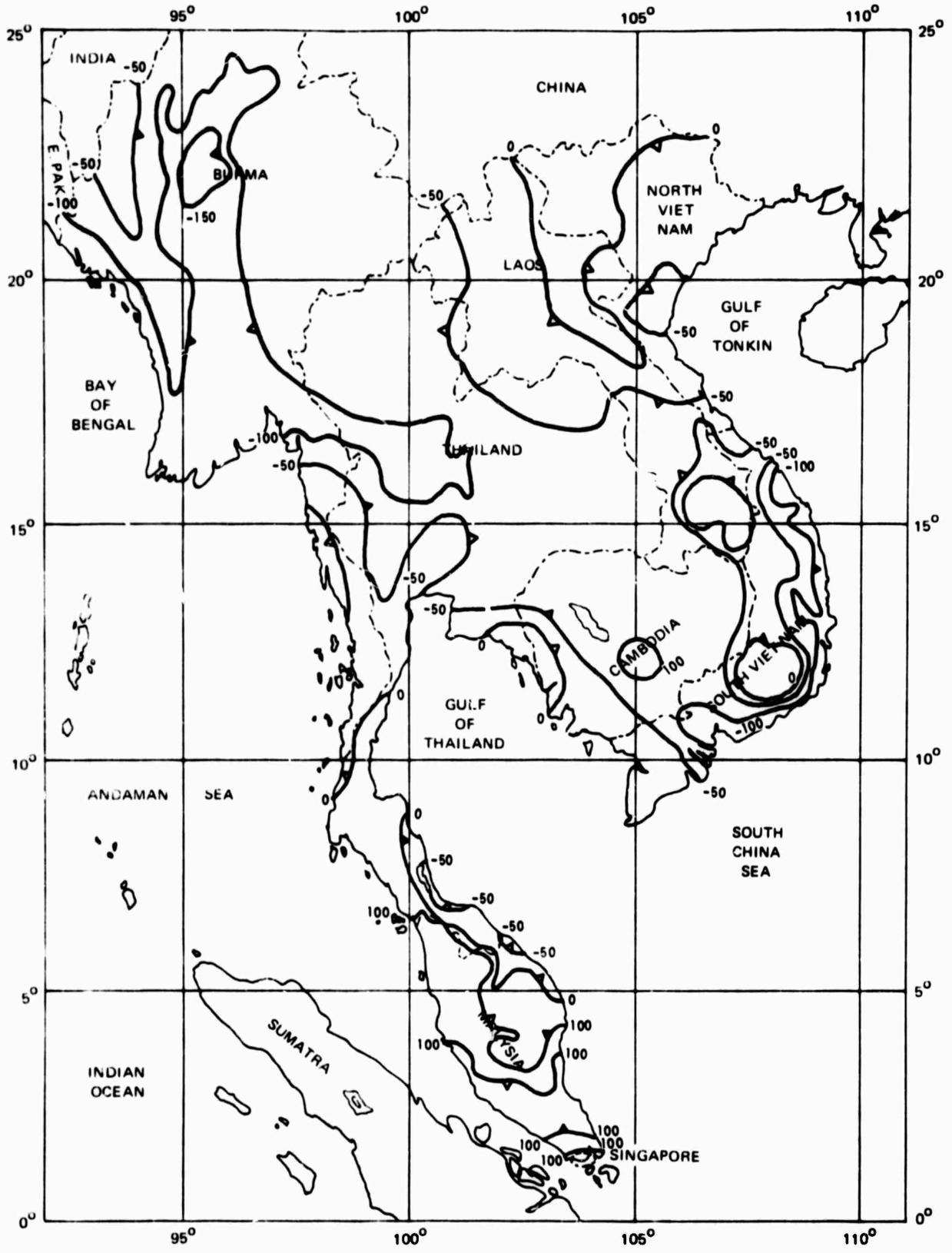

Figure D-1(a) PRECIPITATION MINUS POTENTIAL EVAPOTRANSPIRATION IN MILLIMETERS - APRIL

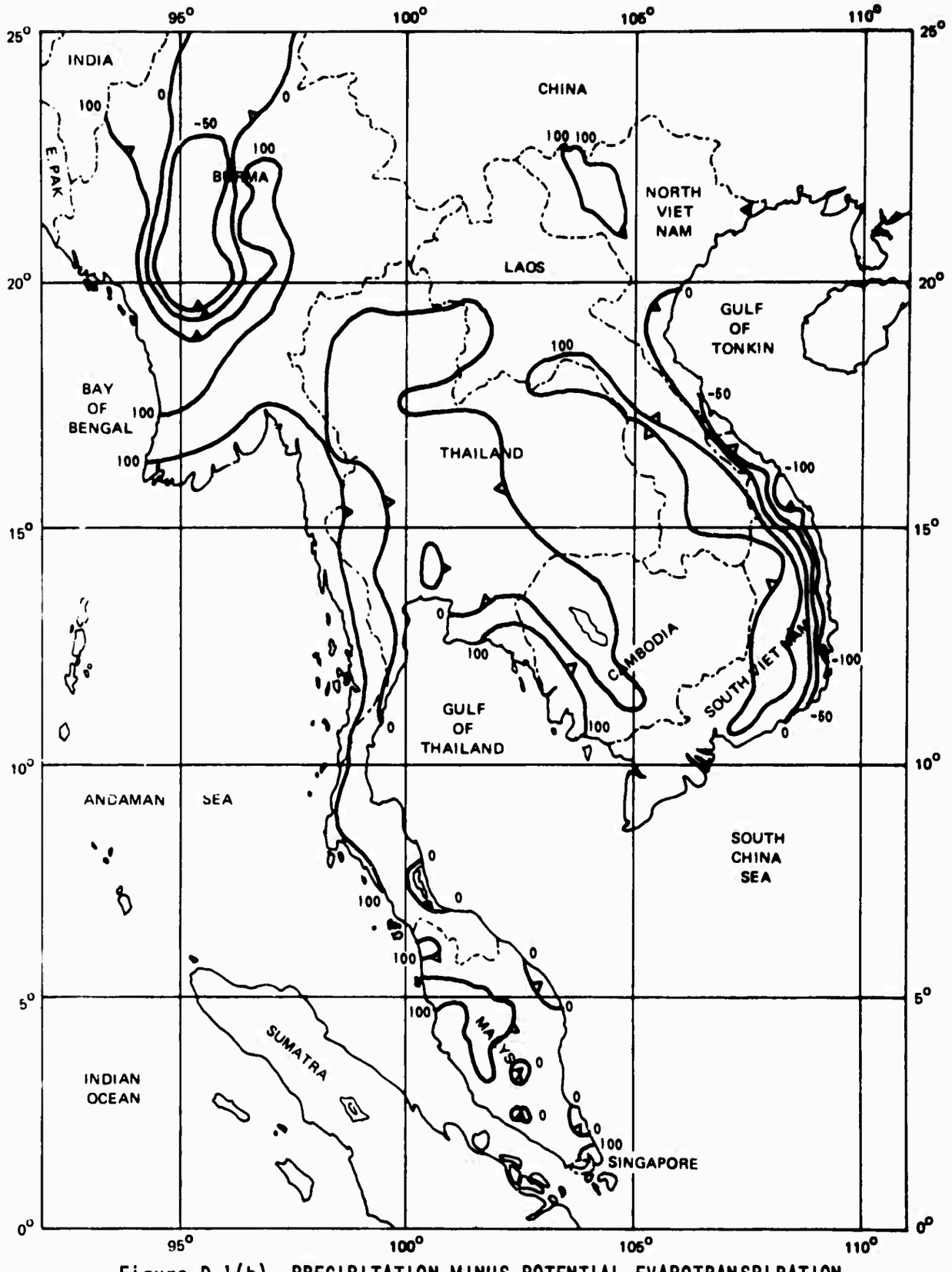

Figure D-1(b) PRECIPITATION MINUS POTENTIAL EVAPOTRANSPIRATION IN MILLIMETERS - MAY

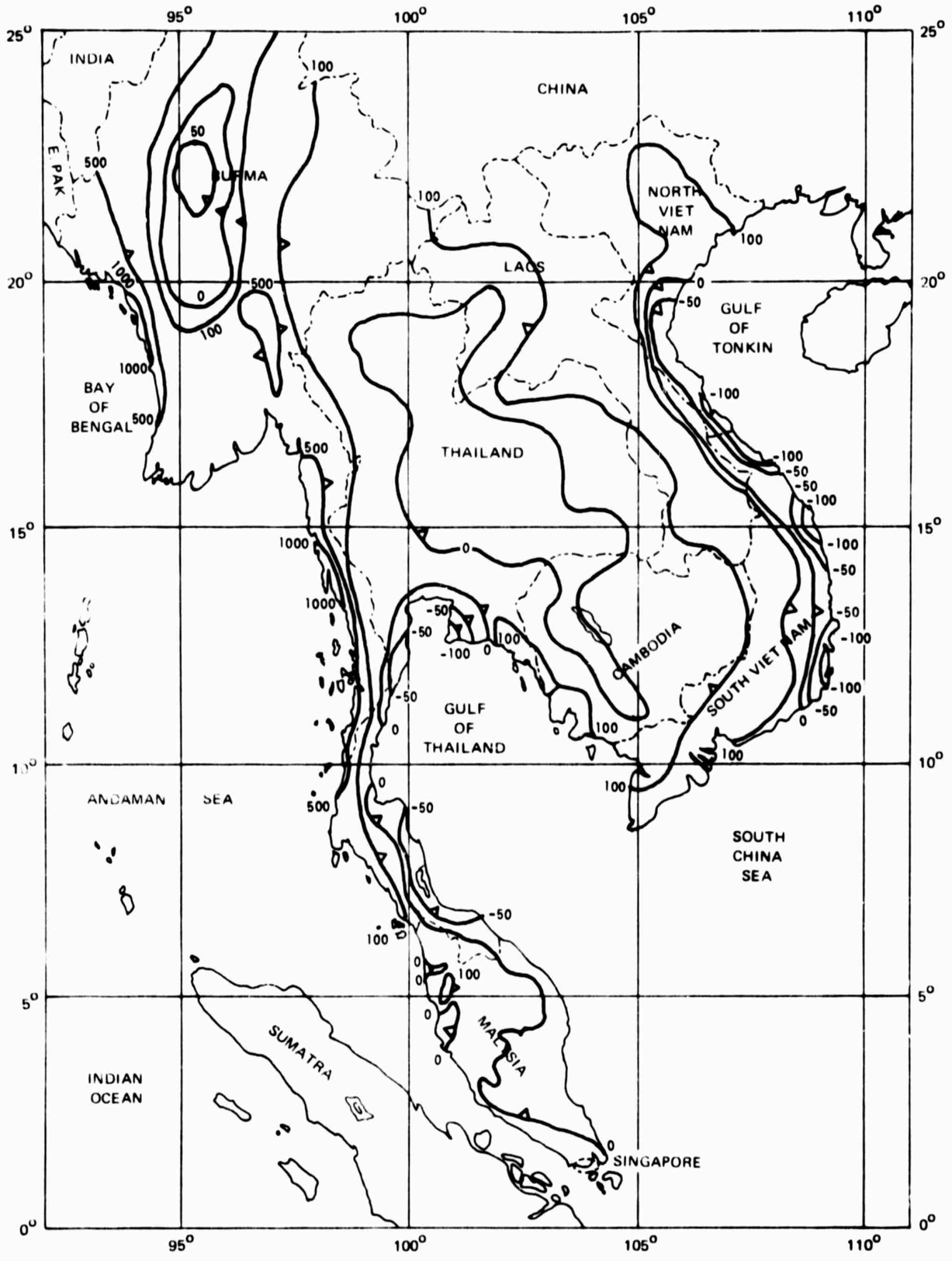

Figure D-1(c) PRECIPITATION MINUS POTENTIAL EVAPOTRANSPIRATION IN MILLIMETERS - JUNE

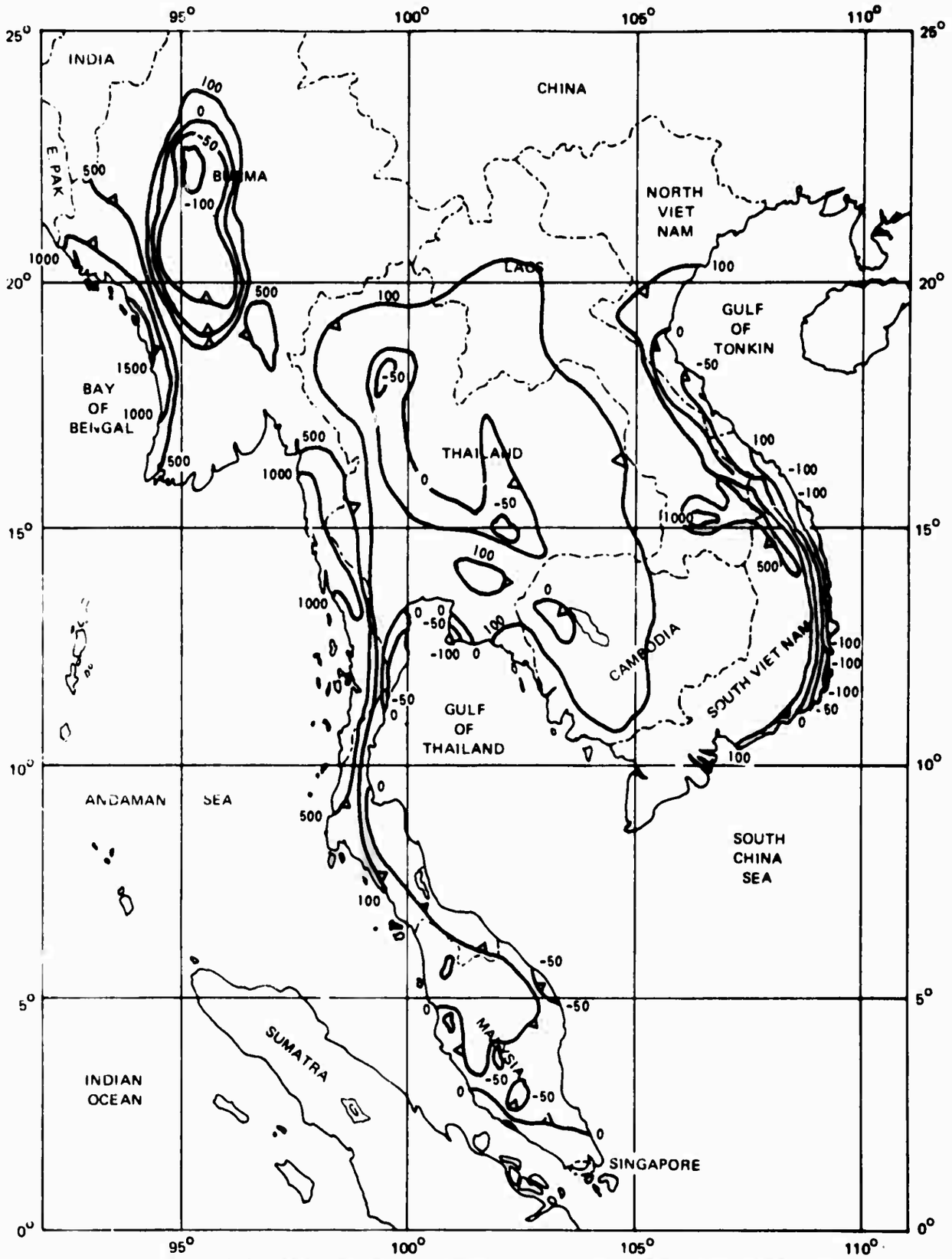

Figure D-1(d) PRECIPITATION MINUS POTENTIAL EVAPOTRANSPIRATION IN MILLIMETERS - JULY

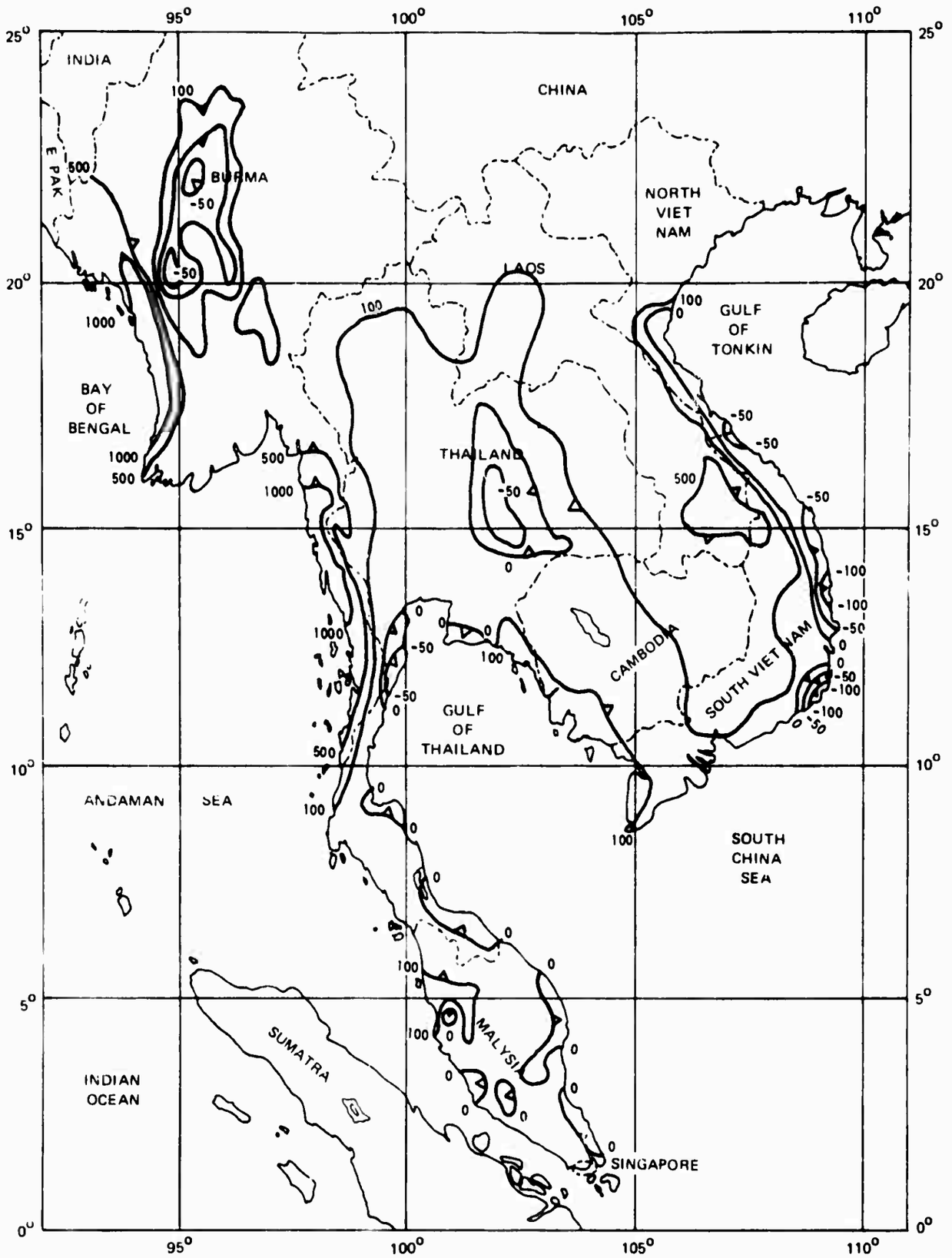

Figure D-1(e) PRECIPITATION MINUS POTENTIAL EVAPOTRANSPIRATION IN MILLIMETERS - AUGUST

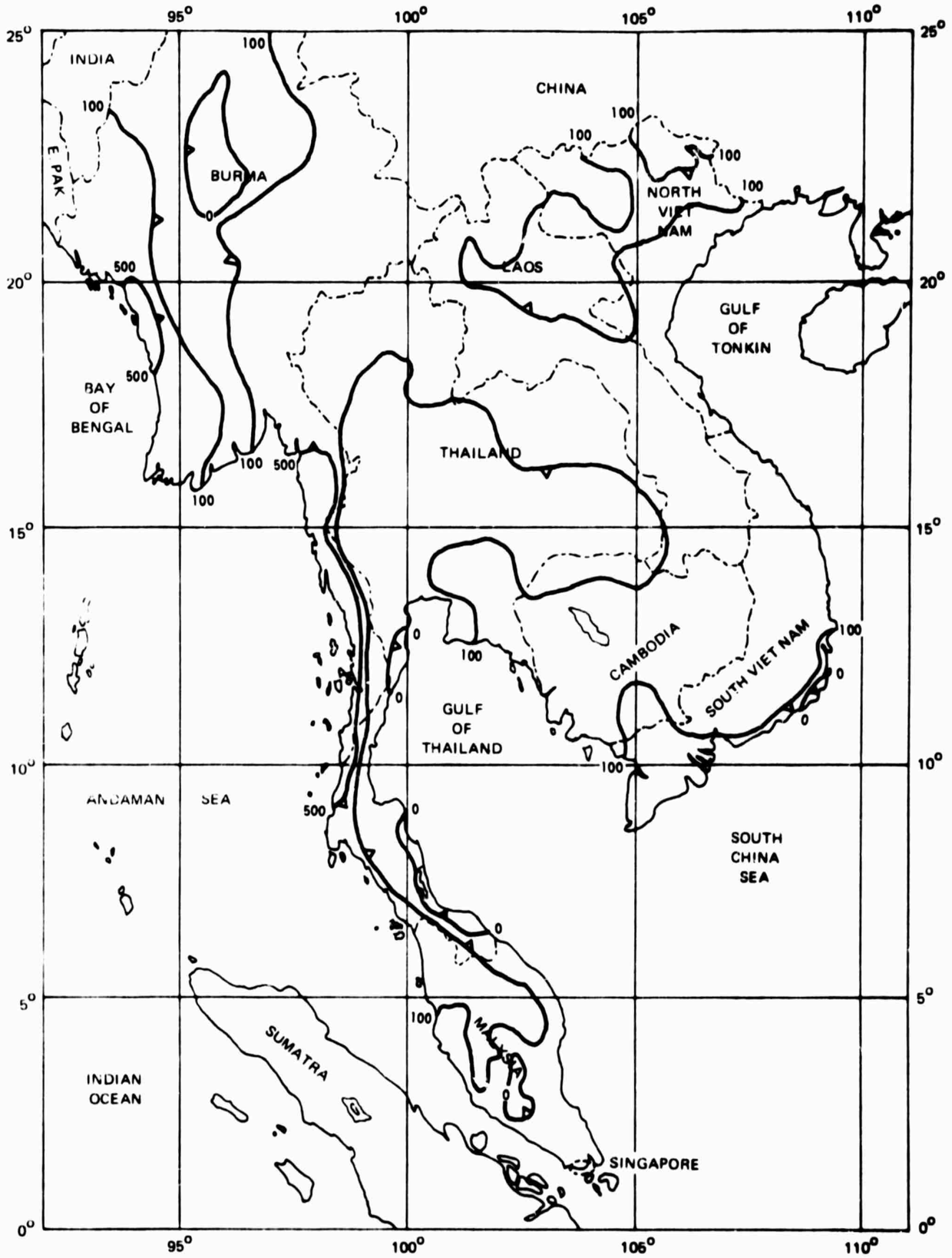

Figure D-1(f) PRECIPITATION MINUS POTENTIAL EVAPOTRANSPIRATION IN MILLIMETERS - SEPTEMBER

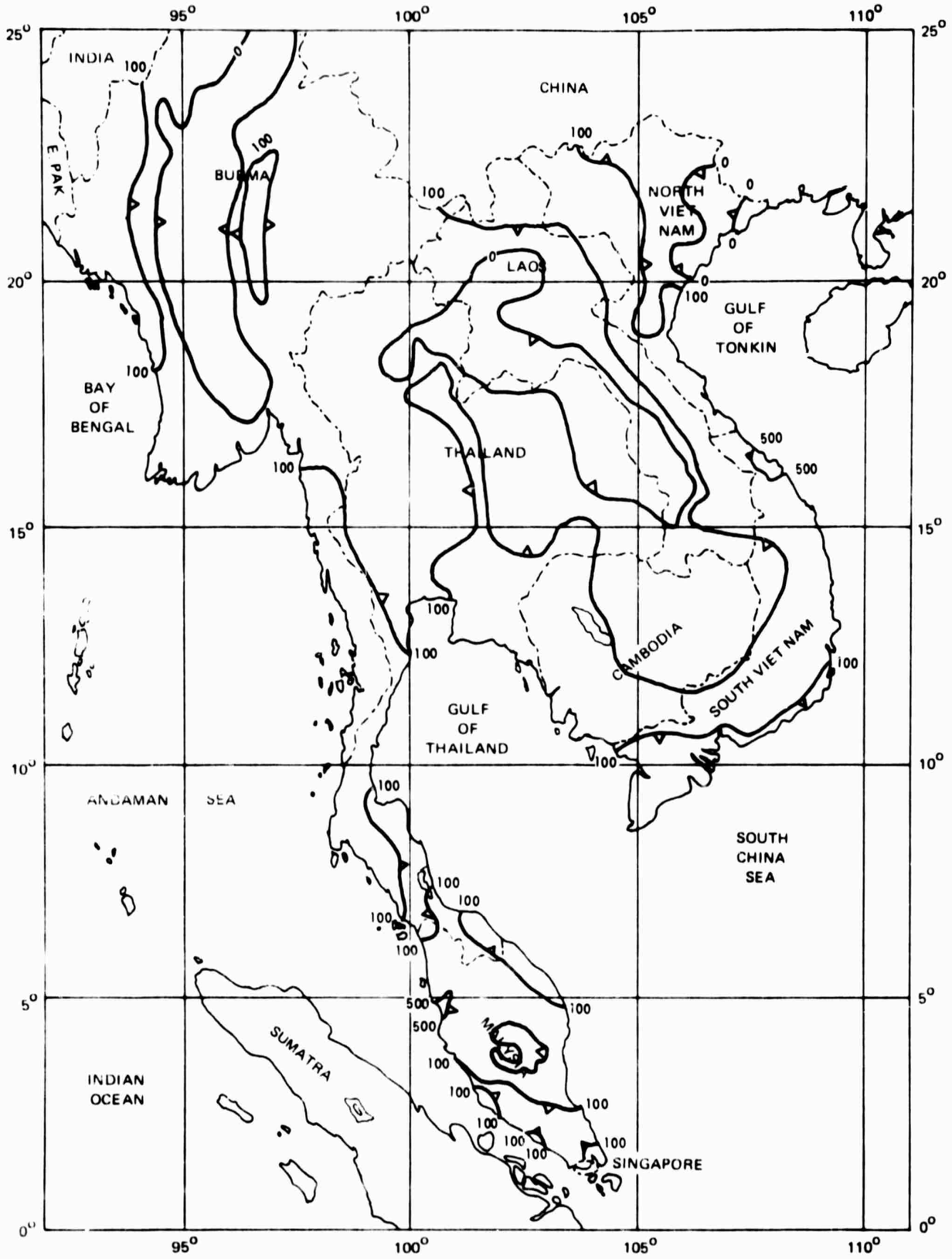

Figure D-1(g) PRECIPITATION MINUS POTENTIAL EVAPOTRANSPIRATION IN MILLIMETERS - OCTOBER

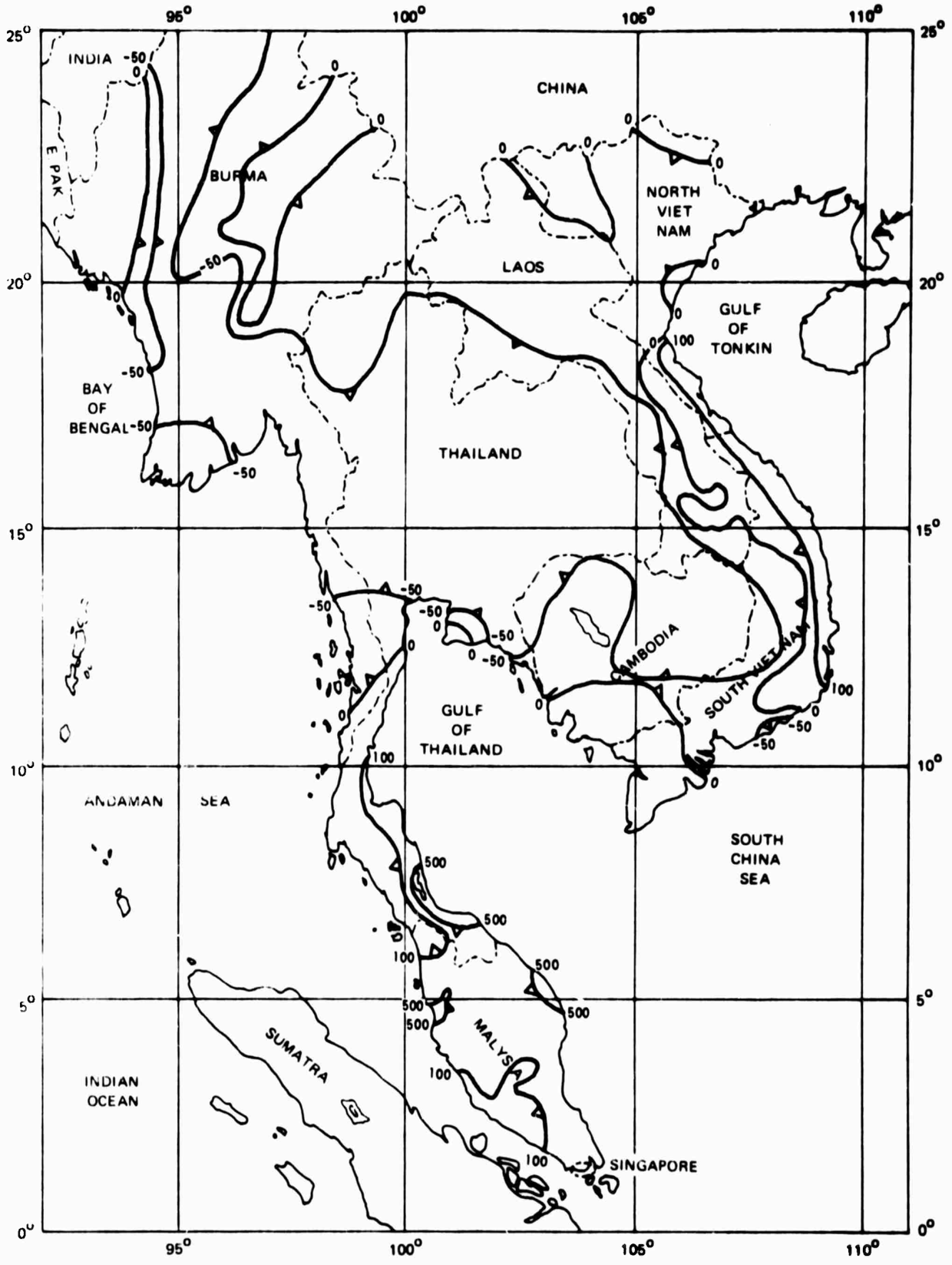

Figure D-1(h) PRECIPITATION MINUS POTENTIAL EVAPOTRANSPIRATION IN MILLIMETERS - NOVEMBER

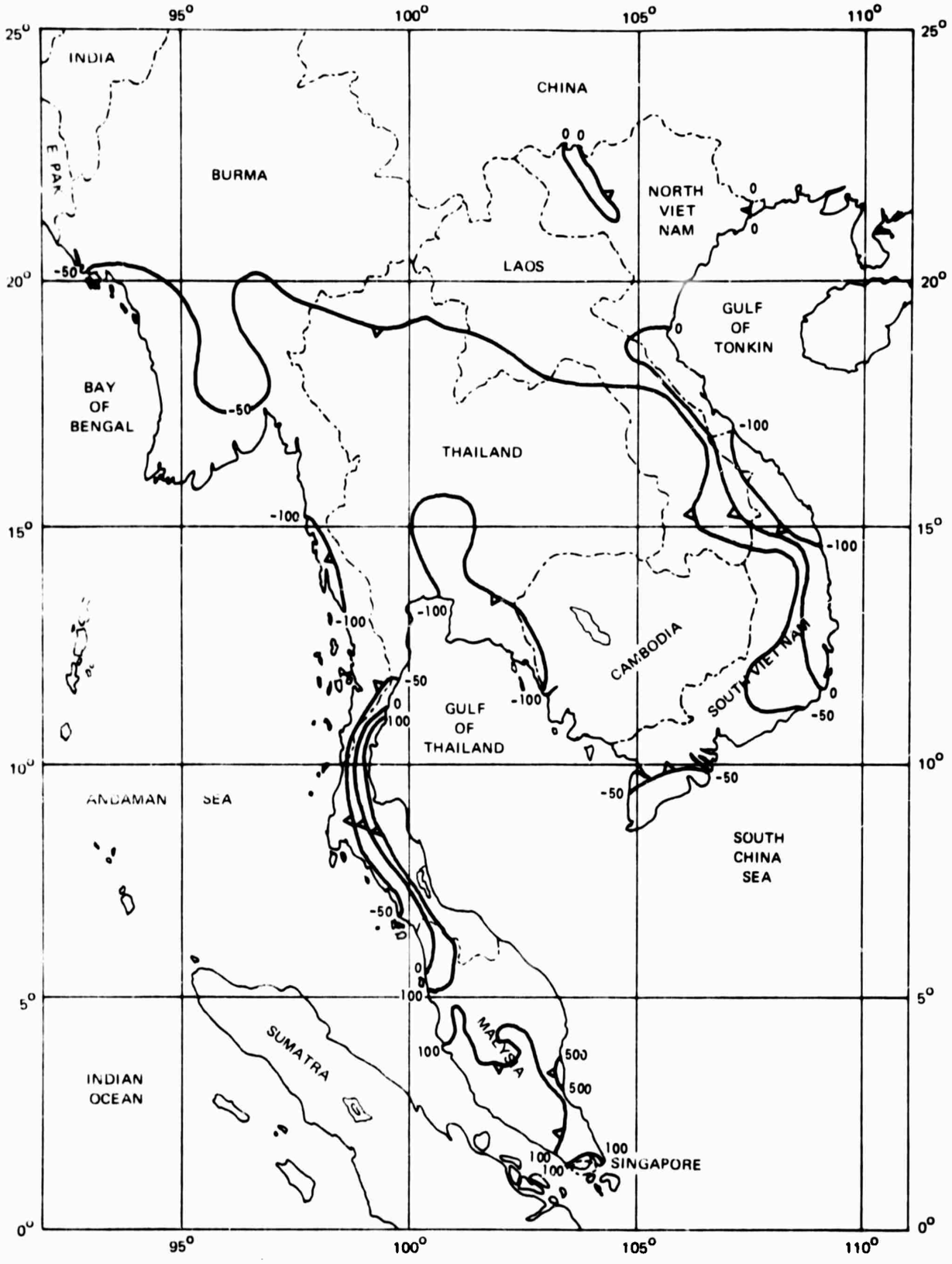

Figure D-1(i) PRECIPITATION MINUS POTENTIAL EVAPOTRANSPIRATION IN MILLIMETERS - DECEMBER

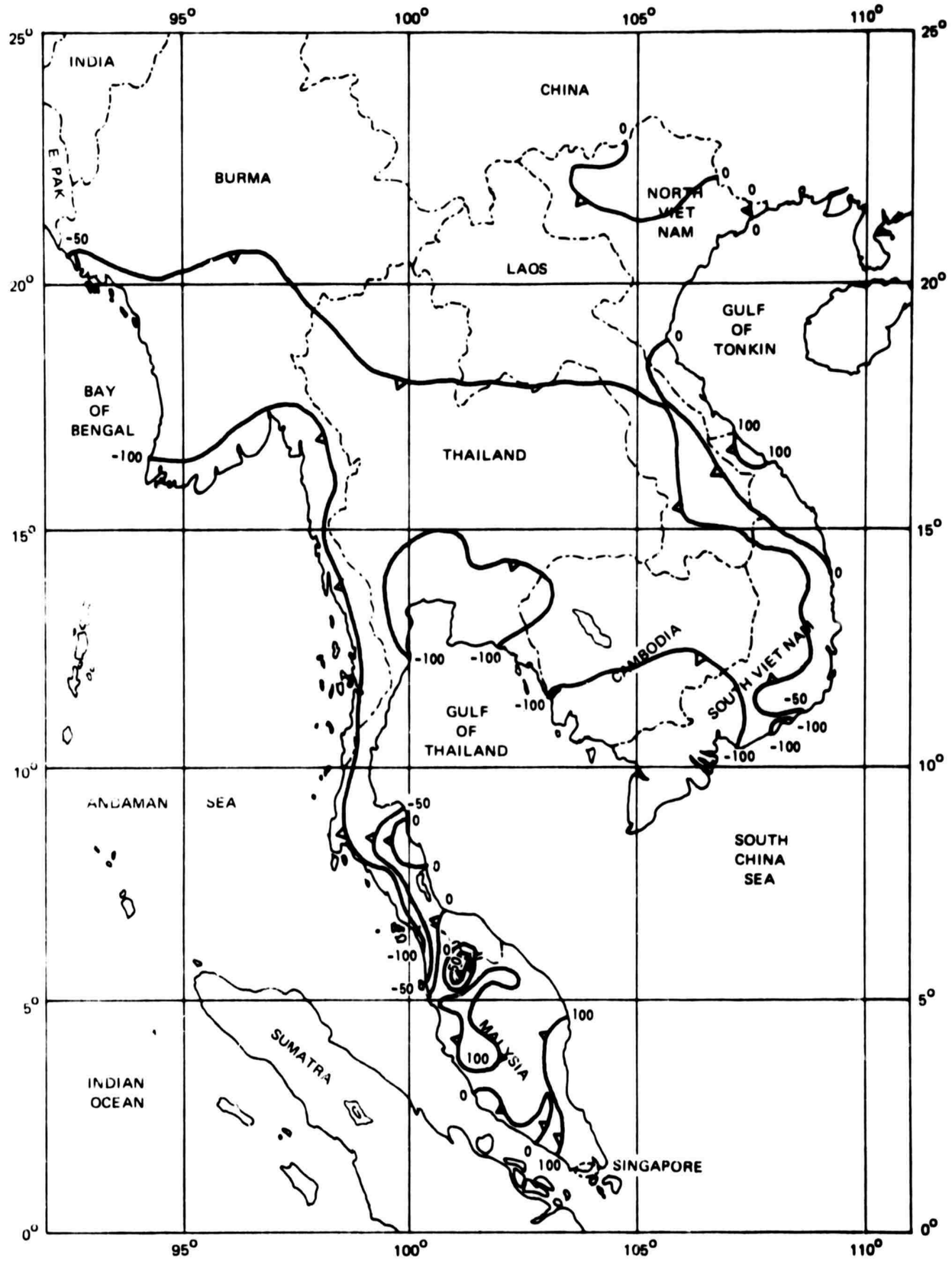

Figure D-1(j) PRECIPITATION MINUS POTENTIAL EVAPOTRANSPIRATION IN MILLIMETERS - JANUARY

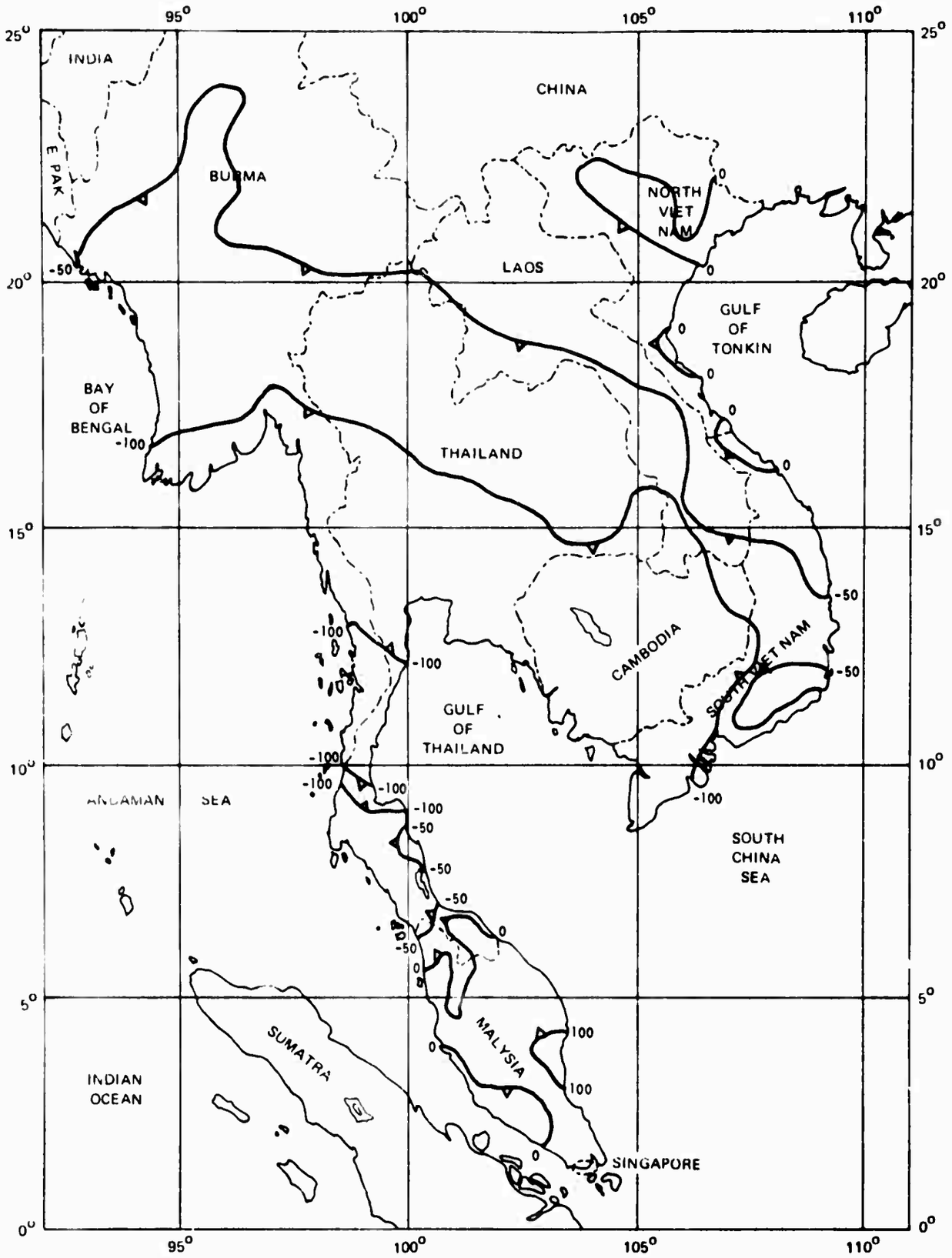

Figure D-1(k) PRECIPITATION MINUS POTENTIAL EVAPOTRANSPIRATION IN MILLIMETERS - FEBRUARY

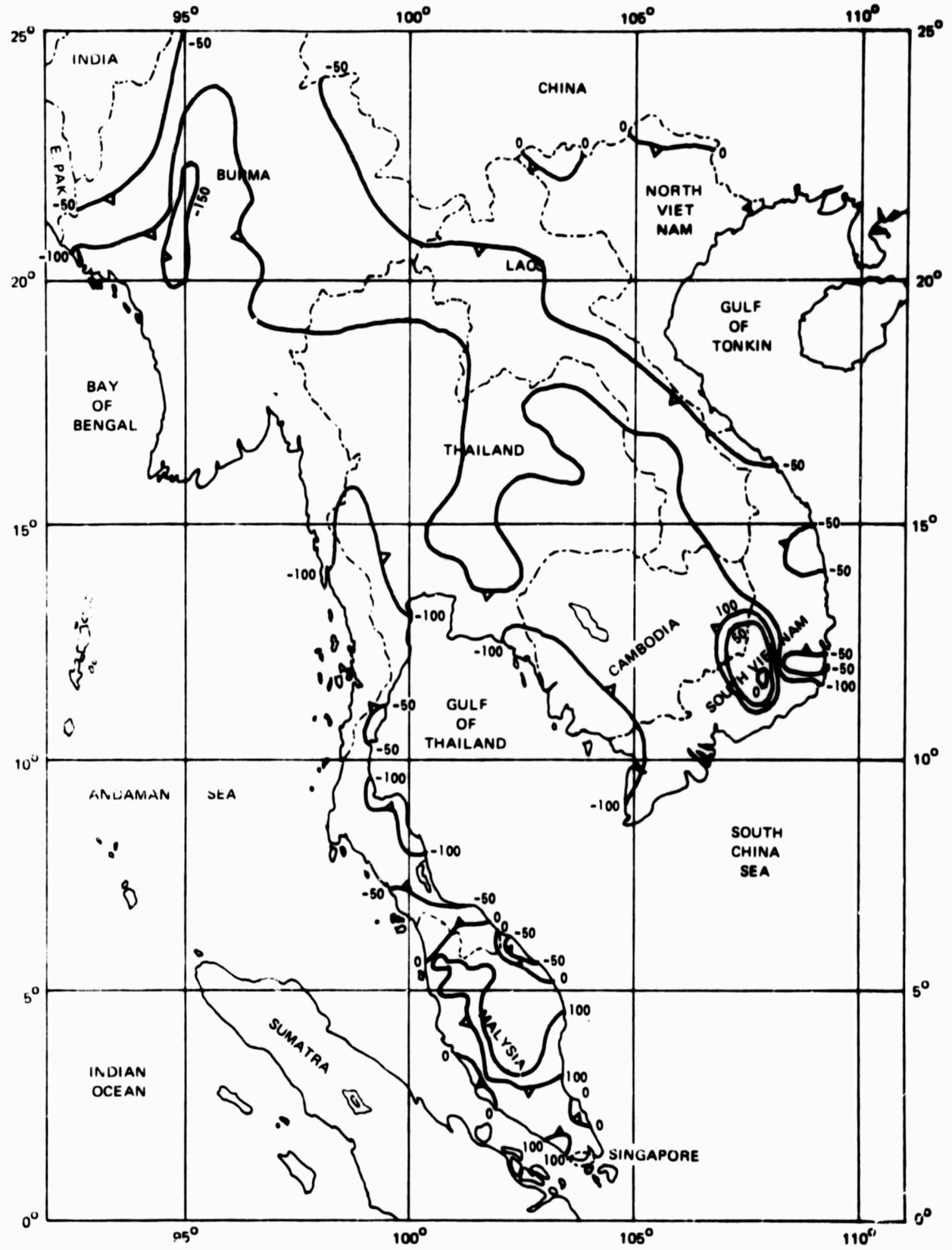

Figure D-1(1) PRECIPITATION MINUS POTENTIAL EVAPOTRANSPIRATION IN MILLIMETERS - MARCH

expected to have shorter dry seasons and longer wet seasons than nearby lowlands, the wet and dry seasons would be expected to occur at the same general me of the year in both types of locations.

Sandoway, Burma at 18° 25'N, 94° 28'E receives an average of 1,686 mm (66.4 in.) of rainfall in July, and several stations in Burma and Thailand receive 2 mm or less during January and February. The station with the highest average potential evapotranspiration is Monywa, Burma at 21° 55'N, 95° 12'E with 197 mm (nearly 8 in.) in May. By contrast Long Son, North Vietnam at 21° 50'N, 106° 46'E in January has only 26 mm (about 1 in.).

Isolines chosen for representing monthly precipitation minus monthly evapotranspiration expressed in millimeters of excess or deficit are 1500, 1000, 500, 100, 0, -50, -100, and -150. Symbols similar to "less than" signs are drawn on the isolines with the points toward the drier side. The zero line is drawn through places where rainfall is equal to potential evapotranspiration. Soils in a high topographic position are expected to have a water content at or near field capacity during most of the month if the previous month has been wet. How deeply into the ground this condition persists will depend on the water balance history for the months immediately preceding the month for which the map is drawn. Soil in a low topographic position could be expected to have a water content between field capacity and complete saturation. Not much water, if any, is added to local streams.

The -50 isoline indicates sub-humid conditions. Only immediately after rains would the top layers of upland soils have moisture up to field capacity. In the same upland sites sub-soil would become progressively drier during the month. Continuously wet soils would be confined to poorly drained spots. Streams flowing through a large area of water deficiency would lose water both through evaporation and seepage. The -100 and -150 isolines represent arid conditions and seldom, if ever, occur unless the previous month or months had been dry also. Stream channels would usually be empty unless

supplied from wetter areas up stream, and soft soils would be difficult to find except in the lowest parts of alluvial areas near such streams.

The 100-isoline condition produces generally wet soil conditions on all types of sites. Immediately after rains, upland soils could be expected to have moisture in excess of field capacity. Time between rains would be short enough to prevent the top layers from drying much below field capacity. Soils in low topographic positions would contain more water than field capacity. Streams would gain water in passing through an area of 100 mm isoline conditions. In an area with a surplus of 500 mm of water, all soils would have water contents of more than field capacity, almost, if not all the time. Stream run-off during the entire month would be at levels experienced only rarely during whole months in middle latitudes.

The highlights of the monthly patterns of excesses or deficiencies of moisture are briefly summarized:

April -- evaporation is high and the 100 mm isoline of excess rain occurs only in Malaya. Parts of the Vietnams and Laos Highlands have an excess of less than 100 mm.

May -- the entire west coast from Singapore to East Pakistan, as well as similarly located parts of Thailand, Cambodia and South Vietnam facing the Gulf of Thailand have an excess of moisture. The 100 mm isoline of excess moisture makes its appearance in the highlands of the Vietnams and Burma. Part of interior Burma and Thailand remain dry. Most of the east-facing coastal lowlands of Vietnam remain dry also.

June -- the 500 and 1000 mm isolines make their first appearance along the West Coast of Burma. Malaya is dryer than in the previous months. The eastward facing coasts of Thailand are in a rain shadow. North Vietnam, north of 20° north, is all noticeably wetter and the highlands all of the way from the border with China to the south China Sea have a water excess of well

over 100 mm. Much of this water flows through the dry coastal lowlands of Vietnam producing the somewhat unusual situation of flooded river valleys in an area where bordering terrain has a deficit of moisture.

July -- the 1500 mm isoline of excess moisture occurs only during this month on the coast of the Bay of Bengal. For the first time a small portion of the lowland has a water deficit of over 100 mm. Interior Thailand and adjoining areas havea greater excess of water overall. Coastal Vietnam between 19^{o} and 11^{o} north remains in a rain shadow. The highlands back from the coast are having their wettest season and as the water runs off, it increases flooding in the streams which flow east through dry Vietnam.

August -- the Southwest monsoon has diminished only slightly and there is very little difference from July.

September -- areas on the west coast of Malaya have an excess of 500 mm of water and small areas of penninsular Thailand experience moisture deficiency. There is no water deficiency in interior Thailand and adjoining areas. Most of Vietnam has an excess of moisture, most of it well over 100 mm.

October -- the northeastern part of North Vietnam has a small moisture deficiency. The remainder of the country has an excess as does South Vietnam. A zone of moisture deficiency reappears in Laos and Thailand and a similar zone is enlarged in Central Burma. Most of the remainder of the area has a moderate excess of water.

November -- the northeast monsoon is established and the flow is strong enough to produce an excess of over 500 mm on parts of the east coast of Malaya as far south as 5^{o} north latitude. The excess of rainfall between 11^{o} and 19^{o} north in Vietnam is due to the same cause. The wet zone along the coast in Vietnam is narrowed down considerably and the interior of the

area centered on Thailand becomes dry with much of it having a deficit of more than 50 mm.

December -- the northeast monsoon is in full force. Virtually every weather station receives less rain than in the previous month. Except for part of coastal Vietnam, the east coast of peninsular Thailand, and Malaya, drought prevails. The -100 mm isoline of water deficiency reappears.

January -- drought intensifies and the areas of moderate water surplus in Vietnam, Malaya, and Thailand all become smaller.

February -- a few places in Vietnam have excess precipitation and only a small part of the east coast of Malaya has over 100 mm water surplus.

March -- most of Southeast Asia is dry except for parts of Malaya which experience more excess rainfall than in the previous month.

Factor Analysis of Vietnam Moisture Data

A portion of the precipitation minus potential evapotranspiration data, more specifically the data for the 30 weather stations in Vietnam, was factor analysed on the month-by-month variance-covariance matrix.

The reasons for doing factor analyses are to deduce the dimensionality of the data, and to try to discover underlying basic patterns in the initial data. One would expect that some basic patterns exist in P-PE data. For example, one would expect a pattern that showed the effects of high rainfall during the wet months, and a pattern indicating the high potential evapotranspiration during the hot months, among others.

The reason for using factor analysis to obtain such patterns rather than just naming them via common knowledge, is that factor analysis determines patterns that are orthogonal to each other. The advantage of

orthogonal patterns is that they are non-interacting or completely independent of each other.

The original data was arranged in a 30 x 12 matrix which was premultiplied by its transpose and solved for eigenvectors and eigenvalues. The methods of computing eigenvectors and eigenvalues will not be discussed here but the general procedures are given in Reference D7. It was found that about 97% of the variance of the original data should be explained by the three eigenvectors with the largest eigenvalues. The eigenvectors and eigenvalues, along with the cumulative variance explained are shown in Table D-1 and Figure D-2.

Since only three eigenvectors were retained, three coefficients b_1, b_2, and b_3 were determined for each station. These values were plotted at the proper map locations and approximate isolines drawn. The results are contained in Figure D-3. Using the eigenvectors and reading the proper coefficients from Figure D-3, excess or deficiency of moisture (P-PE) can be calculated for any location in Vietnam for a desired month by using the formula

$$\text{P-PE} = b_1 E_1 = b_2 E_2 + b_3 E_3$$

A check on the accuracy of the method was done by comparing observed and calculated values for each of the 30 stations and for each month. The root mean square difference between observed and calculated P-PE was about 33 mm of water and when the variance of the calculated and observed values are compared, about 97% of the variance is explained by the calculations.

The values of P-PE obtained by interpolating values of b_1, b_2, and b_3 and using the three eigenvectors seem to be as accurate as those obtained by interpolating on one of the monthly P-PE maps. The accuracy would be increased if the density of stations were higher. The advantage of this

type of analysis is not increased accuracy (there may be none) but that the resulting eigenvectors can be examined to discover causes of the pattern in the original data.*

Table D-1

EIGENVECTORS - EIGENVALUES FOR VIETNAM WATER BALANCE DATA

		MONTHS												EIGENVALUE λ	VARIANCE ACCOUNTED FOR (CUMULATIVE %)
		JAN	FEB	MAR	APR	MAY	JUN	JUL	AUG	SEP	OCT	NOV	DEC		
EIGENVECTORS	E_1	0.01	-0.05	-0.08	-0.09	0.05	0.11	0.24	0.24	0.53	0.59	0.44	0.17	4.0×10^6	49
	E_2	0.10	0.03	0.00	-0.08	-0.28	-0.38	-0.55	-0.45	-0.14	0.25	0.39	0.22	3.3×10^6	90
	E_3	0.35	0.40	0.51	0.49	0.13	0.04	0.08	0.15	-0.11	-0.10	0.22	0.32	4.8×10^5	97

* This technique is clearly applicable to other than P-PE data (e.g., surface temperature, soil strength, etc.)

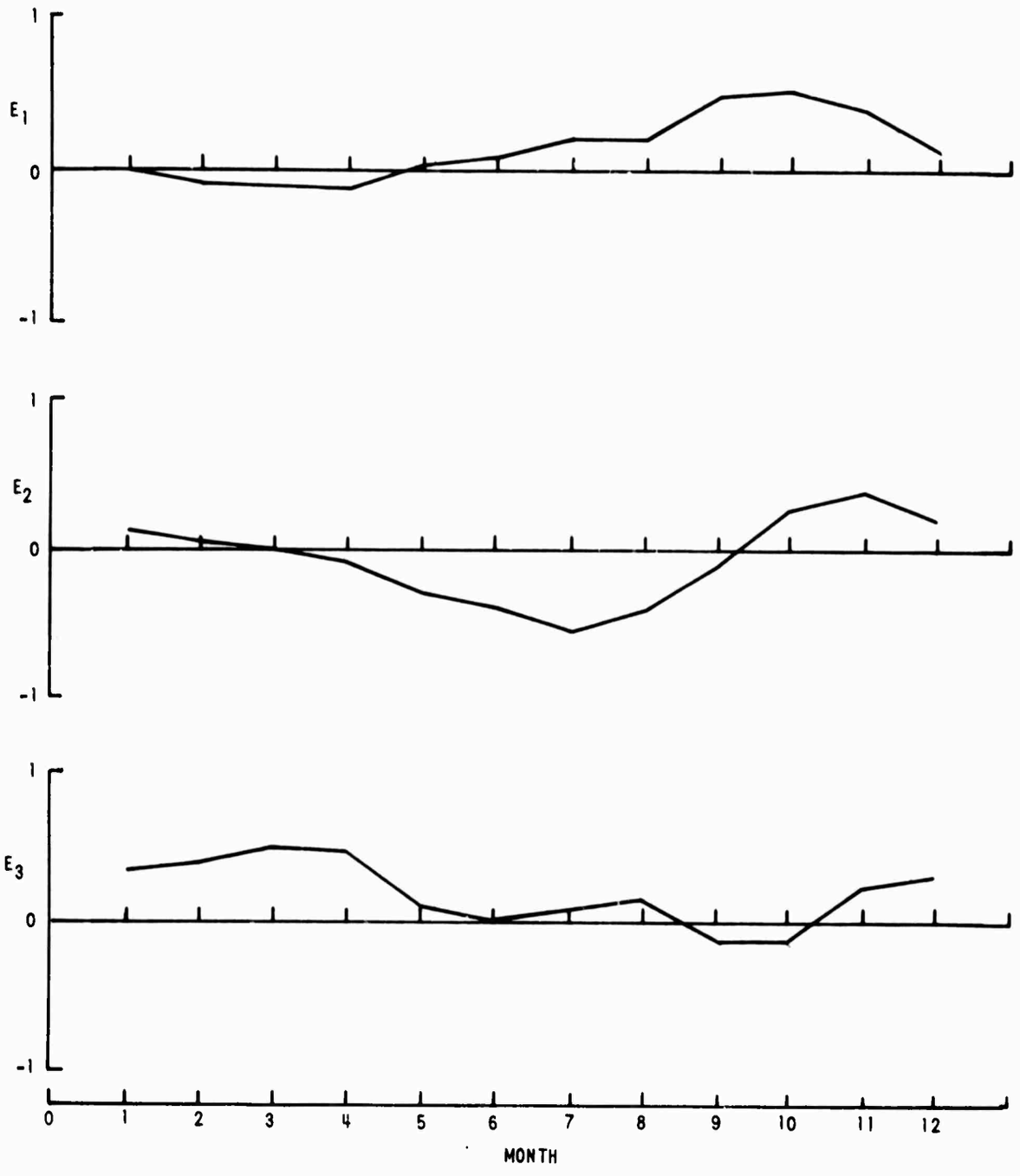

Figure D-2 FIRST THREE EIGENVECTORS OF FACTOR ANALYZED WATER BALANCE DATA

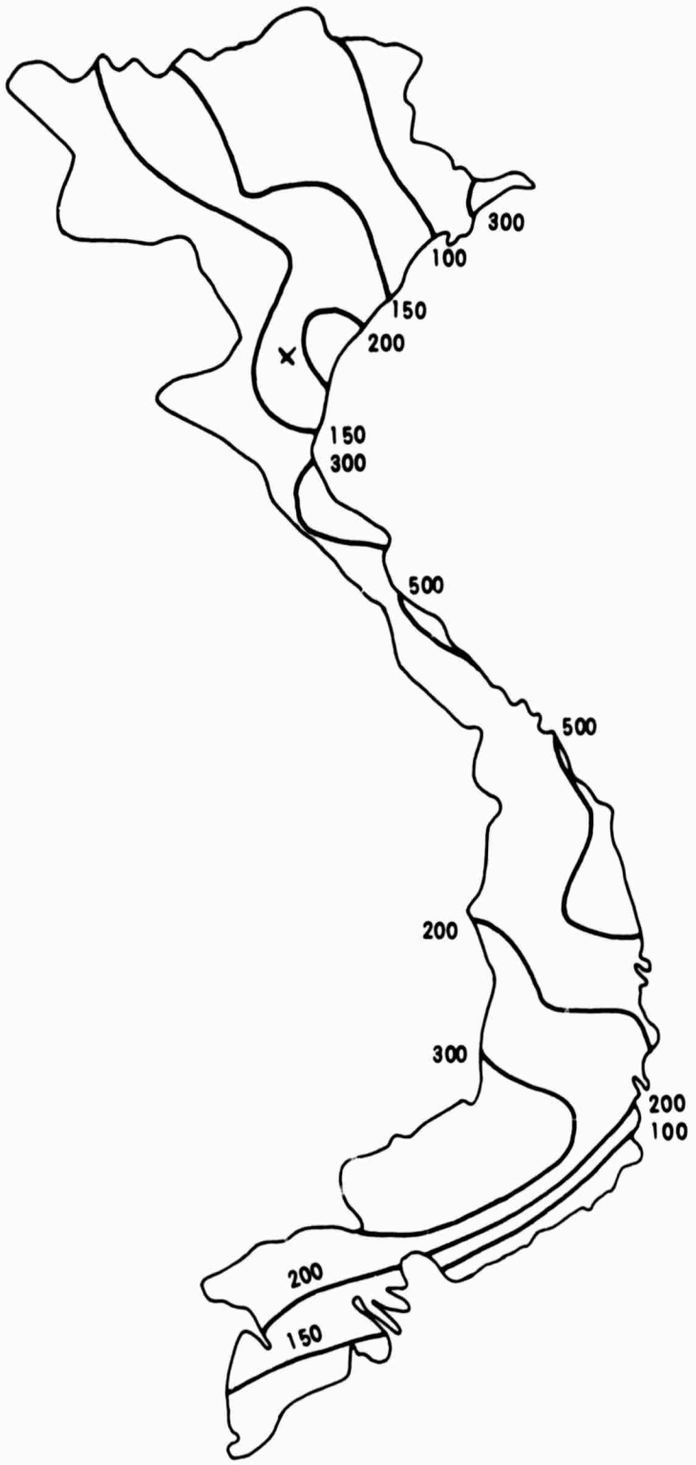

Figure D-3(a) COEFFICIENTS (b_1) FOR E_1 EIGENVECTOR

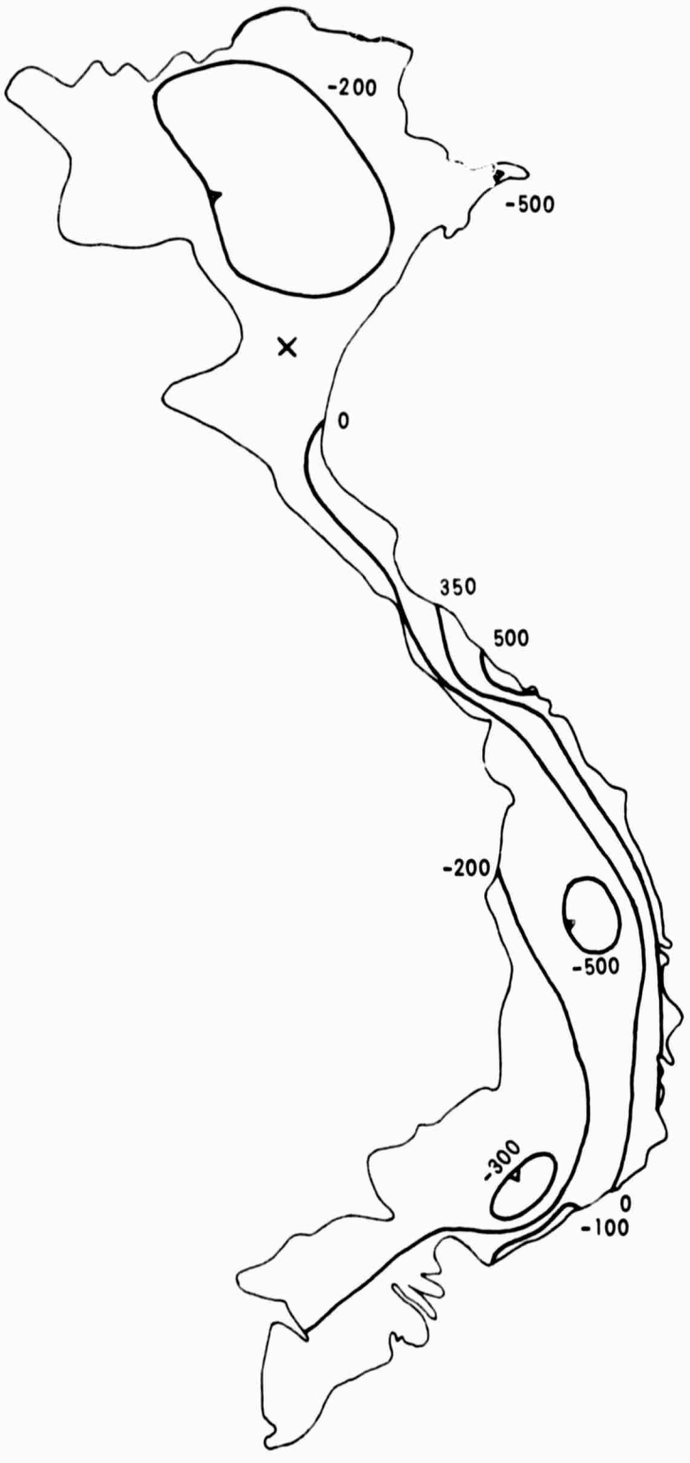

Figure D-3(b) COEFFICIENTS (b_2) FOR E_2 EIGENVECTOR

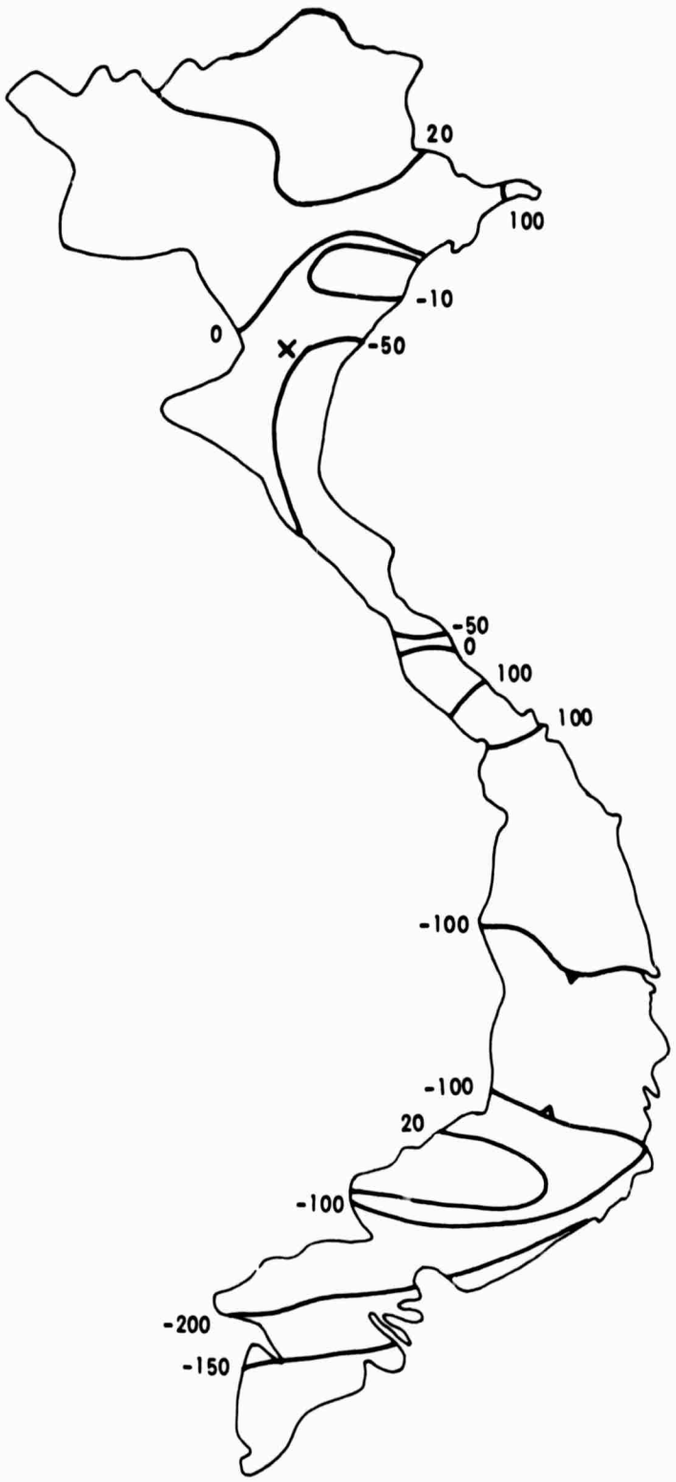

Figure D-3(c) COEFFICIENTS (b_3) FOR E_3 EIGENVECTOR

REFERENCES

D1. Cornell Aeronautical Laboratory, Inc., "Off-Road Mobility Research, 2nd Semi-annual Technical Report". CAL Technical Report No. VJ-2330-G-2, Buffalo, N. Y., September 1967.

D2. Anonymous, "Vicksburg Mobility Exercise A; Vehicle Analysis for Remote-Area Operation," Miscellaneous Paper No. 4-702, U.S. Army Engineer Waterways Experiment Station, CE, Vicksburg, Miss., Feb.,1965.

D3. Thornthwaite, C.W., Mather, J.R., Carter, D.B., and Molyneaux, C., "Estimating Soil Moisture and Tractionability Conditions for Strategic Planning". Air Force Surveys in Geophysics No. 94, Laboratory of Climatology, Centerton, N.J., and Air Force Cambridge Research Center, Bedford, Mass., March 1958.

D4. Thornthwaite, C.W., and Mather, J.W., "Instructions and Tables for Computing Potential Evapotranspiration and Water Balance", Laboratory of Climatology, Centerton, N.J., 1957.

D5. Mather, J.W. (ed.) "Average Climatic Water Balance of the Continents", Laboratory of Climatology, Centerton, N.J., beginning 1962.

D6. Ohman, Howard L., "Climatic Atlas of Southeast Asia", Technical Report No. ES-19, U.S. Army Materiel Command, U.S. Army Natick Laboratories, Natick, Mass., December 1965.

D7. Harman, H.H., Modern Factor Analysis, Chicago: University of Chicago Press, 1960.

Appendix E: STATISTICAL DISTRIBUTION OF SOIL MOISTURE

In the course of collecting trafficability data on soil in humid temperate and tropical climates, the staff of the Waterways Experiment Station made many measurements of soil moisture content. These data can be used to describe the statistical occurrence of moisture levels in various soil types and topographic positions. The resultant statistics can be used as guidelines for deciding upon moisture levels to be used in vehicle testing programs, and also can be of value in prediction of moisture content in remote terrains.

The data which has been treated thus far was collected in the United States [E1] and in Costa Rica[E2]. The manner in which the data were presented dictated somewhat different analyses. The summary tables of the U.S. report give the average wet season moisture contents of the 6-to 12-inch soil layers for a large number of soils throughout humid regions of the U.S. In contrast, the data from Costa Rica were from only five sites, but daily measurements of soil moisture are given. No attempts were made to record rainfall at the U.S. sites, whereas daily rainfall measurements were recorded at the sites in Costa Rica.

In both instances, the moisture contents are reported as percent of the dry soil weight. As part of their analyses, they also reported moisture contents at 0.06 atmospheres tension, which can be considered as field capacity. At field capacity, soils are just able to retain moisture against the force of gravitation. Soils differ widely in their capacity to retain moisture; thus a typical sandy loam may contain 15% moisture and be at 100% field capacity, whereas a silt loam with 15% moisture would be at approximately 50% field capacity.

To take into account the variable moisture-holding capacity of the soils, the moisture contents in the WES data were recalculated by computing the ratio of average wet-seaon moisture content, percent dry

weight, to the moisture content at field capacity (0.06 atmospheres) and expressing this ratio as a percent. As an example, for a soil which has an average wet season moisture content of 25% and a field capacity of 20%, the ratio would be:

$$\frac{\text{Average moisture content, wet season}}{\text{Moisture content at field capacity}} = \frac{25}{20} = 1.25 = 125\%$$

Analysis of U.S. Data

The sites upon which the measurements were made were categorized by WES according to many criteria. The criteria of interest in the present analysis were soil type, slope gradient, and topography class. The soils were grouped according to the Unified Soil Classification System (USCS) classes. An important distinction to be made is whether the site is in a low or high topographic position. A high topographic position is one in which the water table is not within 4 feet of the ground surface any time of the year; a low topographic site will have a water table within 4 feet of the surface at some time of the year.

Frequency distributions of moisture content as percent of field capacity were determined for various soil, soil-slope and soil-slope-topographic class combinations. Surprisingly, the frequency distributions were quite similar for the different soils except the sandy ones (SM, SC, SM-SC) and the organics (OH, OL). Although there were data on few slopes greater than 19%, the figures reflected a marked decrease in average wet-season moisture content on slopes greater than about 19%. Topographic class (high or low) did result in noticeably different distributions.

As a result of the preliminary frequency distributions, all the soils except sandy were considered as one group. The grouping then included MH, ML, CL, CH and ML-CL soils. Any of these soils occuring on slopes up to 19% were included. The soils were segregated on the

basis of their occurrence in either high or low topographic positions.

The resultant frequency distributions of the data are shown in Figures E-1 and E-2. The data were grouped into five-percent intervals and the midpoints plotted. The groups show a fairly normal distribution. The means and standard deviations for low and high topography sites are as follows:

Topographic Class	Mean M.C. as % field capacity	Standard Deviation
High	90.3%	10.8%
Low	99.4	13.3%

This analysis suggests the spectrum of moisture content in the six-to-twelve inch soil layers which realistically represent average wet season conditions for regions with humid temperate climates. Thus tests conducted on other than sandy or organic soils with moisture contents up to 140% of field capacity in the six-to twelve-inch layers should cover over 99% of the average wet season conditions to be encountered in low topography on 0-19% slopes (average low topography plus three standard deviations = 99.4% + 3 (13.3) = 139.3%).

Analysis of Costa Rica Data

Because daily rainfall measurements as well as moisture measurements were made on Costa Rica sites, it was possible to look at the distribution of moisture contents relative to the amount of rainfall. The data from two sites with USCS soil types OH (CR-3, CR-5) and two sites with soil type MH (CR-1, CR-2) were analyzed.

Frequency distributions of moisture contents as percent of field capacity were quite similar for both MH sites, and therefore the data from both sites were combined. Separate frequency distributions were then prepared for all months having between 3-4.9, 5-6.9, 7-8.9, 9-10.9, and

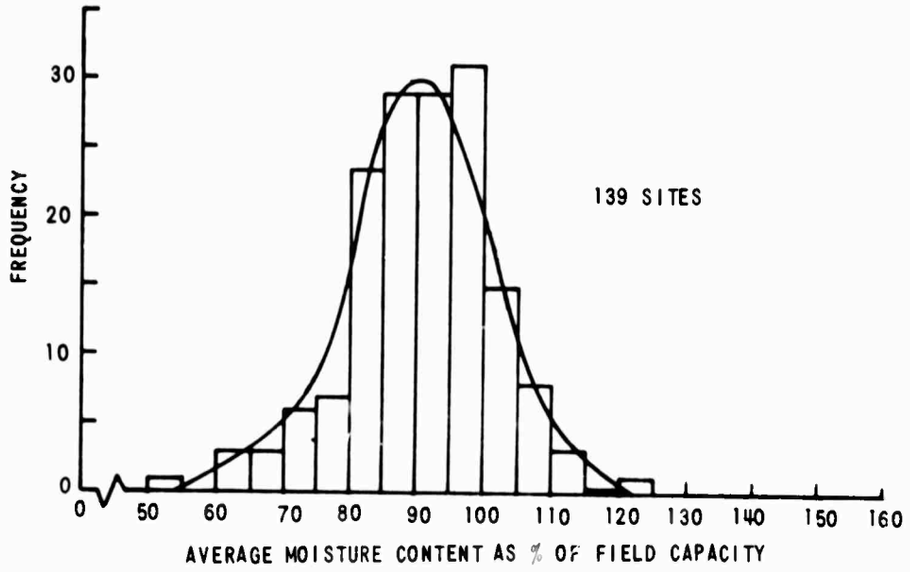

Figure E-1 DISTRIBUTION OF AVERAGE MOISTURE CONTENTS - HIGH TOPOGRAPHY (ML, MH, CH, CL, ML-CL SOILS)

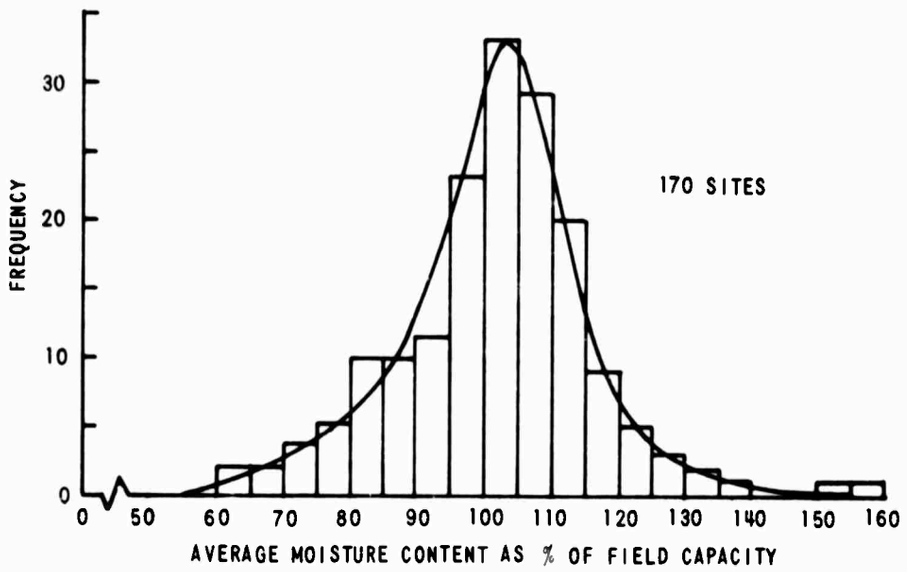

Figure E-2 DISTRIBUTION OF AVERAGE MOISTURE CONTENTS - LOW TOPOGRAPHY (ML, MH, CH, CL, ML-CL SOILS)

11-13 inches of rainfall. The percentage cumulative frequencies were plotted as cumulative probability graphs and gave good indication of normal distributions. The graphs revealed differentiation only between wide increments of rainfall. The resultant plots, means and standard deviations are shown in Figure E-3.

The data for the OH soil types (CR-3 and CR-5) were treated in a similar manner and the results are shown in Figures E-4 and E-5. As with the MH soils, moisture contents increased very little in proportion to the increased rainfalls and standard deviations remained rather constant.

Unlike the MH sites, the OH sites displayed distinctly different distributions and separate means and standard deviations resulted. As one would expect, the highly organic OH soils, which are often associated with wet sites, had higher moisture contents. The differentiation between the two OH sites can be explained by the position of the water table, which was within 12 inches of the surface 100% of the time in the wetter site (CR-3). The overwhelming influence of the permanent water table is demonstrated in Figure E-4, which shows essentially the same cumulative probability distributions for 3-7 inch and 7-13 inch rainfall increments.

The analysis of Costa Rica data suggests that perhaps probability levels for particular moisture levels being met or exceeded can be established for various groups of soils, rainfall increments, and topographic positions. Many different soils tend to exhibit similar statistical distributions when moisture content is expressed as percent of field capacity.

Certainly much more data from many more locations needs to be analyzed to test and develop this hypothesis. WES has collected data from other countries such as Panama, Puerto Rico, Columbia, and Thailand which can be used in such analysis. We intend to do further statistical studies of available data to further develop a predictive method and provide guidelines for test programs.

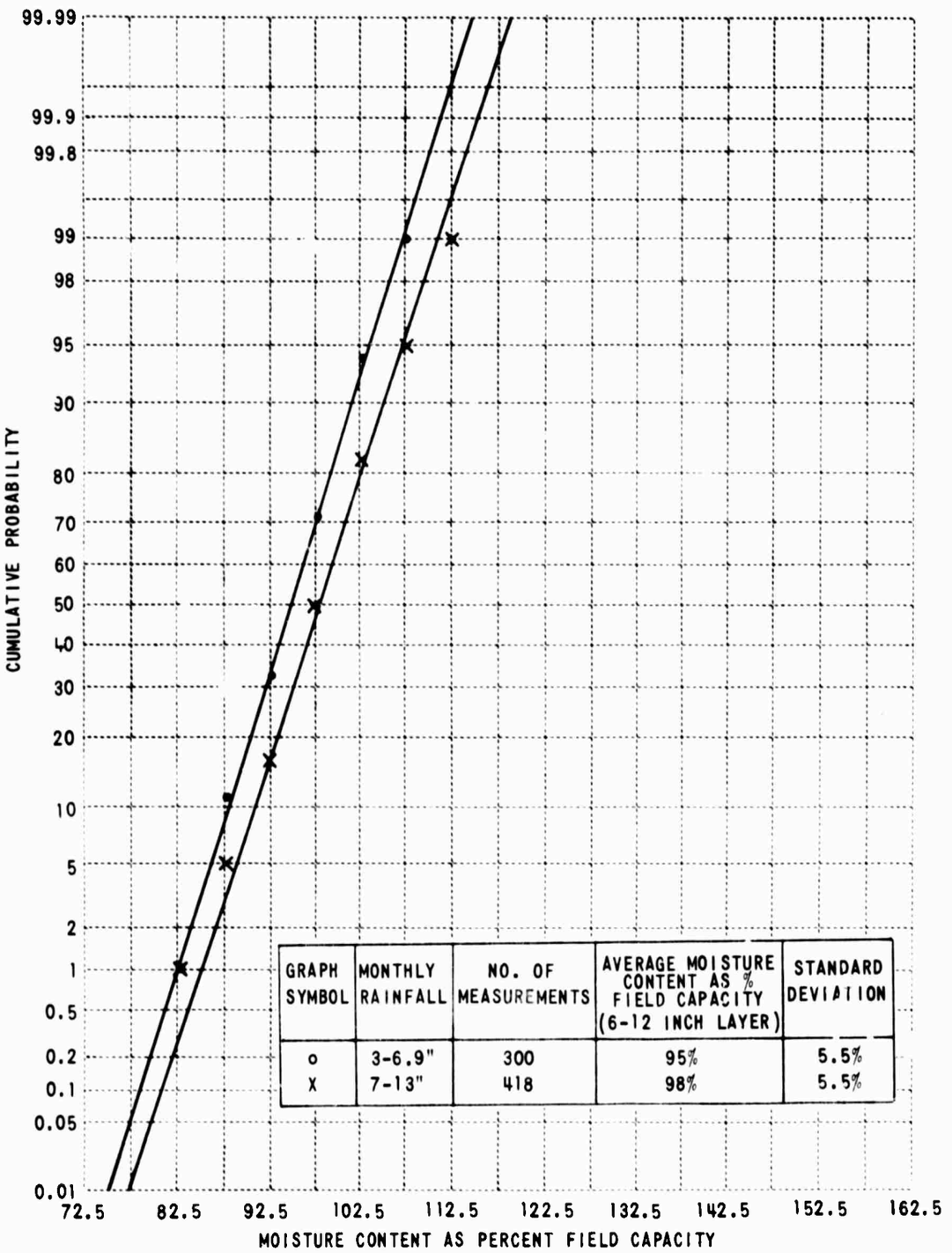

Figure E-3 CUMULATIVE PROBABILITY DISTRIBUTIONS OF MOISTURE CONTENTS IN WES COSTA RICA SITES CR-1, CR-2

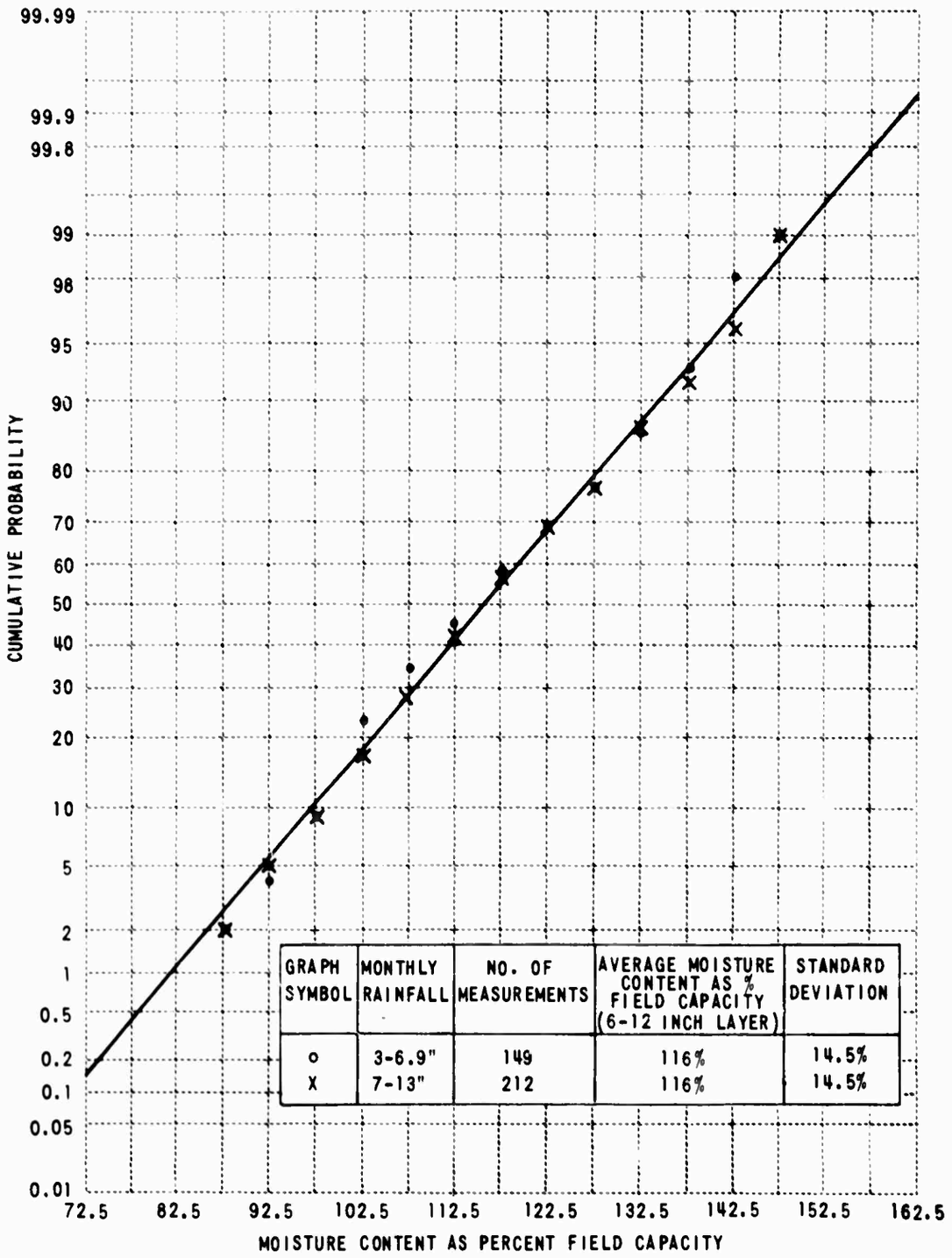

Figure E-4 CUMULATIVE PROBABILITY DISTRIBUTIONS OF MOISTURE CONTENTS IN WES COSTA RICA SITE CR-3

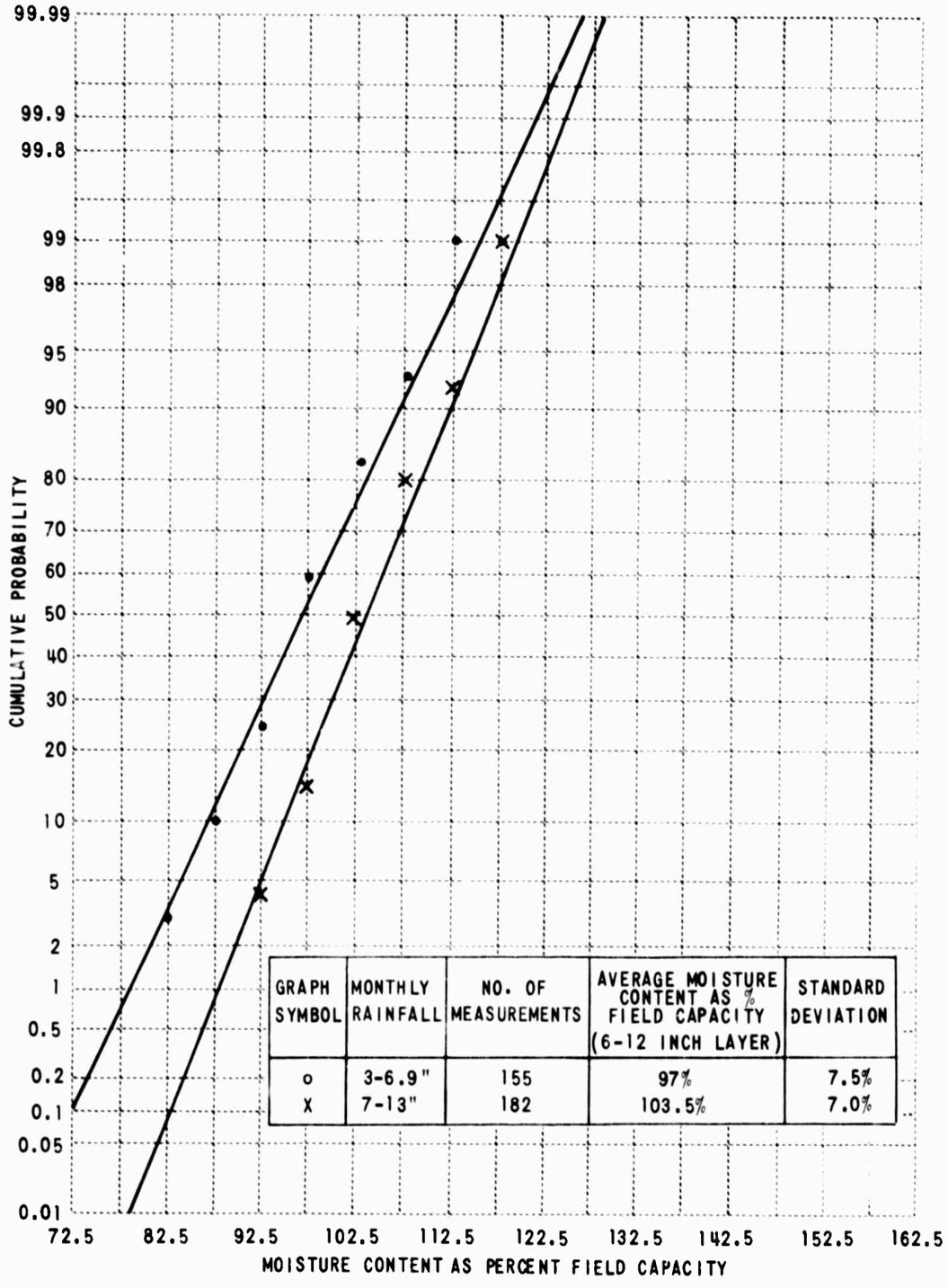

Figure E-5 CUMULATIVE PROBABILITY DISTRIBUTIONS OF MOISTURE CONTENTS IN WES COSTA RICA SITE CR-5

REFERENCES

E1. Anonymous, "Trafficability of Soils; Soil Classification," Technical Memorandum No. 3-240, Sixteenth Supplement, U.S. Army Engineer Waterways Experiment Station, CE, Vicksburg, Miss., June 1966.

E2. McDaniel, A.R., "Trafficability Predictions in Tropical Soils; Costa Rica Study No. 1 (January 1963 - January 1965), " Miscellaneous Paper No. 4-355, Report No. 5, U.S. Army Engineer Waterways Experiment Station, CE, Vicksburg, Miss., December 1967.

BLANK PAGE

Appendix F: GEOMETRIC AND SOIL CHARACTERISTICS OF STREAMS

Streams have characteristic streambed and bank properties which are reasonably consistent and definable within given landscapes. Streams can be categorized as destructional, constructional, or fan. Destructional streams are narrow and steep-sided and occur in the headwaters of drainage basins. They are eroding in local soil or bedrock and do not have alluvial flood plains. Constructional streams are wider with greater average water depths and will have flood plains of fine to medium textured alluvium.

Constructional streams can be further categorized into upstream and deltaic. In upstream constructional streams, the mean water level is significantly below the bank top, whereas in deltaic streams the mean water level is often near the bank top. Deltaic type streams are relatively rare since they must occur on coastal shelves and are actually large rivers. Examples would be in the Mississippi or Mekong Deltas. Streams producing alluvial fans are confined to semiarid regions where coarse textured materials are deposited at the base of mountain ranges.

Figure F-1 illustrates idealized cross-sectional shapes of the stream types discussed previously.

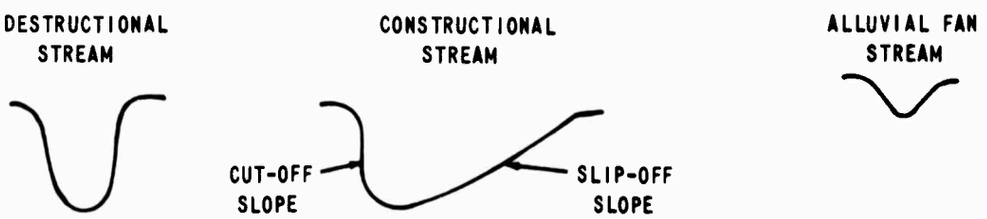

Figure F-1 TYPICAL STREAM CROSS SECTIONS

Tables F-1 and F-2 summarize some bed and bank characteristics which can be expected to normally occur in these streams.

Since destructional streams do not have alluvial flood plains, their bank and bed compositions will vary erratically depending on the nature of the local soil and bedrock. Cross-sectional channel shapes will be symmetric and bank slopes will be nearly vertical. Destructional streams have not developed a meandering pattern.

Constructional streams do meander across their alluvial flood plains and except for relatively infrequent straight reaches, assume typical assymetric cross-sections as shown in Figure F-1. The cut banks occuring on the outside of meanders are normally steeply sloping since they are being undercut by high velocity flow during high water periods, and are cohesive. The suggested slope range for cut banks is 70% to vertical. The slip-off banks are less sloping since water velocity is less on the inside of meanders, and coarse textured, low-cohesion materials are deposited there. The suggested range for slip-off banks is from 10% to 30%. Upland constructional streams will often require vehicle swimming in contrast to destructional streams, which rarely if ever will have sufficient water depth to require swimming. Deltaic streams will almost always require vehicle swimming.

From Table F-1 it is seen that deltaic streams differ from other constructional streams principally in the composition of the slip-off slopes. This results because the bulk of coarse materials have been deposited on shoals much further upstream.

Streams on alluvial fans are confined to arid or semiarid landscapes occurring at the base of mountain ranges. Their beds and banks are predominantly coarse textured. In addition, bank heights rarely exceed three feet. These streams therefore are minor deterrents to off-road movement.

Table F-1

BANK AND BED CHARACTERISTICS OF CONSTRUCTIONAL STREAMS

	CUT-OFF (1) BANK COMPOSITION	CUT-OFF BANK SLOPES	SLIP-OFF (1) BANK COMPOSITION	SLIP-OFF BANK SLOPES	BED MATERIAL
UPSTREAM	CH, CL MH, ML	70% – VERTICAL	GW, GP, SW SP, GM, SM	10 – 30%	GW, GP SW, SP
DELTAIC	CH, CL MH, ML	70% – VERTICAL	CH, CL, SM MH, ML	10 – 30%	SW, SP SM

(1) UNIFIED SOIL CLASSIFICATION NOMENCLATURE

TABLE F-2

BANK AND BED CHARACTERISTICS OF DESTRUCTIONAL AND ALLUVIAL FAN STREAMS

	BANK COMPOSITION (1)	BANK SLOPES	BED MATERIAL
DESTRUCTIONAL	VARIABLE (2)	NEARLY VERTICAL	VARIABLE (2)
ALLUVIAL FAN	GW, GP SW, SP	NOT APPLICABLE (3)	GW, GP SW, SP

(1) UNIFIED SOIL CLASSIFICATION NOMENCLATURE

(2) DETERMINED BY NATURE OF LOCAL SOIL AND BEDROCK

(3) BANK HEIGHTS RARELY EXCEED THREE FEET

Tables F-1 and F-2 can be used to delimit what soil and geometric conditions can generally be expected for those landscapes containing either destructional, constructional or alluvial fan streams. It must be remembered that destructional and constructional stream segments occur in the same watershed as illustrated in Figure F-2.

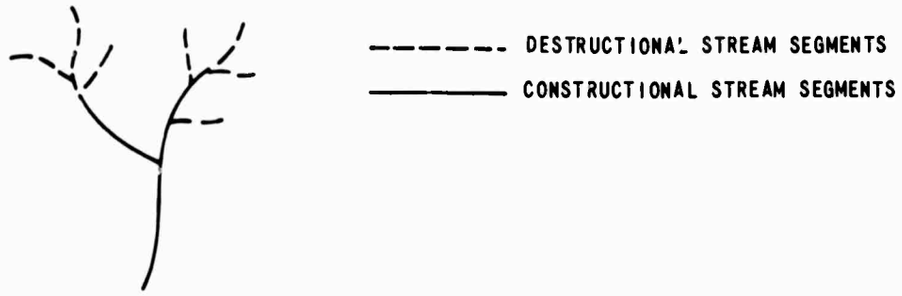

Figure F-2 CONSTRUCTIONAL AND DESTRUCTIONAL STREAM SEGMENTS

Mathematical Model of Stream Bank Heights

The geometric relationships of streams to their drainage areas depend upon a spectrum of rainfall and runoff flows which in turn are related to the vegetation and soil cover of the bedrock.

An idealized cross-sectional configuration which most alluvial streams approach is shown in Figure F-3. The following discussion will be referenced to this figure.

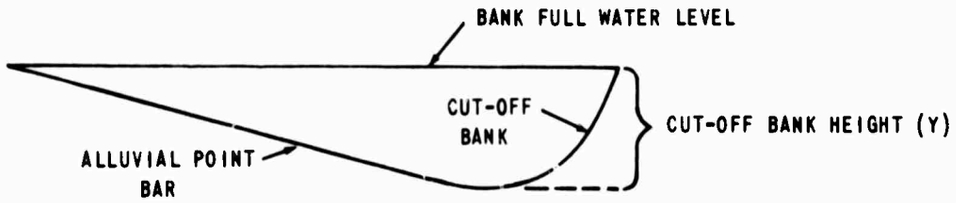

Figure F-3 TYPICAL CROSS-SECTION OF ALLUVIAL STREAM

The slope which the alluvial point bar makes with the horizontal for many naturally occurring streams is 15% and therefore will be assumed in this model.[F1] The cross-sectional area of Figure F-3 therefore is

$$A = \frac{\pi}{4} Y^2 + \frac{1}{2} \cdot \frac{Y^2}{0.15} \tag{1}$$

The hydraulic radius of a stream is defined as A/P where P is the wetted perimeter of the channel [F2]. In the above figure $r \simeq 0.5Y$

The classic and well-established formula for relating the erosive properties of a stream to its geometry and bank materials is Manning's formula[F2]:

$$V = \frac{1.49}{n} r^{2/3} S^{1/2} \tag{2}$$

where:

V = erosive velocity in feet per second (fps)
n = channel roughness factor
r = hydraulic radius
S = water surface slope $\simeq$ channel slope

The value for n in small streams $\simeq$ 0.07 and this value will be assumed here. Substituting 0.07 for n and 0.5 Y for r in Equation 2:

$$V \simeq \frac{1.49}{0.07} (0.5Y)^{2/3} S^{1/2} \simeq 13.4 Y^{2/3} S^{1/2} \tag{3}$$

$$Y \simeq 0.02 V^{3/2} S^{-3/4} \tag{4}$$

Therefore bank height Y can be expressed in terms of erosive velocity V and channel slope S. The empirical data of Ref. F1 shown in previous ORMR reports [F3, F4] are in general agreement with Equation 4. Analysis

of existing data as shown in Figure F-4 shows that V varies from 2.5 ft/second for sand to some 13 ft/second for the most resistant basalts. Objectives of future work would be to more precisely establish values for V, especially in soil materials, to correlate values of S with local relief, and test the models by checking predictions from the model with the actual geometries of natural streams.

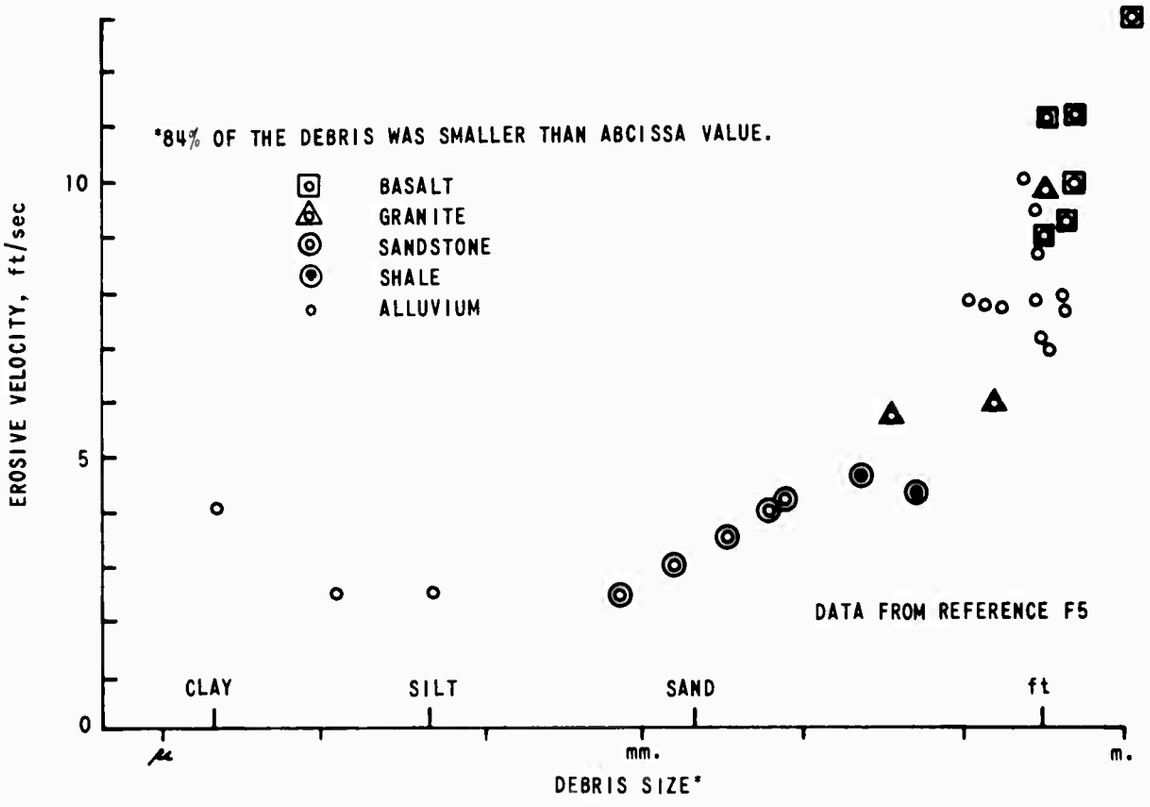

Figure F-4 PEAK FLOOD WATER VELOCITIES WHICH INITIATE EROSION OF VARIOUS DEBRIS SIZES

REFERENCES

F1. Leopold, L.B., Wolman, M.G., and Miller, J.P., Fluvial Processes in Geomorphology. San Francisco, W. H. Freeman & Co., 1964.

F2. Chow, V.T., Open Channel Hydraulics. New York: McGraw-Hill Book Co. Inc. 1959.

F3. Bartlett, G.E., Kaufman, S., and Deutschman, J.N. (coeditors), "Off-Road Mobility Research", Second Semiannual Technical Report, Report VJ-2330-G-2, Cornell Aeronautical Laboratory, Inc., Buffalo, New York, September 1967.

F4. Bartlett, G.E., Kaufman, S., McAdams, H.T., and Smith, R.L. (coeditors), "Survey and Program Definition for Off-Road Mobility Research", 1st Semiannual Technical Report, Report VJ-2330-G-1, Cornell Aeronautical Laboratory, Inc., Buffalo, New York, March 1967.

F5. Barnes, H.H., "U. S. Geological Survey", Water Supply Paper No. 1849, 1967.

BLANK PAGE

Appendix G: INSTRUMENTATION FOR MEASUREMENTS WITHIN SOILS

We report below on (1) our effort toward improvement in the X-ray method for measuring marker displacement, (2) the applicability of microwave techniques for this and other purposes, (3) the feasibility of measuring pore water pressure by small gages imbedded in the soil and (4) the feasibility of remotely measuring the output of imbedded sensors.

X-ray Measurement of Marker Displacement

One of the major difficulties in interpreting the flash X-ray data from the rigid wheel experiments performed for CAL at McGill University has been that the flow field was recorded on several 8x10 in. X-ray films with consequent considerable uncertainty as to marker position at junction points. Therefore, we examined the capabilities of more powerful improved flash X-ray equipment presently being marketed. It was found that the new equipment will permit, in addition to one-shot recording of the entire flow field, penetration through wider soil bins, at higher contrast and with increased pulse repetition rate. The latter is desirable for observation of transient phenomena.

The present McGill equipment is a 300-kv unit and the new, a 600-kv unit; both made by the same manufacturer*. X-ray beam attenuation varies with X-ray wavelength and follows an exponential law:

$$I = I_o e^{-\sum_{i=1}^{n} \left(\frac{\mu}{\rho}\right)_{i\lambda} \omega_i \rho_c x}$$

where I = X-ray intensity at distance x

I_o = X-ray intensity at source

---

* Field Emission Corporation, McMinnville, Oregon.

$\sum_{i=1}^{n} \left(\frac{\mu}{\rho}\right)_{i\lambda} \omega_i$ is the mass absorption coefficient of the compound at the wavelength λ

ρ_c is the density of the compound

x is the amount of material which must be traversed.

If the X-ray beam must traverse two or more different materials, then the total attenuation is computed by multiplying by the attenuation of each of those materials. Our calculation was based on traversing a bin 8" wide, contained by 1" thick Plexiglas walls. Compound density and mass absorption coefficient were taken for kaolin and 60% (by weight) of water. In the calculation of the mass absorption coefficient the simplifying assumption was made that all the X-ray energy is of the wavelength corresponding to 40% of the peak voltage.

Figure G-1 shows the geometry on which the calculations are based.

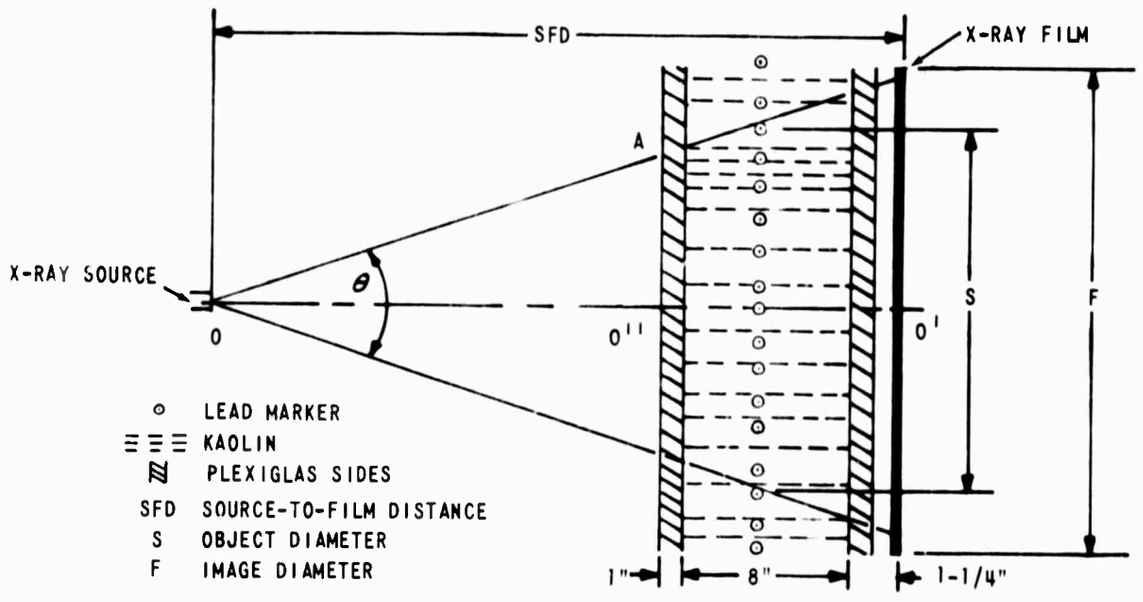

Figure G-1 GEOMETRY FOR MEASUREMENT OF MARKER DISPLACEMENT

The system parameters for both X-ray units under consideration are listed below:

	Summary of System Parameters	
	300 kv Unit	600 kv Unit
Source Size	5 mm	5 mm
X-ray beam cone angle	30^{o}	60^{o}
Resolution of marker	1 mm	1 mm
S.F.D. (maximum)	21"	31"
S (object diameter)	8.24"	29.6"
F (Image diameter)	10.5"	36"
Repetition Rate (pulses/sec)	2	5

The cone angle for both units is based on the minimum energy required at the film which is 0.2 milliroentgen for Royal Blue X-ray film backed by a pair of calcium tungstate intensifying screens.

The 600-kv unit is available with a repetition rate of 5 pulses/sec and the contrast is expected to be improved over the 300-kv unit because twice as much energy is available at the edge of its 60^{o} field than at the edge of the 30^{o} field of the older unit.

Microwave Techniques

There are only two regions of the electromagnetic spectrum where soils have significant transparency. These are the X-ray or hard X-ray region, which was discussed in the preceding section, and the microwave region at wavelengths of 3 cm or more.

Microwaves offer an additional degree of freedom to the experiment designer in that they are reflected from suitable targets; therefore, he is not limited to measurement of transmitted energy as in X-ray work. A possible advantage of the method would be the acquisition of information on displacements in the interior of a soil volume in a continuous rather than an intermittent mode. On the other hand, their reflection properties also limit their usefulness by scattering from many materials, including sensors, and the wheel. Their most severe limitation - one which has not been examined quantitatively - may be heating and consequent water movement in the soil. Since practically no data on microwave penetration in soil were available, a few simple experiments were conducted. Evaluation of these experiments was reported to be in progress at the time of publication of Reference G-1 and significant results are reported below.

Attenuation in sands of different water content was measured at a wavelength of 10.53 cm (S-band). On the basis of measurement of input, reflected and transmitted power, skin depth (the depth of sand at which power has been attenuated to $1/e$ of its magnitude at the surface) was calculated. Working depth in sand at this frequency compared favorably with that of X-rays. At water contents of 0, 4, and 16%, skin depths of 700, 50 and 20 cm, respectively, were found. Total marker displacement measurements were made with the interferometer setup shown in Figure G-2.

Target, sand box and stub tuner make up the test arm and the line stretcher, attenuator and phase shifter the reference arm. When the standing wave patterns in each arm annul each other at the coaxial hybrid, the crystal detector indicates the null by having a zero output.

With this set-up, displacements were computed from phase shift measurements; their accuracy was found to be strongly dependent on the distance of the horn from the sandbox. A distance of several wavelengths appeared to be preferable to distances below one wavelength. In view of

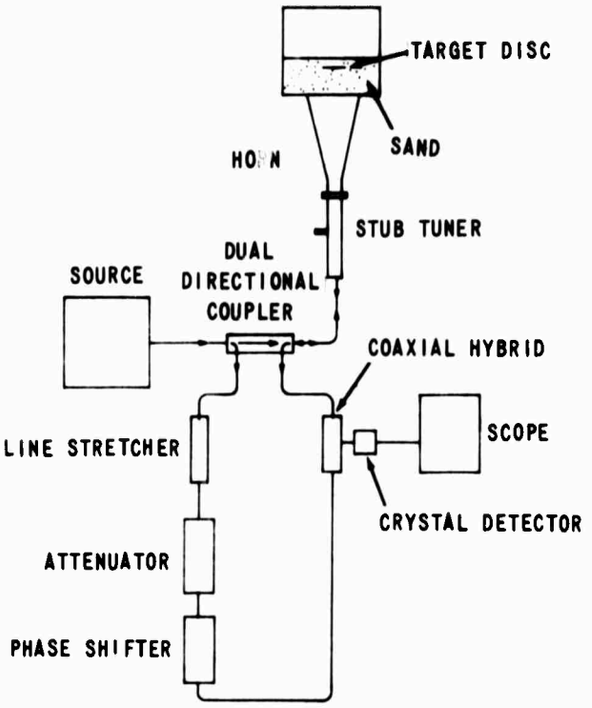

Figure G-2 INTERFEROMETER FOR MEASURING MARKER DISPLACEMENT AT S-BAND

the fact that due to its shorter wavelength, the X-ray method is inherently more accurate. It was concluded that development of a microwave method to replace the X-ray technique as currently used is not warranted.

Pore Pressure Measurement

The response time, t, of a pore pressure measuring setup is given by Bishop and Henkel[G2] as

$$t = \frac{\pi}{4} \frac{1}{c_v C_c^2} \left(\frac{d}{D}\right)^4 \left(\frac{\Delta x}{\Delta p}\right)^2$$

where c_v = coefficient of consolidation

C_c = coefficient of compressibility

d = gage diameter

D = specimen diameter (e.g., diameter of triaxial test cell)

Δx = displacement at tube diameter

Δp = pressure change associated with Δx

The test geometry for which the formula applies is shown in Figure G-3

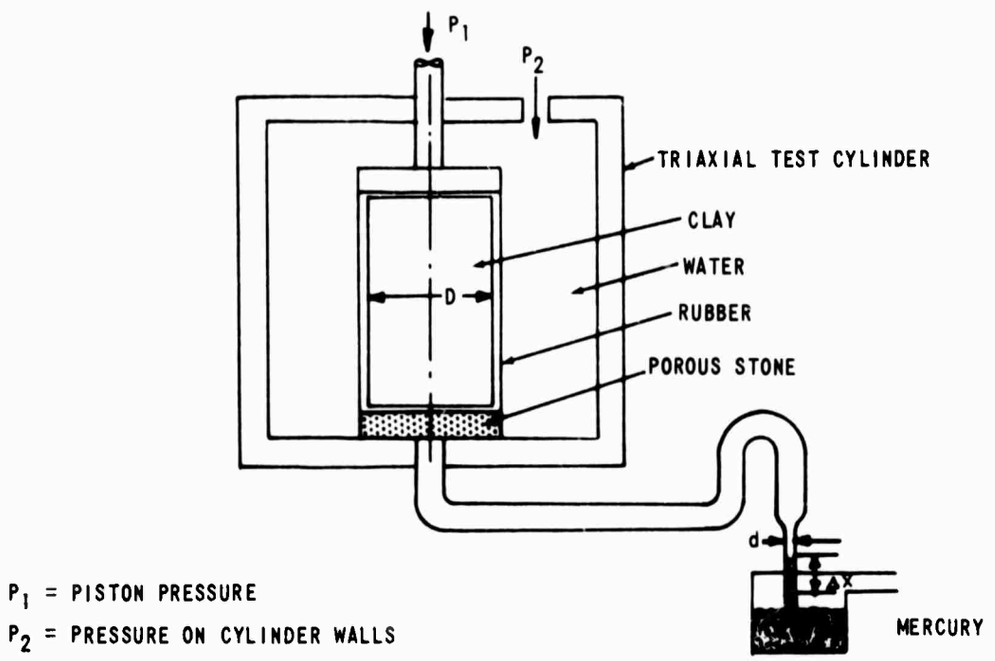

Figure G-3 PORE PRESSURE MEASUREMENT

This test geometry is used in the triaxial test. Here pore pressure is measured for the entire volume under test, this volume is large and the gage response time is long.

It is seen that the response given in the equation is a function of soil material properties, test geometry and gage characteristics. Actual pore pressure changes, whether observable or not, depend only on c_v and C_c. Generally gage response, i.e., the pressure change actually measured and the response time, will depend on the soil volume observed and on the displacement required to obtain a measurement. If both are made small, then the gage will be sensitive and will have a short response time. Such a gage will measure local pore pressure changes that may occur even though no change occurs in a large surrounding volume.

Some progress toward the development of small sensitive and fast pore pressure gages was reported by MIT [G3] in 1963. Our review of that work and recognition of improvements in sensor material since that time encourage us to recommend development of a small pore pressure gage.

The MIT report indicates that several fast response gages appeared technologically feasible, e.g., based on electrical resistance change in a semiconductor, change in resistance in a transistor, change in electrostatic charge of a piezoelectric crystal, and a proprietary pressure-sensitive resin compound. Only the last of these appears to have been built - with poor results due to material failure.

Of these schemes, the pressure sensitive transistor was investigated independently at the same time at CAL *. In principle, transistors having a

---

*"Stressed-Transistor Pressure Transducer", Internal Memo, 26 July 1963.

very thin n-layer and transition layer (1-2 microns) diffused on a p-type crystal appear to exhibit ambient pressure sensitivity. Best results in terms of sensitivity and signal-to-noise ratio , were obtained when such a transistor was operated in the diode mode. However, the device was also found to be highly temperature sensitive and was not further developed at CAL.

The device which is recommended for further development has the geometry shown in Figure G-4.

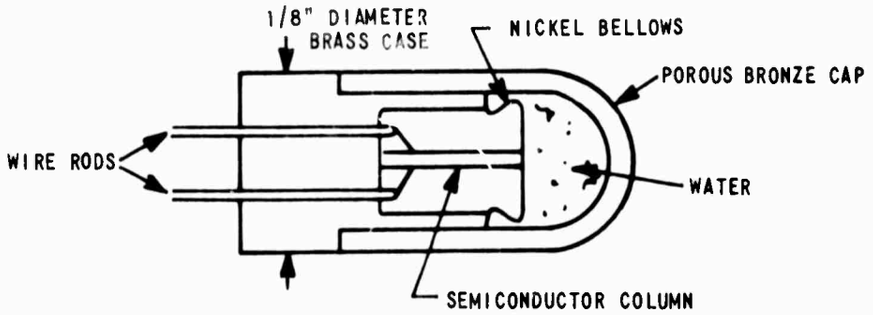

(FROM REFERENCE G3)

Figure G-4 SEMICONDUCTOR COLUMN PORE PRESSURE DEVICE

The sensitive element is a semiconductor column which has one end in contact with metal bellows which is in turn exposed to water within a hemispherical porous shell. The shell is acted upon by the pore water pressure of the soil medium in which the entire gage is embedded.

The semiconductor column changes resistance with pressure. A power source and a bridge circuit are required to sense this change in resistance.

According to the cited MIT report the semiconductor column will have a Δx of only 4.10^{-5} inches at a rated load of 100 psi. The optimum stiffness of the transducer and its response time have yet to be determined. Response time of such a gage (say in water), should be well below one millisecond. The supplier of the semiconductor material* has been contacted and has expressed interest in development of the device.

Remote Sensing

The pore pressure gage described in the previous section is powered from outside the soil and is connected to the power source by two wires. Disturbance of the soil medium, particularly if many such local measurements are to be made, would be much less if this external connection were not needed. The feasibility of three devices; a completely passive, a self-powered, and a pulsed device, for wireless, or remote, sensing was explored. Such "endoradiosondes" have been used to transmit physiological information from within the human or animal body. The devices examined in our brief survey were all developed for such purposes. As a consequence, they have been built for power pressures and for shorter source-to-sensor distances than would be suitable for soil measurements, but in principle they appear highly applicable. The development of a passive, i.e., battery-less, device designed to transmit pressure information from within the eye has recently been reported [G4]. It comprises two flat spiral coils that are electrically equivalent to a parallel resonant circuit and whose resonant frequency is a function of the spacing between the coils. As the surrounding pressure forces the coils closer together, the resonant frequency is changed and a remote frequency-swept transmitter that is coupled to the circuit provides an indication at the frequency at which the energy absorbed by the parallel resonant circuit is a maximum.

For implantation into the eye, the coils are packaged into a cylindrical capsule and capsules have been built 2,4 and 6 mm in diameter and 1 to 2 mm thick. The largest of the capsules resonates near 120 MHz; the resonant frequency changes approximately 10 MHz per mm change in coil

* Bytrex, Inc.

separation. The pressure sensitivity is, of course, a function of the stiffness of the capsule faces that transmit the pressure to the enclosed coils.

The main difficulty in implementing this scheme for the application at hand will be to achieve a close enough coupling between the transmitter outside and the passive resonant circuit within the soil bin - the circuit must absorb a sufficient portion of the transmitted energy for it to be detected by the transmitter. The author indicates that a practical limit to the distance between the transmitter and the radiosonde is approximately 25 times the radius of the coils. However, with antennas or lenses that focus the energy onto the capsule, it should be possible to extend the range considerably. At 120 MHz, such a focusing system would probably be a very large device; at higher frequencies the energy absorption of the soil will become a problem.

An active radiosonde with a self-contained battery was described by Mackay and Jacobson [G5, G6] in 1957. The device was a capsule 2.8 cm long and 0.9 cm in diameter, transmitting both temperature and pressure information at a frequency of approximately 500 KHz. The circuit was basically a transistorized Hartley oscillator; the pressure was sensed by the movement of a diaphragm that moved an iron slug in the oscillator coil, thus controlling the oscillator frequency. The unit was capable of operating for about two weeks.

An improved version of the active radisonde described above was reported by Mackay [G7] in 1959. Also operating in the broadest band (about 500 KHz), this unit was enclosed in a capsule 0.8 cm in diameter and 2.7 cm long, and the transmitter signal was picked up with a 2 1/2 inch diameter coil and fed into a standard broadcast receiver. One mercury cell would power the unit for about 3 days. For indefinite operation, a rectifier diode could be added to the circuit and the mercury cell replaced with a

rechargeable nickel-iron-cadmium cell [G8]. The battery could be recharged from the external oscillator inductively coupled to the rectifier in the radiosonde. A similar endoradiosonde is described by England et al. [G9]

Externally generated pulses charge up a storage capacitor in the Hartley oscillator, of another device, and the time interval between the trailing edge of the externally generated pulse and the beginning of oscillation is a measure of the magnitude of a blocking capacitance in the circuit.[G10] In the reported device temperature and pH control the magnitude of the capacitance, but pressure control appears just as possible. The operating frequency of the charging circuit was 700 KHz. The capsules measured 8 mm in diameter and 25 mm in length.

It is evident that none of the devices surveyed is immediately applicable to laboratory or field experiments in soil. Adaptation to the pressure range of interest would inherently also make them more rugged. Extension of their transmitting range may be a bigger problem. As an immediate step we recommend consideration of a pore pressure probe as described earlier, with built-in battery. Battery life should be less of a problem than in human inplants.

We should also note the potential of such gages for measurements of variables other than pore pressure, e.g., uniaxial solid pressure, temperature or position.

If, as noted earlier, many such gages are to be used in array, then a variation of the method appears attractive in which a high power transmitted pulse excites a passive device into oscillation. One exciter could be used for a number of pressure transducers set to different quiescent frequencies and, by using a time gated transmitter-receiver switch, very high sensitivity receivers adequate to detect the transducer signals could be used without incurring damage from high power transmitted pulses. Locations of the pressure transducers in the soil could be determined between runs by ultrasonic or X-ray means.

REFERENCES

G1. Bartlett, G.E., Kaufman, S., Deutschman, J.N. (co-editors) "Off-Road Mobility Research" Second Semi-Annual Technical Report, Report No. VJ-2330-G-2, Cornell Aeronautical Laboratory, Inc., September 1967.

G2. Bishop, A.W. and Henkel, D. J., The Measurement of Soil Properties in the Triaxial Test. E. Arnold, London, 1964, p. 192.

G3. Miller, E.T., "Further Study of a Rapid Response Pore Pressure Gage", Report No. R63-42, Dept. of Civil Engineering, MIT, Nov. 1963.

G4. Collins, C.C., "Miniature Passive Pressure Transensor for Implanting in the Eye", IEE Trans. on Bio-Medical Eng., Vol. BME-144, No. 2, p. 74 April 1967.

G5. Mackey, R.S., Jacobson, B., "Endoradiosonde", Nature, Vol. 179, p. 1239-1940, June 1957.

G6. Mackey, R.S., Bio-Medical Telemetry, John Wiley, 1967.

G7. Mackey, R.S., "Radio Telemetering from Within the Human Body", IRE Trans. on Med. Elect., Vol. 6, p. 100, June 1959.

G8. Mackey, R.S., "Endoradiosondes: Further Notes", IRE Trans. on Med. Elect., Vol. ME-8, p. 67-B, April 1960.

G9. England, R.J.M., Pasamanick, B., "Radiotelemetry of Physiological Responses in Laboratory Animals", Science, Vol. 133, p. 106, January 1961.

G10. Nagumo, J., et al, "Echo Capsule for Medical Use (A Batteryless Endoradiosonde)", IRE Trans. on Bio-Medical Electronics, July 1962.

Appendix H: INTERPARTICLE FORCE CALCULATION FOR CLAY

Clay particles have a surface charge density which depends on the type of clay and the exchangeable cations on the clay. Figure H-1 shows the crystal structure of montmorillonite [H1], indicating that the clay surface can only be negatively charged.

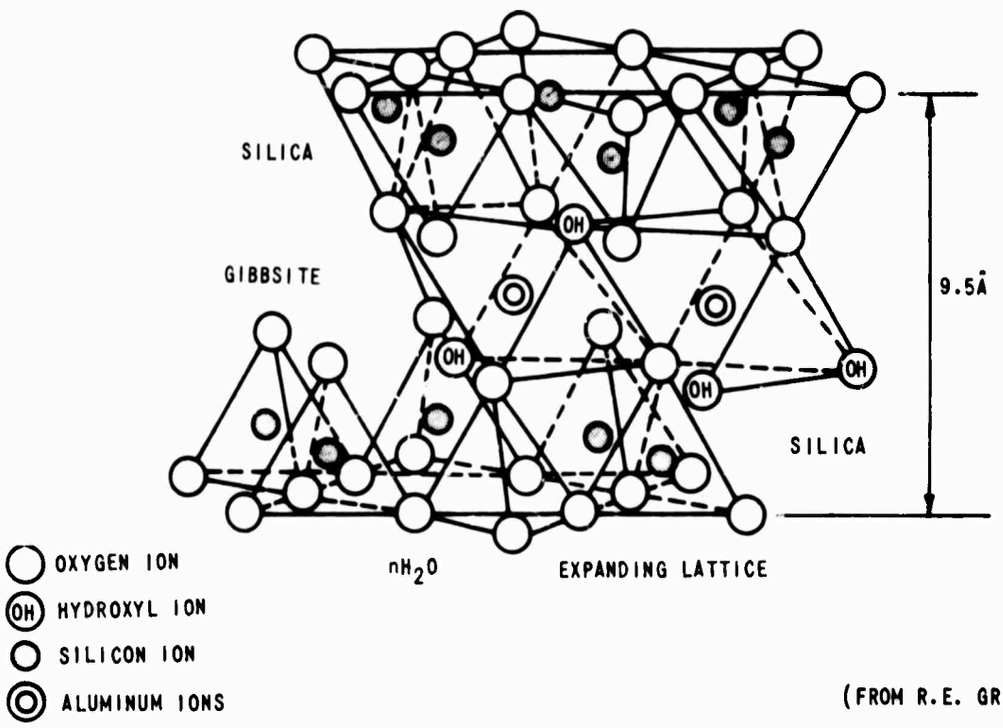

Figure H-1 CRYSTAL STRUCTURE OF MONTMORILLONITE

Montmorillonite consists of alternate layers of tetrahedral silica units and octrahedral hydrous aluminum oxide (gibbsite) units. This alternate layered structure of silica and gibbsite is shown schematically in Figure H-2. The negatively charged silica surfaces attract water which occupies the space between the silica layers. The spacing between the elemental silica-gibbsite-silica sheets depends upon the amount of water available to occupy the space. The expandable lattice of montmorillonite is seen to be due to this interlayered water.

---

* Grim, R.E., "Applied Clay Minerology", McGraw-Hill Book Company, Inc., New York 1962.

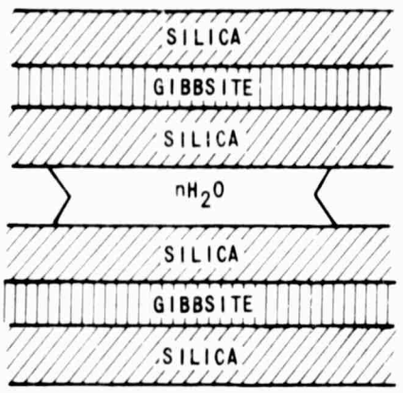

Figure H-2 MONTMORILLONITE SHOWN SCHEMATICALLY

Under water-saturated conditions, the montmorillonite platelets can be separated into elemental silica-gibbsite-silica sheets having a thickness of approximately 10Å (see Figure H-1). It will be shown for 0.1 N solution of NaOH and constant surface charge of 3.0×10^{-4} esu/cm^2 that a zero pressure between the platelets predicts each flat surface will attract a viscous water layer of 40Å. Under these zero pressure conditions, the platelets are separated by 100Å. In general, montmorillonite occurs in sheet form having lateral dimensions of 1000 - 5000Å and a thickness of 10-50Å. The water absorbed on a clay platelet consists of the bound water and the viscous water. Figure H-3 depicts the states of water about a clay particle.

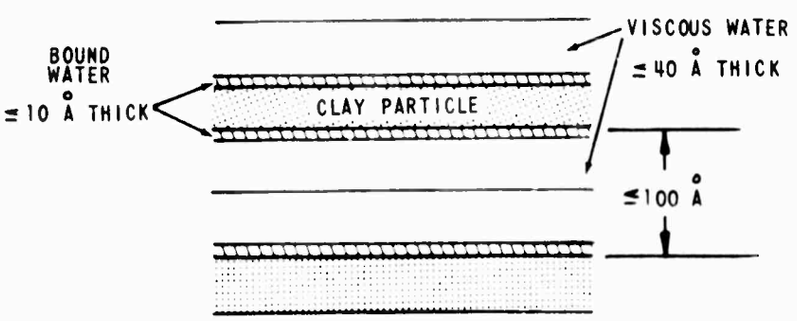

Figure H-3 STATE OF WATER ABOUT A CLAY PARTICLE

Since a clay particle is charged, it interacts with the electrolyte and drags the viscous water around with it as the clay particles move in solution. The interaction of two charged plates in an electrolyte has been calculated by Van Olphen [H2] for one plate separation and the extension to other separations will be presented below. The interaction comes about because the clay particles have an electrostatic field about them, due to their charged surface, which interacts with the ions in the electrolyte. This phenomenon is described by the electric double layer theory. Under equilibrium conditions, a charged platelet in an electrolyte will have a local concentration of ions at a distance X from the platelet's surface which can be related to the potential at that point. Using Boltzmann's theorem, we can express the local ion concentration at some point within the electrolyte as a function of the potential at that point. The appropriate equations* are:

$$n_- = n_-^* \exp(\nu_- e\phi/kT) \tag{1}$$

$$n_+ = n_+^* \exp(-\nu_+ e\phi/kT) \tag{2}$$

$$\rho = \nu_+ e n_+ - \nu_- e n_- \tag{3}$$

where n_-, n_+ local ion concentrations of negative and positive ions

ν_-, ν_+ valence of negative and positive ions

ϕ potential at point in question

n_-^*, n_+^* ion concentrations of negative and positive ions far away from the surface

---

*Much of this work follows the outline given by Van Olphen [H2] in his Appendix III.

ρ	charge density at the point
e	electron charge
k	Boltzmann constant
T	Absolute temperature

If we consider the case for which $\nu_+ = \nu_- = \nu$ or equivalenced ions, then $n_+^* = n_-^* = n$. Using the above equations with this **simplification** in the Poisson equation we get

$$\frac{d^2\phi}{dX^2} = -\left(\frac{4\pi}{e}\right)\rho = \frac{8\pi n\nu e}{\epsilon}\sinh\left(\frac{\nu e\phi}{kT}\right) \tag{4}$$

where ϵ is the dielectric constant of the medium.

If $\frac{\nu e\phi}{kT} << 1$ then $\phi << \frac{kT}{\nu e}$

At room temp $\phi < 25\ m\nu$

Then Equation 4 can be written as

$$\frac{d^2\phi}{dX^2} = \frac{8\pi n\nu e}{e}\left(\frac{\nu e}{kT}\right)\phi = K^2\phi \tag{5}$$

where $$K^2 = \frac{8\pi n\nu^2 e^2}{\epsilon kT} \tag{6}$$

so $\phi = \phi_o e^{-Kx}$ where ϕ_o is the expotential (7)
of the plate.

Equation 7 describes the decay of potential ϕ_o with distance from the platelet. The quantity $1/K$ represents the thickness of the double layer and is called the Debye length.

$$\frac{1}{K} = X_0 = \sqrt{\frac{ekT}{8\pi n \nu^2 e^2}} \tag{8}$$

The double layer charge is given by

$$\sigma = -\int_0^\infty \rho dX \tag{9}$$

- σ the surface charge
- ρ volume charge density

Using Poisson's equation we get

$$\sigma = -\frac{\epsilon}{4\pi}\left[\frac{d\phi}{dX}\right]_{X=0} \tag{10}$$

Evaluating expression (10) we have

$$\sigma = \sqrt{\frac{2\epsilon nkT}{\pi}} \sinh\left(\frac{\nu e\phi_o}{2kT}\right) \tag{11}$$

We can now use this expression to determine the potential of the surface for a plate of constant charge density. Table III of Reference H2 gives the results for a plate of constant surface charge of 11.7 $\mu C/cm^2$ at various electrolyte concentrations and charges.

Table III OF REF. H2
SURFACE POTENTIAL ϕ_o FOR CONSTANT CHARGED SURFACE OF 11.7 MICROCOULOUMBS/cm^2

NORMALITY, C	1-1 VALENT		2-2 VALENT	
	$1/\kappa$	Φ_o	$1/\kappa$	Φ_o
10^{-5} N	10^{-5} cm	355 mV	0.5×10^{-5} cm	178 mV
10^{-3} N	10^{-6} cm	240 mV	0.5×10^{-6} cm	120 mV
10^{-1} N	10^{-7} cm	130 mV	0.5×10^{-7} cm	65 mV

Equation (4) can now be evaluated with appropriate boundary conditions to give the potential between interacting flat double layers of the Gouy type. Explicit use is made of the fact that we are dealing with a constant surface charge, not with a constant surface potential.

Figure II-4 below shows the potential between interacting parallel plates in one dimension.

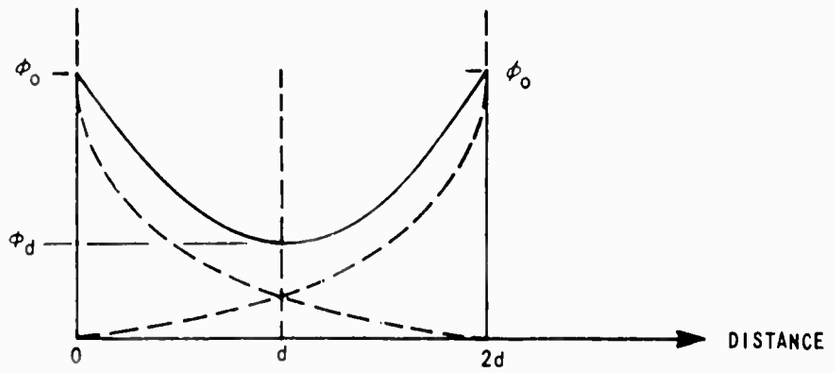

Figure II-4 POTENTIAL BETWEEN INTERACTING PARALLEL PLATES

The boundary conditions are at $X = d$, $\frac{d\phi}{dX} = 0$, $\phi = \phi_d$; $X = 0$, $\phi = \phi_o$

integrating $$\frac{d^2\phi}{dX^2} = \frac{8\pi n \nu e}{\epsilon} \sinh\left(\frac{\nu e\phi}{kT}\right)$$

gives $$\left(\frac{d^2\phi}{dX}\right)^2\Bigg]_0^{\frac{d\phi}{dX}} = \frac{8\pi nkT}{\epsilon} \cosh \frac{\nu e\phi}{kT}\Bigg]_{\phi_d}^{\phi_o}$$

so $$\frac{d\phi}{dX} = -\left(\frac{8\pi nkT}{\epsilon}\right)^{\frac{1}{2}} \left[2\cosh \frac{\nu e\phi}{kT} - 2\cosh \frac{\nu e\phi_d}{kT}\right]^{\frac{1}{2}} \qquad (12)$$

The gradient of the potential in Equation (12) is used in Equation (10) to relate the hypothesis of constant charge to a calculation of the midway potential, ϕ_d. The equation which results is

$$\left[2\cosh\left(\frac{\nu e\phi_d}{kT}\right) - 2\cosh\left(\frac{\nu e\phi_d}{kT}\right)\right]^{\frac{1}{2}} = \sigma\left(\frac{2\pi}{\epsilon nkT}\right)^{\frac{1}{2}} = \text{const.}$$

Given the electrolyte concentration, plate separation and charge density on the platelets, Van Olphen calculates sets of values for $-u$, where $u = \frac{\nu e\phi_d}{kT}$ and $-Z$, where $Z = \frac{\nu e\phi}{kT}$ and defines $-u$ and $-Z$ as the midway and surface potential respectively. This information can now be used to calculate the pressure between two flat double layers. Langmuir [H3] derived the expression given in Equation (13). This expression gives the total repulsive pressure acting on two flat charged planes in an electrolyte as a sum of osmotic pressure terms. The total pressure is constant across the space between the planes and is evaluated midway between the plates. This equation strictly applies for an equilibrium ion solution.

$$\begin{aligned} P &= \left[n_o\left(e^{\nu e\phi/kT} + e^{-\nu e\phi/kT}\right) - 2n_o\right] kT \\ &= 2nkT\left(\cosh\frac{\nu e\phi}{kT} - 1\right) \end{aligned} \qquad (13)$$

The pressure between two flat charged plates can now be evaluated. Initially we specify:

(1) Charge layers are of the Gouy type

(2) Constant surface charge - take 3×10^{-4} esu/cm^2 = 11.7 μC/cm^2

(3) Plate separation = 2 d; take 2 d = 100 Å

(4) Electrolyte and normality - take NaCL, 0.1N

Using this information we find K which is given as 10^7 cm^{-1} = 10 Å in Table III of Reference H2. We calculate $\left(\frac{dy}{d\xi}\right)_0 = \frac{\sigma(5.7 \times 10^{-5})}{\sqrt{N'}} = 5.6$ and Kd; where $y = ve\phi/kT$ and $\xi = Kx$. Using these values we look up the value of $u = ve\phi_d/kT$ in Reference H2. For the example chosen $P = 0.023$ atm.

Figure H-5 shows the magnitude of repulsive pressure versus various plate separations; as shown qualitatively in text books (e.g., Scott). For the case shown, there is no electric double layer interaction between the plates when the plate separation is approximately 100 Å or greater.

The attractive Van der Waals pressure [H4] between the neutral atoms on the platelets can be calculated from

$$P = \frac{A}{6\pi\delta^3} \tag{14}$$

where A is the Hamaker constant

δ the separation of two thick plates

The material properties of the plates come into the calculation of A since $A = \pi^2 q^2 \left(\frac{4}{3}\alpha^3 h\nu\right)$. q^2 is the number of atoms per cm^3 of the plate material and α is the polarizability of an atom and $h\nu$ is its ionization energy. This expression applies for the case of additive London-Van der Waals forces.

For most elements the Hamaker [H5] constant is experimentally found to be of the order of 10^{-12} to 10^{-13} erg. Using A = 10^{-13} erg we calculated the attractive pressure using Equation (14). These results are plotted in

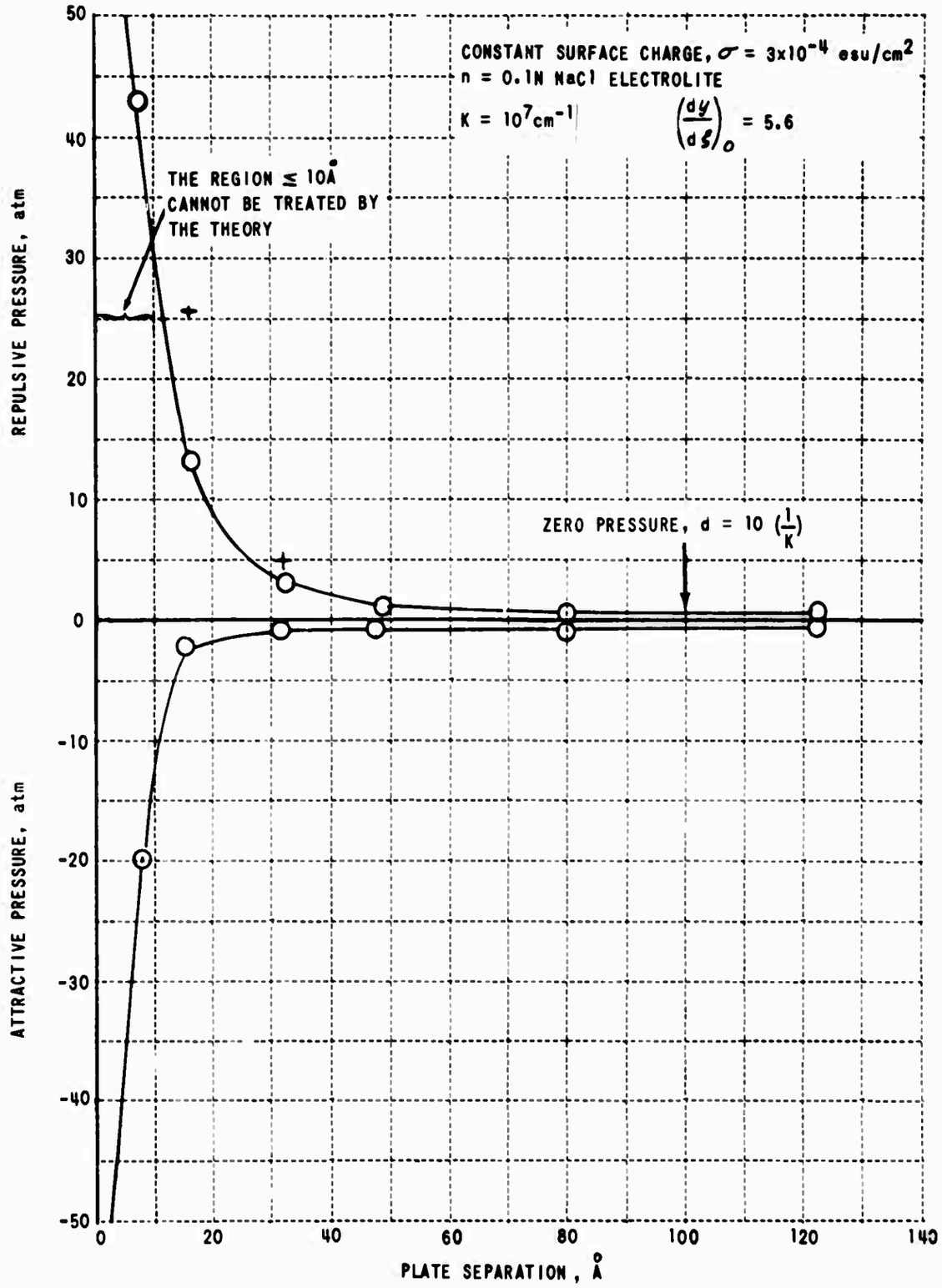

Figure H-5 INTERPARTICLE PRESSURE RELATIONSHIP

Figure H-5 for direct comparison with the repulsive pressure. Figure H-5 indicates that the parallel plate separation of 10Å is not physically meaningful, since this would require the ions to penetrate the bound layers of water. Also, it is physically impossible for the electrolyte concentration to reach the potential calculated at this point.

Figure H-5 represents the results of interparticle pressure calculation for an idealized two particle system. Similar calculations could be made for other electrolyte concentrations and surface charge.

In a system of many finite size particles having a particle separation of 100 Å or more, we can assume that the particles do not interact. The possibility of a new interaction, such as that produced by the edge of the platelets which carried a different sign charge density requires further consideration. If the particle separation is 100 Å, the particle thickness 25 Å, the particle density 2.6 gm/cm^3, and all voids are filled with water, the sytem would contain 155% water by weight. Such a system would have very little shear strength. If the separation between particles is reduced and the plate thickness increased, water contents in the vicinity of the plastic limit result.

REFERENCES

H1. Means, R.E., Parcher, J.V., Physical Properties of Solids, p 23 -

H2. Van Olphen, H., Clay Colloid Chemistry.

H3. Langmuir, I., "The Role of Attractive and Repulsive Forces in the Formation of Tactoids, Thexotropic Gels, Protein Crystals and Coacervates", Journal of Chemical Physics, Vol. 6, 1938, pp 873-896.

H4. Sparnaay, M. J., "Measurement of Attractive Forces Between Flat Plates", Physica XXIV, pp 751-764, 1958.

H5. Overbeek, J. Th. G., Sparnaay, M. J., London-Van Der Waals Attraction Between Macroscopic Objects, Disc. Farad. Soc. 1954, pp 12-24.

BLANK PAGE

Appendix I: SOIL FABRIC STUDIES

An earlier report [11] pointed out that the spatial configuration of the soil particles, called "fabric" (as distinct from "structure" which also includes consideration of interparticle forces) is an indicator of soil state. Fabric is defined by the spacing between particles, their angular orientation and their size. Extremes are random fabric, in which the particles are not in contact and are randomly oriented; flocculated fabric, in which the particles are randomly oriented but make contact along their edges; and fully oriented fabric, in which the particles are closely spaced with their plate faces generally parallel to one another. These fabrics are the result of interparticle forces (e.g. those related to the pH of the liquid medium) and of applied loads. Consolidation pressures, say during soil bed preparation, tend to produce fully oriented fabric. Particles near shear planes have been reported to be more closely spaced than those away from these planes. Fabric is an indicator of the internal and external forces that have acted on a soil long enough to be propagated. Hence, changes in fabric are indication of energy dissipated in the soil.

Our efforts toward development of quantitative measures of clay fabric were based on three methods of fabric observation: (1) polarizing microscopy, (2) X-ray diffraction and (3) electron microscopy.

Specimen Preparation

Common to these methods is the problem of extracting and preserving an undisturbed soil specimen in a form suitable for observation. The method usually adopted is to replace the soil water by a solid material. A series of water soluble polythylene glycol waves have been used for this purpose.

These waxes vary in specific gravity from 1.0 to 1.2 and in melting point from 35 to 70° C with corresponding variation in hardness. The choice of wax within this range was found to be controlled by two conflicting requirements: The desire to make the wax as hard as possible so that it can be cut and polished readily, and the need to prevent alteration of the clay fabric during the impregnation process. Prior information on overall dimensional distortion was somewhat contradictory. Quigley and Thompson[I2] reported linear shrinkage of from 7.2 to 8.8% with a wax having a melting point of 65° C. Rosenquist [I3] found a linear shrinkage of 15% with a wax of unspecified melting point, whereas Leitch and Yong [I4] reported a linear shrinkage of 1-2% for an equal-volume mixture of two waxes having individual melting points of 45 and 42 C. Experience at McGill University during experiments performed for CAL under ORMR [I5] indicated the desirability of going to the lower melting point waxes, because additional problems, typically large wax-crystal formation upon drying, appeared to be associated with wax mixtures and with the high melting point waxes. The effort at CAL was more concerned with the ability to cut and polish impregnated specimens without distorting the fabric or without smearing the wax. These tests clearly indicated the superiority of the higher melting point waxes.

A double substitution procedure, in which a first impregnation with low temperature wax was followed by immersion in a high melting point wax appeared to give the best results at CAL. No data are available on other aspects of wax choice, e.g. the completeness of the substitution process. The latter might be important in preparation of the impregnated specimens for electron microscopy, as will be explained later.

Polarizing Microscopy

Fabric observation by polarizing microscopy yields information on the angular orientation of crystalline soil particles. When a single birefringent crystal is viewed in plane polarized light under crossed Nicols prisms, it will transmit no light when the direction of the optical axis

coincides with the polarizing direction of the incident beam and a maximum will be transmitted at 45° to that direction. If the crystal axis is inclined with respect to the angle of polarization, then the angle through which it must be rotated to obtain maximum (or minimum) light transmission is a measure of the orientation of the crystal. Similar behavior is exhibited by an aggregate of birefringent crystals; maximum (or minimum) light transmission will no longer differ so much and the angle of rotation necessary to obtain the maximum (or minimum) is now a measure of the average orientation of the aggregate. This principle is used to measure the orientation of clay particles in fabric specimens. The optical rotation introduced by the inclined crystallites is also proportional to their thickness in the direction of the optical axis. In order to obtain observable maxima and minima a section thickness of 25 μ has commonly been employed, necessitating the use of a microtome to obtain uniform sections. A field several millimeters in diameter is customarily viewed in the microscope. A typical kaolin plate - which is an aggregate of several tightly bonded platelets - is estimated to be 100Å thick and about 1 μ in diameter. It is apparent then that the method gives some average of the orientation and thickness of many particles. Morgenstern and Tchalenko[I6] have shown that the method works for various models of the distribution of spatial particle orientation. Leitch and Yong[I4] showed qualitatively that measures of orientation can be developed based on measurement of angular retardation.

Under subcontract to CAL, Prof. Yong [I5] made orientation determinations on the kaolin used in the rigid-wheel tests. One of the difficulties associated with the method stems from the need to use thin sections. A hand drawn microtome knife, used at first, produced a saw-tooth-like layered section and uneven drying of the higher melting point waxes also caused non-uniformities. With the cutting technique developed under the subcontract, involving a mechanized microtome and a softer wax, improved specimen uniformity was obtained. Briefly, it was found that black and white photography of retardation maxima (or minima) of clay specimens taken from

the bin before and after passage of a load did not produce significant information. Subsequent exploratory effort at CAL indicated that a graphic record of intensity of transmitted light vs microscope stage angle would probably produce useable orientation data. The route successfully chosen at McGill University was to transpose the light retardation by means of a "Gypsum Red Plate" further into the visible region and to record the resulting patterns on color film. The McGill Report [I5] contains a number of color prints from clay specimens; these were orginally prepared as an acidic slurry (flocculated fabric) and as a basic slurry (oriented fabric) and were subsequently equilibrated at a number of suction pressures approximating various degrees of consolidation. The colors recorded range from red $\overline{+}$ which is characteristic for light transmitted perpendicular to the plate faces of oreinted clay - to green and brown - which correspond to 45 and 135^{o} edge orientations, respectively. A practical method for quantitative interpretation of these colors in terms of the orientations they represent should not be difficult to develop. Whether the method has advantages over the X-ray diffraction method, which is discussed next, has yet to be determined.

X-Ray Diffraction

Determination of clay orientation by X-ray diffraction is based on identifying the Bragg angles of the plate and edge facrs of the clay crystallites under consideration and comparing the intensities of radiation reflected at these angles.

A rigorous method for measuring platelet orientation by this principle has been established by Martin [I7]. For kaolinite the intensities of the $\langle 002 \rangle$ and the $\langle 020 \rangle$ reflections are measured with the aid of a pole figure device. The mean ratio of these intensities is the measure of orientation and the standard deviation in the ratio is a measure of fabric inhomogeneity.

At CAL a simpler X-ray diffraction technique has been tried and found promising. Fabric is determined on the basis of diffraction from the plane face of a clay block; intensity is recorded as a function of Bragg angle by the diffractometer. The area illuminated in the diffractometer used (GE Model XRD-5) is 1/4 x 1/2 inch and the X-rays penetrate to a depth of 25 μ. Hence, the orientation of many crystallites is averaged. A rough check on the presence of texture effects (which - if strong - would necessitate the use of a pole figure device) was made by determining the <002> and <020> intensities of a block, first while stationary and then while spinning about an axis perpendicular to the face under examination. No significant change in the intensities was noted. As a further check on the significance of texture, a section about 125 μ thick, microtome-cut from a clay block previously measured in the diffractometer, was examined by transmission Laue photography. The degree of texture found was deemed too small to invalidate the simple diffractometer method. However, more specimens must be measured before an error analysis can be made.

Some initial difficulties in the use of the method were related to smearing of wax during microtomy. This presents a more serious problem to X-ray diffraction than to polarizing microscopy, because in the former case the layers that are closest to the surface - and most likely to be smeared - are the strongest contributors of reflected X-ray energy, whereas in the latter all layers of the specimen contribute equally to light retardation regardless of their proximity to the surface.

Other difficulties were associated with non-uniformity and looseness of specimens removed from the soil prepared for the wheel tests. In order to get better acquainted with the capabilities of the X-ray method these difficulties were circumvented by examining a specially consolidated specimen of the same kaolin that was used in the wheel tests. It was expected that the specimen surface perpendicular to the direction of consolidation would have stronger reflection from the plate face (<002> direction) and that a face parallel to the consolidation direction would reflect more strongly from the clay edges <020> directions) as indicated schematically below:

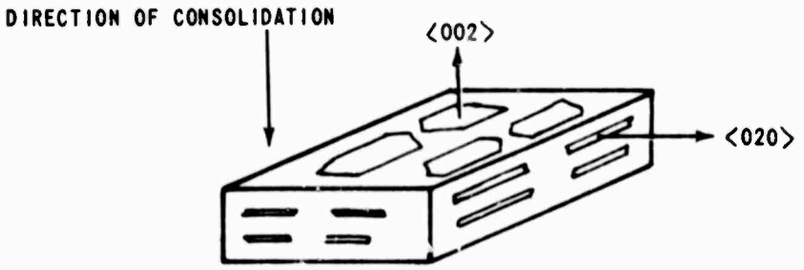

Actually the <002> peaks were higher than the <020> peaks for both surfaces. However, the ratio of these peaks had the expected trend, having a magnitude of 140 for the face perpendicular to the consolidation direction and 6 for the parallel face. In the table below we list our values for the peak ratio $(\frac{\langle 002 \rangle}{\langle 020 \rangle})$ along with those found by other observers.

<002>/<020> Peak Ratios for Kaolin

	Surface Perpendicular to Consol. Direction	Surface Parallel to Consol. Direction	Specimen Preparation
Martin [I7]	200		Dispersed kaolin dried on a glass slide
Nowatzki [I8]	33		Parallel oriented, consolidation condition not known
	3.3	2.1	Consolidated at 500 psi and subjected to shear stress
CAL	140	6	Consolidated

Comparison of these values indicates agreement only in trends. A question still to be answered is what these ratios should be for extreme cases of

preferred orientation. In particular we want to know whether the magnitude of the $\langle 002 \rangle / \langle 020 \rangle$ peak ratio can ever be less than one.

Electron Microscopy

Electron microscopy is attractive as a tool for fabric assessment because it can provide information on all three descriptors of fabric: particle size, orientation and spacing. It is also the least developed of the three methods of fabric observation whose development as quantitative tools is under investigation.

Soil specimens are viewed in direct transmission, if ultra-thin sections ($\sim 0.1\mu$ thick) are prepared or thin-film replicas of the specimen are viewed in transmission. The most recent method is scanning electron microscopy which is suitable for bulk specimens. The former two methods have been used by many investigators to study clay particle shape and size [I9]. In many cases dry clay particles are examined; if direct transmission electron microscopy of undisturbed fabric is desired the soil water must be replaced by a solid which will not melt in the electron beam, as attempted by Smart [I10, I11]. He made an extensive comparative study of methods of specimen preparation and electron microscopy. His best visual results were obtained by scanning electron microscopy which produces images of considerable depth; however, these images are difficult to assess quantitatively.

The method selected for study at CAL is replication. This decision was largely based on schematics published by Sloane and Nowatzki [I12] indicating that quantitative fabric information may be deduced from such electron micrographs.

Ideally, the thin film replica is a faithful and reproducible negative of the specimen surface, which must have been undisturbed by the preparation method. The replica must be free of artifacts and of such detail that the outline of each clay particle can be clearly recognized. Although many variations in preparation procedure have been explored such replicas have not yet been obtained reproducibly. Figure I-1 is representative of early results obtained; the clay particles are well defined but, since the replica was taken from a face parallel to the direction of consolidation, absence of any particles on edge must be taken as evidence of fabric distortion. Some success was attained with a variation in preparation, further described below, in which clay particles are left attached to the replica. The table below lists the variables of preparation procedure in seven categories. It should be noted that not all combinations of variables were explored and the tabular arrangement does not indicate any correspondence along horizontal lines.

PROCESS VARIABLES IN ELECTRON MICROSCOPY OF CLAY

WAX MELTING POINT	STORAGE	SURFACE PREPARATION		REPLICATION	SHADOWING	RELEASE
		MECHANICAL	CHEMICAL			
37-40 °C 53-56 °C 60-63 °C	REFRIGERATOR DESICCATOR	FRACTURE MICROTOMY ULTRA-MICROTOMY 600μ SiC POLISH 1μ DIAMOND POLISH FREEZE POLISH	ETCH WAX "FEW" DROPS DICHLORETHYLENE 100 DROPS DICHLORETHYLENE ETCH CLAY HF-SOLUTION HF-VAPOR	PARLODION CARBON	ROTARY CARBON GERMANIUM UNDIRECTIONAL CARBON GERMANIUM	STILL WATER ULTRASONICALLY AGITATED WATER HF-SOLUTION

Figure I-1 ELECTRON MICROGRAPH OF DISTURBED SURFACE

With the exception of a consolidated and sheared specimen from Cornell University (impregnated at CAL) and an unimpregnated, dried and very dense specimen from the University of Arizona, all clay specimens were received wax-impregnated at CAL. Re-impregnation of the lower melting point waxes with a higher melting point and harder wax proved beneficial in two respects: (a) cutting and polishing of the harder wax without obvious fabric disturbance was easier, (b) uncontrolled surface changes due to water absorption and consequent wax dissolution were less obvious. Storage of the clay at household refrigerator temperature in order to harden the wax appears to be a common practice - one which unfortunately brings about moisture condensation upon exposure to room temperature and humidity. It should be noted again that such changes at the surface are much more important when surfaces are examined, as in electron microscopy, than in polarizing microscopy even though the specimen thickness there is also only 25 μ . At CAL, vacuum desiccation of the impregnated specimen blocks proved beneficial in that upon removal from the desiccator the specimen blocks had a less "waxy" feel and the moisture condensation problem was reduced.

The surface of an impregnated clay block must be further prepared for electron microscopy or for any of the other examination methods discussed here, because it is wax-rich and the fabric was disturbed during rough cutting before impregnation. The purpose of all the mechanical surface preparation methods listed in the table is to produce a surface that is representative of an undisturbed plane in the interior of the soil under examination. Being composed of many plans, a facture surface does not meet this criterion. Nevertheless, one fracture surface was replicated and examined in the microscope, because it did not require any other surface preparation. The other mechanical preparation methods listed were all explored but will not be discussed here, because at this stage of the investigation no significant advantage can be claimed for any one method.

Chemical surface preparation is necessary in order to obtain relief. If the clay surface (or any other surface to be examined) would be perfectly smooth, then a surface replica would also be perfectly smooth and thus would not contain any information on the particles making up the surface. In the case of our replicas one has then a choice of creating relief by etching the clay or by removing the wax. In either case, the objective is to obtain an outline on the replica of both the clay particles and the wax matrix as they existed on the surface before etching. A method for removing a thin layer of wax by a dichlorethylene "etch" was used by Sloane and Nowatzki [12] and a visit was made to Professor Sloane at the University of Arizona to become familiar with the method. On the basis of numerous experiments following this consultation we have come to the conclusion that his method, designated as " ~100 drops" in the table, is unsuitable for specimens containing much wax (i.e. a large void ratio before impregnation); apparently too many clay particles of such specimens become loose and change position or are covered with partially dissolved wax. Attempts to modify the procedure by using only a few drops of the wax-etchants produced erratic results. Attempts to etch the clay particles with hydrofluoric acid (HF) also were doomed to failure, because even when HF vapor was employed, loss of wax in subsequent rinse was unavoidable.

The variations in the replication and shadowing procedure in the Table are only listed to indicate the large number of tests that may be required to fully explore the potential of the procedure. Briefly, they indicate whether the primary replica was either a plastic one or one where the carbon was applied to the clay specimen directly. To obtain contrast, germanium was usually applied following carbon coating using one of the two shadowing procedures indicated.

The last column in the Table indicates the procedures used for removing clay or wax particles adhering to the replica prior to its insertion into the electron microscope. Actually, some of the best qualitative indication

of the orientation and spacing of clay particles was obtained when the wash in HF was omitted so that clay particles adhered to the replica, as shown in Figures I-2a and I-2b. These electron micrographs are from adjacent regions of one side of a consolidated specimen. The flocculated areas could be seen with the unaided eye throughout the specimen and are shown at low magnification in Figure I-3. However, we deem this procedure not suitable for quantitative work because loss of some clay particles that wash away with the wax cannot be controlled or, in some instances, too many clay particles adhere so that the replica becomes opaque to the electron beam.

Our problem is to obtain a characterization from a two-dimensional image which is valid for a three-dimensional body. The approach planned is to draw a number of diameters across representative image areas and to measure particle size, spacing, and orientation along these diameters. Alternatively the number of particle-particle contacts along such a diameter might serve as a relative measure of spacing. One of the main checks on the method, in fact one that can be applied to all three methods, is to view three sections of the specimens that form a cube. The observations, and the measures eventually established must be mutually compatible and must satisfy volume relationships.

Summary of Fabric Studies

Since knowledge of chemical composition and water content do not permit predicting soil strength properties, its state must be described by additional measures. Such measures can be developed from fabric observation. Techniques for preparing specimens for such observation by replacing the liquid phase with a hard wax have been applied. Observations of orientation, spacing and size of particles by polarizing microscopy, X-ray diffraction and electron microscopy have been made.

We found that the techniques, as described in the literature, produced fabric changes during the preparation process and considerable techniques

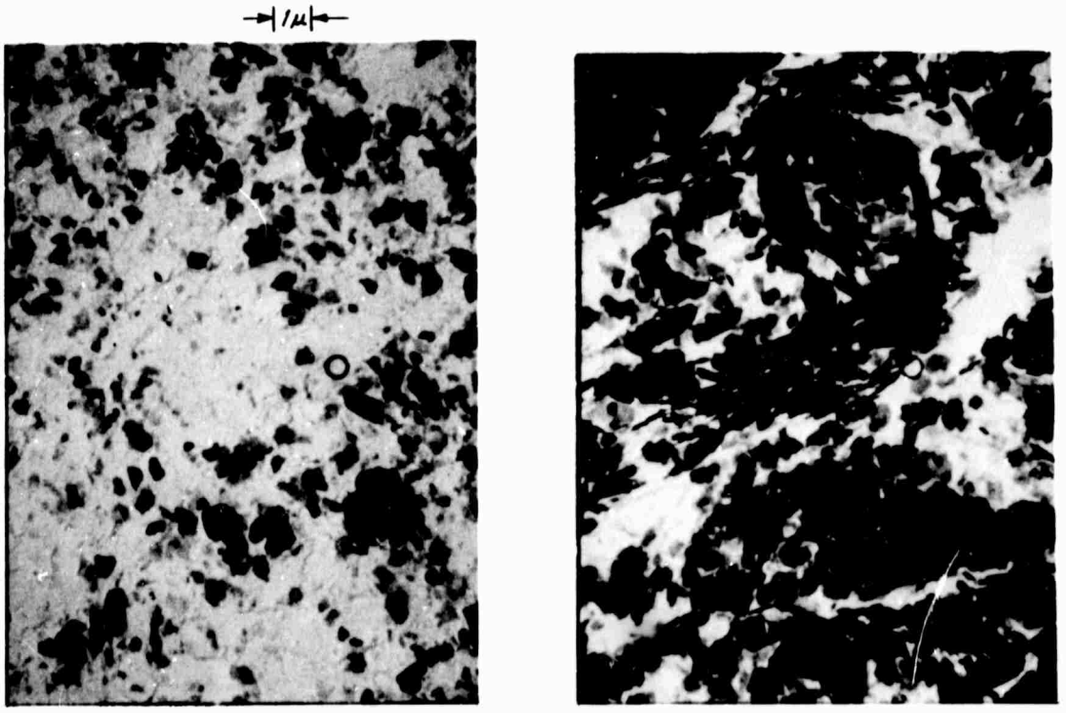

(a) AREA BETWEEN "FLOCCS"

(b) FLOCCULATED AREA

Figure I-2 ELECTRON MICROGRAPHS OF CONSOLIDATED SPECIMEN

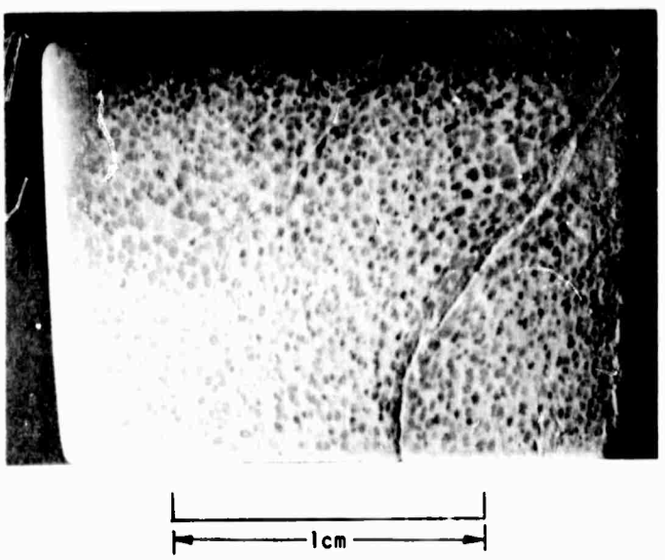

Figure I-3 PHOTOGRAPH OF CONSOLIDATED SPECIMEN OF FIGURE I-2

development effort has been required. While our examination of the wax impregnation method has only been exploratory, we conclude that problems encountered with preparation of specimens for electron microscopy make it advisable to explore alternate methods of water-substitution.

REFERENCES

I1. Bartlett, G.E., Kaufman, S., and Deutschman, J.N.(co-editors) "Off-Road Mobility Research" Second Semiannual Report, Report VJ-2330-G-2, Cornell Aeronautical Laboratory, Inc., Buffalo, New York, September 1967.

I2. Quigley, R.M. and Thompson, C.D., "The Fabric of Anisotropically Consolidated Sensitive Marine Clay", Canadian Geotechnical Journal, III, 2, 61-73, 1966.

I3. Rosenquist, I.T., "Investigations into the Clay-Water Electrolyte System", Norwegian Geotechnical Institute Publication No. 9, 1955.

I4. Leitch, H.C., and Yong, R.N., "The Rate Dependent Mechanism of Shear Failure in Clay Soils", McGill University, Soil Mechanics Series No. 21, August 1967.

I5. Yong, R.N., and Japp, R.D., "Soil Water Relationsips and their Engineering Applications", McGill University Report to CAL, September 1968.

I6. Morgenstern, R.N. and Tchalenko, J.S., "The Optical Determination of Preferred Oreintation in Clays and its Application to the Study of Microstructure in Consolidated Kaolin", Proc. Royal Soc. A, 300, 218-250, 1967.

I7. Martin, R.T., "Quantitative Fabric of Consolidated Kaolinite", MIT, Dept. of Civil Engineering, Research Report R65-47, September 1965.

I8. Nowatzki, E.A., "Fabric Changes Accompanying Shear Strains in a Cohesive Soil", Doctoral Thesis, Department of Civil Engineering, University of Arizona, 1966.

I9. Beutelspacher, H. and Van der Marel, H.W., Atlas of Electron Microscopy of Clay Minerals and Their Admixture, Elsevier Publishing Co., 1967.

I10. Smart, Peter, Soil Structure, Mechanical Properties and Electron Microscopy, Ph.D. Dissertation, Cambridge U., October 1966.

I11. Smart, Peter, Particle Arrangements in Kaolin, 15th Confer. on Clay and Clay Minerals, Pergamon Press, 11, 241-254, 1967.

I12. Sloane, R.L., and E. A. Nowatzki, "Electron-Optical Study of Fabric Changes Accompanying Shear in Kaolin Clay", Third Panam. Conference on Soil Mechanics and Foundation Eng., 1967.

BLANK PAGE

Appendix J: VISIBILITY STUDY--PLANS FOR FIELD TESTING

Test plans have been developed for the initial phases of a field study dealing with the effects of light level and obscuration on the driving of an off-road vehicle. This investigation is designed to obtain quantitative field data concerning system performance under various test driving conditions and to provide a basis on which to design simulator experiments. The field data are intended to serve as checkpoints against which simulator data can be compared and evaluated and this would be used to validate simulator data. Only grossly different conditions are included in the field study plan. The simulator can be utilized to obtain a more precise and comprehensive examination of the various driving conditions of interest. As a body of simulator data accumulates and the validity and reliability of the simulator is determined, it is expected that the design of future field studies would be oriented more and more toward the verification aspects of the role of the driver in off-road mobility and the simulator would become the basic research tool.

In the plan for the first field study, the task of the subjects is to drive a vehicle along a pre-selected, winding path over relatively smooth terrain. The goal of this study is to determine the effects on system performance of driver visual degradation that occurs (1) under various nighttime driving conditions and (2) under conditions in which trees, brush and other objects obscure the driver's view of the forward field of travel.

This initial study would be conducted in five phases. These are described below.

PHASE I - Installation and checkout of vehicle instrumentation

Instrumentation to provide permanent records of the following continuous measurements is requred:

(1) elapsed time;
(2) vehicle velocity;
(3) distance traveled;
(4) accelerator position (with transmission position indicated);
(5) steering device/brake position;
(6) fuel consumption;
(7) motion accelerations - (bounce, pitch, roll and surge);

The data from these records are needed to provide measures of system performance that can be used as baseline measurements in the analysis of subsequent test data. These measures include:

(1) total elapsed time and average velocity for the entire course;
(2) time required and average velocity for individual segments of the course, e.g., a single curve, curves or a straight section of the course;
(3) relative system efficiency as measured by fuel consumption, frequency and pedal pressures associated with brake-accelerator actions, number of course correction actions;
(4) ride quality as determined by the motion data.

The motion acceleration data also provide a reference input source driving the motion platform of the simulator. Video records can also be obtained on some of the test runs for simulator use.

PHASE II - Basic System Performance Checkout

During this phase, the vehicle would be driven through various maneuvers to ascertain basic system performance characteristics over flat and relatively smooth terrain. No visual obstructions should be present. Since the primary concern is with system performance, not vehicle capabilities, several experienced drivers (4 or more) would be used to collect these data. The basic data, collected after system performance in the maneuvers has stabilized for each of the drivers, would include:

(1) Maximum attainable safe velocity

(2) Acceleration characteristics

(3) Deceleration characteristics

These data would serve as guidelines for the conduct of the test path checkout (see Phase IV) and would provide a basis against which to evaluate the Phase IV data. Since terrain irregularities and path obscuration will be present in the test path, the influence of these factors can be ascertained by reference to the data obtained in this basic system checkout phase. These data also would establish certain of the test path requirements such as the required length of the straightaways.

PHASE III - Test Path Layout

This phase, in part, could be conducted simultaneously with Phase I and Phase II.

The test path would have the following basic characteristics:

-- The path would represent an unimproved terrain.

-- Within constraints imposed by the terrain, the curves in the path would be similar to those that would be detailed during Phase II, i.e. radii of the curves would be approximately 25, 50 and 100 feet and turn angles would be 30^{o}, 45^{o}, 90^{o} and 180^{o}. Both single and compound curves would be represented.

-- A straightaway to permit attainment and maintenance of the predetermined maximum safe velocity for at least 10 seconds would be provided between curves or a combination of curves. (At 15 miles per hour, for example, this would require a minimum of 230 feet plus run-up distance.)

-- Each basic curve or combination of curves would appear both in terrain that affords a relatively clear view of the entire curve or combination of curves and in terrain that, because of trees, brushes or other objects,

effectively obscures the driver's view of the curve or curve combinations. This can most readily be accomplished by using open field areas for the unobscured portions of the path.

-- Insofar as possible, the test path would course through basically flat terrain although some local changes in elevation undoubtedly would occur along the path.

-- Preliminary layout could be done using aerial photographs of the test site, but the final layout would be determined on site where topographical and other considerations can best be appraised. Tree removal and brush clearance requirements would be kept at the lowest practicable level.

-- Minimum path length tentatively is estimated at three miles. This would permit each type of curve to be represented twice under each of the obscuration conditions.

-- A short warm-up track also would be provided. This would be a simplified version of the test path and would be used for practice and familiarization purposes. It can be constructed entirely in the open.

PHASE IV - Test Path Checkout

The primary purpose of this phase is to determine to what extent, if any, characteristics of the test path other than those under study affect performance. Path characteristics that could affect performance include, for example, terrain irregularities and soil texture. A precise knowledge of these factors is necessary so that in the actual tests effects due to experimental variables are properly evaluated. The data obtained in this checkout would provide a basis for weighting performance measures obtained in the field study proper so that results attributable to unique characteristics of the test path such as terrain irregularities or soil differences can be accounted for and the test data can be appropriately weighted for analysis.

PHASE V - Field Test #1

It is well known that vehicle system performance suffers when visibility is degraded, but the extent to which performance is affected under various visibility and operating conditions has yet to be adequately determined.

The purpose of this first field test is to obtain quantitative data concerning system performance under various conditions of illumination and obscuration of critical features of the forward path of travel such as might occur in woods or dense brush. It is assumed that dangerous obstacles, the locations of which are unknown to the driver, will be present along the path.

There are some basic considerations underlying the design of this study that should be noted. Because of the response times of the driver and the vehicle, a certain finite amount of time is required to effect changes in system operation that may be required as a result of visual information afforded the driver. Since primary tasks of the driver are to guide his vehicle along some selected path of travel and to avoid colliding with any dangerous obstacles that may be present in the path, it can be assumed that the driver takes his response time and the vehicle response time into account and thus looks along the path to at least a distance that will enable him to efficiently guide or stop his vehicle to avoid obstacles, negotiate curves, etc., that he might sight. System response time thus establishes the minimum distance at which an obstacle must be sighted to permit appropriate corrective action to be implemented at the speed of travel. The maximum sighting distance is determined by factors such as the level of illumination and the extent of obscuration of the forward path of travel. The visual detection task is a critical determinant in system performance and must be specified before the effects of reduced visibility on performance can be adequately assessed. If the visual detection task is such that, under specified velocity and visibility conditions, a critical object or feature of the path cannot be detected and recognized and corrective action taken in time to avoid a collision, then the driver has little recourse but to attempt

to alter system performance. In this case, he probably would slow down to achieve safer travel. The visual task in the first study will be designed to be sufficiently difficult to effect such changes in performance in the test situation compared to performance in the checkout phases.

The basic experimental design is a 2x4 factorial design with repeated measures over both factors. The independent variables are:

1. Light level (measured with brightness meter and standard test plate)

   (a) 50 fL or more (daylight)
   (b) -0.0001 - 0.001 fL (moonlight)
   (c) 0.00001 - 0.0001 fL (starlight)
   (d) below 0.00001 fL (moonless, overcast)

2. Obscuration level

   (a) Heavily wooded terrain (sufficient to block view of path around curves)
   (b) Open terrain (no trees or brush obstructing the driver's view of critical path features).

In addition to negotiating the curves in the path, the driver would be instructed to avoid hitting "dangerous obstacles" that are present on the path. These obstacles would be represented by stakes mounted on knock-down bases. The exact dimensions and contrast characteristics of the stakes would be such that under optimal viewing conditions they could be detected at about the minimum distance required to come to a safe, controlled stop from the maximum safe velocity (as determined in Phase II). Thus, under degraded viewing conditions, the driver must slow down to avoid hitting a stake. At least 10 obstacles would be presented during each run and would be randomly

placed along the test path. The obstacles would contain symbols which the subject would identify. This is to enable the experimenter to verify reports by the driver that he has detected and identified an obstacle. All subjects would encounter both obscuration conditions under all light levels.

The subjects would be instructed to proceed at the maximum velocity they believed safe (as long as it was within prescribed safety limits established for the curves and the straightaways), to stay on the path, to avoid hitting unidentified test obstacles and to avoid undue risk to either personnel or the vehicle.

Performance measures would include:

1) total elapsed time to traverse the entire test course and average velocity over the course

2) time required to complete each segment of the course (each straightaway section, each curve and each combination of curve) and average velocity for each segment

3) fuel consumption

4) number of braking, accelerator and course correction actions taken over the entire course and over individual segments

5) locations and relative times at which velocity changes are effected upon entering and upon exiting the curves

6) number of unidentified obstacles knocked down

7) distances at which obstacle is detected and identified (verbal report)

8) "ride" measures derived from the motion data.

The various measures would be analyzed using analysis of variance techniques.

These data should provide a firm basis for establishing criteria used to evaluate performance on the simulator. (Estimating operational performance on the basis of simulator data without operational validation of these data is known to be a tenuous procedure.) The field tests are intended to be reasonably realistic representatives of certain operational activities. The results of these tests and the knowledge gained concerning field test procedures would also be of benefit in proposed future investigations such as those involving the effects of fog, dust, rain and other environmental factors on performance.

The data regarding the distance at which the "obstacles" are identified can be used to examine the effects of operating a moving vehicle on basic visual detection. Finally, the motion data would provide reference inputs to the motion simulator.

Appendix K: AUXILIARY DISPLAYS FOR IMPROVING OFF-ROAD MOBILITY

It is necessary for a human vehicle operator to integrate information from many sensory modalities to perform a number of operations. In aerospace vehicles, a large amount of the burden incurred from processing this information has been alleviated by the use of instruments which report system conditions. In contrast, ground vehicle systems have not utilized many information displays. Reference K1 points out that there is reason to believe that increased performance would be obtained from an off-road vehicle driver if additional systems and environmental information were made available to him.

An example of potentially useful information which could be made available is a measure of slip taking place between the running gear of the vehicle and the ground surface. To this end a slip-indicating device was selected for study and an experiment was conducted to evaluate the benefits to the driver of this added information. Also we were interested in developing methods for assessing the advantages of a wide variety of displays.

A vehicle is slipping when its running gear velocity exceeds its actual forward velocity. Slip, in percent, is defined by the expression $(1 - \frac{V}{r}) \times 100$ (See Appendix A of this report.) Weiss [K2] has shown that the use of a slip control governor resulted in lower fuel consumption and increased travel speeds. Whether this control should be automated (i.e., use of a governor) or left to the operator (i.e., use of a display), is a question which depends on many factors. These factors include the diversity of slip conditions to be encountered and the reliability of the mechanical governor. They also include the ability of the operator to perform the slip governing task. It remained to be determined if an operator could make use of a slip information display for controlling vehicle slip.

The experienced vehicle operator has available to him several sources of sensory information which, taken together, inform him of vehicle slip:

a) He can hear the engine and running gear noises (which generally increase in amplitude under slip conditions).
b) He can see the rate of forward progression of the vehicle.
c) He can feel the rate of forward progression of the vehicle.
d) He can feel the amount of depression of the accelerator pedal.

In addition, the driver has system displays, a speedometer and often a tachometer, which inform him of the running gear speed and engine rpm. To perform his task optimally, the operator must be able to integrate over all this sensory information to determine the amount of slip the vehicle is experiencing and to determine what effects his control actions have on slip changes.

In this study two questions were asked:

a) Can a driver make use of currently available cues, and if so, is it possible to determine the relative usefulness of these cues?
b) Can a new display (a slipmeter) present slip information in a more useable form?

The slipmeter used was a device which computes slip as a function of actual forward speed and running gear velocity and presents this information to the driver. The desired operating slip value varies according to the particular vehicle characteristics, soil conditions and mission requirements. In order to avoid requiring difficult mental computations on the part of the driver, the nominal "best" value of slip as displayed by the slipmeter could be specified for the operating situation, i.e., type vehicle, terrain and mission. For this experimental investigation a slipmeter was used that displayed the difference between running gear velocity and vehicle forward

speed. To construct a slipmeter suitable for operational use from a human factors standpoint would require:

1. the determination of a function of slip that can be displayed as a constant value independent of velocity and
2. the determination of the "best value" of slip for each operating condition to be encountered (these slip values could be memorized, or listed for use, by the driver).

The driver's task in this experiment was to drive a vehicle over a track with a low coefficient of friction starting from rest and progressing to a specified point in the shortest time possible. The usefulness of the various sources of slip information (e.g., vehicle noise, speedometer, slipmeter) was evaluated by presenting this information singly or in combination, to the driver on a series of trial runs. The scoring of these trials was achieved by making use of two measures: a) the total time required to traverse the track; and b) the total amount of slip accrued as measured by the integral of slip during the total time of the run.

Five experimental conditions, each consisting of a different set of available information were administered to each driver. In two of the conditions, the auditory cues provided by the vehicle noise (motor and tires) were masked by means of a sufficiently loud white noise played binaurally through earphones. For one of these conditions, both the speedometer and the slipmeter were obscured from view, and in the other condition the driver was allowed to view the speedometer. Under each of the remaining three conditions, the auditory cues were available to the driver (i.e., the white noise was not administered). Under one of these three conditions, both meters were obscured; in another, only the slipmeter could be seen; while in the last condition only the speedometer was visible.

When the test conditions are ranked according to performance, one finds that the white noise-only conditions (i.e., no additional displays or auditory cues) yielded the poorest performance. This condition was followed in order by: white noise plus speedometer; auditory cues plus slipmeter; auditory cues with no displays; and auditory cues plus speedometer. This ranking holds for both performance measures (total time and integrated slip).

The rank ordering of the five display conditions is statistically significant for both measures. Therefore, it can be concluded that the methods used in this study permitted evaluation of the effects of various sources of information. The integrated slip measure indicated the extent to which the drivers used this information to control the amount of vehicle slip while the time measures showed the effect of his control on acceleration. The best system performance (shortest times) resulted when the total slip was lowest.

Before the differences between the individual display conditions are considered, a special comment is needed concerning the two conditions which prevented drivers from hearing the vehicle noise cues. Under these conditions white noise was used to mask the sounds. In choosing this technique, it was understood that such a procedure not only made the vehicle noises inaudible, but might have provided a source of stress. It was concluded, however, that this method of stimulus control was valid for our purposes, since it is only through loud masking noises that a driver would be deprived of vehicle running gear sounds.

A pronounced effect is observable in the data and is related to the availability of auditory cues (vehicle noise) to the driver. The best scores (lowest times) were associated with the conditions in which the drivers were allowed to hear the vehicle running gear sounds. The scores were similar among those three conditions (auditory cues plus slipmeter, auditory cues with no displays, auditory cues plus speedometer). The performance was not as good for the "white noise" trials, but for those two conditions (white noise alone,

white noise plus speedometer) the scores were similar. Further distinction among the conditions cannot be made on the basis of the data gathered. It is evident from this preliminary work that some statistically significant differences may be obtained with a small number of subjects. Increasing the number of subjects in future work would allow the use of more powerful statistical tests to discriminate more finely among the test conditions.

Future studies should address the following problems:

1. Determine the slip function which requires the least interpretation by the driver.

2. Evaluate the variety of displays which may be employed to present the slip information.

In addition to a slipmeter (which may, in fact, be an auditory or visual display), one must evaluate the amount of slip information that the driver receives from the present displays and running gear noise. From the results of the present study it appears that useful slip information is derived from the running gear noise. An analysis of this source of cues should be carried out to determine if there is some combination of training and controlled noise presentation which allows the driver to maintain the most desirable slip conditions.

The types of measures used in this study and the experimental methods used to rank the usefulness of various sources of information are applicable on all levels of investigation, i.e., field testing, simulated field studies (e.g., as in the present study), and laboratory simulation. Laboratory simulation is especially promising since that method provides for more exacting control over the sources of information. Only by bringing all relevant cues under the control of the experimenter is it possible to properly evaluate: (1) the usefulness of information to the driver, (2) the drivers' abilities in comparison to the performance of automatic control systems.

REFERENCES

K1. Bartlett, G.E., Kaufman, S. and Deutschman, J.N. (co-editors) "Off-Road Mobility Research" Second Semiannual Technical Report, Technical Report No. VJ-2330 G-2, Cornell Aeronautical Laboratory, Inc., September 1967.

K2 Weiss, S.J., "An Experimental Off-the-Road Governor for Transport Vehicles", Research Report No. 3, Land Locomotion Research Laboratory, Detroit Arsenal, 1956, pp. 20-30.

Appendix L: DESIGN FOR VEHICLE MOTION SIMULATION

This Appendix discusses the design efforts related to a moving base motion simulator which incorporates roll, pitch, and bounce motions and provides a description of two possible designs:

(1) a "short throw" motion simulator capable of ± 6.0 inches; in the bounce mode;

(2) "long throw" motion simulator capable of ± 12.0 inches vertical displacement at ± 45 degrees pitch.

"SHORT THROW" MOTION SIMULATOR

The design of a "short throw" (± 6.0 inches) motion simulator with freedom in pitch, roll and bounce consisted of the following tasks:

(a) conceptual design;

(b) selection of motion limits, determination of the hydraulic power requirements and development of the mechanical specification; and

(c) preparation of design sketches.

Design Concepts

Two concepts were investigated in an attempt to produce angular motions. One used a spherical bearing and the other used gimbals. The latter concept was pursued because of the availability of commercial bearings, ease of structural fabrication, and ease of measuring and controlling the angular motions. In this design the bounce mechanism was mounted on the pitch-roll platform. This permitted minimizing the weight to be driven in bounce and hence minimized power requirements. In this concept the bounce motion is always perpendicular to the combined pitch-roll plane.

Design Specifications

This task dealt with the selection of motion specifications as dictated by human tolerance limits and vehicle motions, determination of the hydraulic power requirements and development of specifications for the mechanical driving components (cylinders). The roll and pitch excursions used in the designs were dictated by existing vehicle capabilities. The accelerations in roll, pitch and bounce were arrived at through considerations of both human tolerance limits and hydraulic power considerations. The rate of change of acceleration characteristics were derived from existing vehicle considerations. The results of this task are summarized in Table L-1. The motion specifications consist of a long-duration sinusoidal motion and a transient motion (such as caused by a hump, boulder or chuck hole) which are assumed to peak at the same time, hence are added to yield the total motion. Note further that the total design weight is 2,000 lbs. (1,000 lbs. for the bounce mechanism, crew station and driver, and 1,000 lbs. for the roll-pitch platform). This design weight will require a flow rate of 150 gpm at a supply pressure of 3,000 psi.

Design Details

Based upon the foregoing concepts and specifications, a set of preliminary designs have been prepared. A single cylinder will drive the motion simulator in roll, a second cylinder will drive it in pitch and two cylinders, supported by the roll frame will be used to drive the bouncing crew station. The guides and cylinder supports are positioned to maintain a low center of gravity of the system.

"LONG THROW" MOTION SIMULATOR

The design of a "long throw" ($\pm$ 12.0 inches vertical displacement at $\pm$ 45 degrees pitch) motion simulator with freedom in pitch, roll and vertical displacement included the same tasks as those for the previous design; namely:

Table L-1

MOTION SPECIFICATIONS, HYDRAULIC POWER REQUIREMENTS, AND MECHANICAL SPECIFICATIONS FOR A "SHORT THROW" (±6 IN.) MOTION SIMULATOR

PARAMETERS	SLOW SINUSOIDAL MOTION	TRANSIENT MOTION	TOTAL
1. BOUNCE (PAYLOAD = 1000 lbs)			
MAXIMUM DISPLACEMENT, ft	±0.50		±0.5
MAXIMUM VELOCITY, ft/sec	3.2	5.2	8.4
MAXIMUM ACCELERATION, g's	0.6	4.0	4.6
FREQUENCY, Hz	1.0		
SUPPLY PRESSURE, psi			3,000
NET PRESSURE, psi			2,000
NET AREA, sq. in.			2.3
FLOW RATE, gpm			60.2
CYLINDER STROKE, ft			1.0
2. PITCH (PAYLOAD = 2000 lbs, LENGTH = 8 ft, INERTIA = 332 lb-ft-sec^2)			
MAXIMUM DISPLACEMENT, deg	±45°		±45°
MAXIMUM VELOCITY, deg/sec	141	100	241
MAXIMUM ACCELERATION, deg/sec^2	443	1,200	1,643
FREQUENCY, Hz	0.5		
SUPPLY PRESSURE, psi			3,000
NET PRESSURE, psi			2,000
TORQUE ARM, ft			1.0
CYLINDER NET AREA, sq. in.			4.76
FLOW RATE, gpm			62.5
CYLINDER STROKE, ft			2.0
3. ROLL (PAYLOAD = 2000 lbs, LENGTH = 5 ft, INERTIA = 130 lb-ft-sec^2)			
MAXIMUM DISPLACEMENT, deg	±30°		±30°
MAXIMUM VELOCITY, deg/sec	92	100	192
MAXIMUM ACCELERATION, deg/sec^2	300	1,800	2,100
FREQUENCY, Hz	0.5		
SUPPLY PRESSURE, psi			3,000
NET PRESSURE, psi			2,000
TORQUE ARM, ft			1.0
CYLINDER NET AREA, sq. in.			2.38
FLOW RATE, gpm			25.0
CYLINDER STROKE, ft			2.0

(a) conceptual design;

(b) selection of motion specifications, determination of the hydraulic power requirements and development of the mechanical specifications; and

(c) preparation of preliminary design sketches.

Design Concepts

The basic mechanism concepts investigated here were:

(1) a vertically guided platform driven differentially by means of two hydraulic cylinders so as to provide vertically guided and pitch motions simultaneously; and

(2) a roll frame driven by a rotary hydraulic actuator.

In this design the crew station is attached directly to a roll frame which, in turn, is mounted on a pitch-vertical displacement platform. Here, the linear motion is vertical whereas in the "short throw" simulator the linear motion is perpendicular to the combined roll-pitch platform.

Design Specifications

The development of design specifications followed the same steps used in the design of the "short throw" motion simulator. These steps and the results are tabulated in Table L-2. The major differences in the specifications are:

(1) a vertical displacement of $\pm$ 2.0 ft. for zero pitch as compared to a bounce of $\pm$ 0.5 ft in the case of the "short throw" motion simulator;

Table L-2

SPECIFICATIONS AND POWER REQUIREMENTS FOR A "LONG THROW" (±12 IN.) MOTION SIMULATOR

PARAMETERS	SLOW SINUSOIDAL MOTION	TRANSIENT MOTION	TOTAL
1. BOUNCE (PAYLOAD = 1,200 lbs, ACCESSORIES = 800 lbs)			
MAXIMUM DISPLACEMENT, ft	±2.0		±2.0
MAXIMUM VELOCITY, ft/sec	3.2	5.2	8.4
MAXIMUM ACCELERATION, g's	0.6	3.0	3.6
FREQUENCY, Hz	0.25		
MAXIMUM FORCE, lb	(TWO CYLINDERS)		9,200
SUPPLY PRESSURE, psi			3,000
NET PRESSURE, psi			2,000
NET CYLINDER AREA, sq. in.	(TWO CYLINDERS)		4.60
FLOW RATE, gpm			120.7
CYLINDER STROKE, ft			4.0
2. PITCH (PAYLOAD = 1,200 lbs, LENGTH = 8 ft, INERTIA = 200 lb-ft-sec^2)			
MAXIMUM DISPLACEMENT, deg	±45		±45
MAXIMUM VELOCITY, deg/sec	141	100	241
MAXIMUM ACCELERATION, deg/sec^2	443	1,200	1,643
FREQUENCY, Hz	0.5		
MAXIMUM TORQUE, lb/ft			5,720
TORQUE ARM, ft			1.0
MAXIMUM FORCE, lb	(TWO CYLINDERS)		5,720
SUPPLY PRESSURE, psi			3,000
NET PRESSURE, psi			2,000
CYLINDER NET AREA, sq. in.	(TWO CYLINDERS)		2.86
FLOW RATE, gpm			75.0
CYLINDER STROKE, ft			4.0
3. ROLL (PAYLOAD = 1,200 lbs, LENGTH = 5 ft, INERTIA = 78 lb-ft-sec^2)			
MAXIMUM DISPLACEMENT, deg	±30°		±30°
MAXIMUM VELOCITY, deg/sec	92	100	192
MAXIMUM ACCELERATION, deg/sec^2	300	1,800	2,100
FREQUENCY, Hz	0.5		
MAXIMUM TORQUE, lb/ft			3,000
SUPPLY PRESSURE, psi			3,000
NET PRESSURE			2,000
TORQUE FACTOR, in.^{3}/rad			24.9
FLOW RATE, gpm			21.7

(2) the maximum vertical displacement attainable being dependent upon the pitch motion, e.g., at ± 45 degrees pitch the maximum attainable bounce is ± 1.0 ft.;

(3) a vertical displacement flow rate requirement of 120.7 gpm as compared to 60.2 gpm for the bounce mode of the "short throw" design (this is due to twice as much mass-2,000 lbs.-being moved);

(4) the cylinder stroke of 4.0 ft. demanding added structure; and

(5) the additional requirement for a rotary actuator.

Design Details

Two cylinders drive the pitch-vertical displacement platform differentially. A rotary actuator drives the roll frame (and the crew station that will be attached to it). In this design the rotary hydraulic actuator is mounted on top of the pitch-bounce platform.

UNCLASSIFIED

Security Classification

DOCUMENT CONTROL DATA - R & D

(Security classification of title, body of abstract and indexing annotation must be entered when the overall report is classified)

1 ORIGINATING ACTIVITY *(Corporate author)*

Cornell Aeronautical Laboratory, Inc.
Buffalo, New York

2a. REPORT SECURITY CLASSIFICATION

2b. GROUP

3 REPORT TITLE

Summary Report on Off-Road Mobility Research

4 DESCRIPTIVE NOTES *(Type of report and inclusive dates)*

Technical Report (2 Vols.) - Summarizing the studies performed between August 1966 and Oct. 1968 with emphasis on period Sept. 1967 to October 1968.

5 AUTHOR(S) *(First name, middle initial, last name)*

Co-editors George E. Bartlett
Jerome N. Deutschman

6 REPORT DATE

November 1968

7a. TOTAL NO. OF PAGES

7b. NO. OF REFS

8a CONTRACT OR GRANT NO

DAHC04 67 C 0005

b. PROJECT NO

ARPA Order No. 841 dated 7 May 1966

c.

d

9a. ORIGINATOR'S REPORT NUMBER(S)

CAL Report No. VJ-2330-G-3

9b. OTHER REPORT NO(S) *(Any other numbers that may be assigned this report)*

10 DISTRIBUTION STATEMENT

Distribution of this document is unlimited.

11 SUPPLEMENTARY NOTES

Contracting Agency - U.S. Army
Research Office-Durham

12 SPONSORING MILITARY ACTIVITY

ARPA

13 ABSTRACT

A summary of research and engineering studies conducted on a long-range program of off-road mobility research is presented in Vol. I of this two-volume report. These studies, some of which are only partially completed, are directed at providing technical knowledge which is required to match off-road vehicles with military mobility requirements.

A hybrid computer model is described which will permit predicting vehicle dynamics performance of simulated vehicles traversing a broad spectrum of off-road situations. A critique of existing soil trafficability theories is made based on a review of the literature which treats the comparison of vehicle performance prediction with experimental results. Analytical and experimental studies of the velocity field and soil fabric in clay soil exposed to dynamic loads are summarized. A general method is discussed for processing mobility related environmental information and for mapping vehicle performance by computer methods. A concept is introduced for testing vehicles in relation to the total environment in order to define the vehicle performance envelope.

Also a method is introduced for displaying potential vehicle performance in selected geographic areas and for producing "testable" specifications for off-road vehicles. Engineering studies of an off-road driving simulator for synthesizing dynamic visual displays and vehicle motion in the laboratory are reviewed.

Recommendations pertaining to future off-road mobility research and engineering studies are presented.

Volume II contains Appendices that complement the material presented in Volume I.

DD FORM 1 NOV 65 1473

UNCLASSIFIED

Security Classification

14. KEY WORDS	LINK A		LINK B		LINK C	
	ROLE	WT	ROLE	WT	ROLE	WT
Off-Road Mobility						
Mobility Systems Studies						
Vehicle-Terrain Interaction						
Human Factors						
Environment						
Soil Mechanics						